(2)

CHEMICAL RESEARCH, DEVELOPMENT & ENGINEERING CENTER

CRDEC-SP-005

INDEPENDENT RESEARCH PROGRAM ANNUAL REPORT FY88

H. Dupont Durst, Ph.D.
Susan F. Hallowell
RESEARCH DIRECTORATE

Prepared by Denise Pobedinsky
PROGRAMS & RESOURCE MANAGEMENT DIRECTORATE

Edited by Cecilia B. Neumann
Patricia J. Reeves
RESEARCH, DEVELOPMENT & ENGINEERING SUPPORT DIRECTORATE

April 1989

U.S. ARMY ARMAMENT MUNITIONS CHEMICAL COMMAND

Aberdeen Proving Ground, Maryland 21010-5423

Disclaimer

The findings in this report are not to be construed as an official Department of the Army position unless so designated by other authorizing documents.

Distribution Statement

Approved for public release; distribution is unlimited.

UNCLASSIFIED

SECURITY CLASSIFICATION OF THIS PAGE

REPORT DOCUMENTATION PAGE

Form Approved OMB No. 0704-0188

1a. REPORT SECURITY CLASSIFICATION UNCLASSIFIED	1b. RESTRICTIVE MARKINGS
2a. SECURITY CLASSIFICATION AUTHORITY	3. DISTRIBUTION/AVAILABILITY OF REPORT Approved for public release; distribution is unlimited.
2b. DECLASSIFICATION/DOWNGRADING SCHEDULE	
4 PERFORMING ORGANIZATION REPORT NUMBER(S) CRDEC-SP-[illegible]05	5. MONITORING ORGANIZATION REPORT NUMBER(S)
6a. NAME OF PERFORMING ORGANIZATION CRDEC	6b. OFFICE SYMBOL (If applicable) See Reverse
6c. ADDRESS (City, State, and ZIP Code) Aberdeen Proving Ground, MD 21010-5423	7a. NAME OF MONITORING ORGANIZATION
8a. NAME OF FUNDING/SPONSORING ORGANIZATION CRDEC	8b. OFFICE SYMBOL (If applicable) SMCCR-PMP
8c. ADDRESS (City, State, and ZIP Code) Aberdeen Proving Ground, MD 21010-5423	9. PROCUREMENT INSTRUMENT IDENTIFICATION NUMBER
	7b. ADDRESS (City, State, and ZIP Code)

10 SOURCE OF FUNDING NUMBERS

PROGRAM ELEMENT NO.	PROJECT NO.	TASK NO.	WORK UNIT ACCESSION NO.
	1L161101	A91A	

11. TITLE (Include Security Classification)

Independent Research Program Annual Report FY88

12. PERSONAL AUTHOR(S)
See reverse

13a. TYPE OF REPORT	13b TIME COVERED	14 DATE OF REPORT (Year, Month, Day)	15. PAGE COUNT
Special Publication	FROM 87 Oct TO 88 Sep	1989 April	103

16. SUPPLEMENTARY NOTATION

17. COSATI CODES			18 SUBJECT TERMS (Continue on reverse if necessary and identify by block number)
FIELD	GROUP	SUB-GROUP	
19	06	03	Independent research, IRP, Laboratory research, Basic research, Exploratory development, Chemical defense research.

19. ABSTRACT (Continue on reverse if necessary and identify by block number)

The objectives of the Independent Research Program (IRP) are to improve the quality of U.S. Army Laboratories, fund new thrusts in laboratories mission areas, fund seed projects for future programs, attract and retain top, young scientists and engineers, and give the Technical Director some flexibility for technical entrepreneurship. IRP funds are allocated directly from the Assistant Secretary of the Army (RDA) to laboratory commanders and directors on the basis of the previous year's performance. This annual report of the IRP at the U.S. Army Chemical Research, Development and Engineering Center details the accomplishments achieved during FY88, the innovativeness of the research projects, and the relevance of the program to the Center's missions.

a. Ion trap mass spectrometry

b. Infrared radiative pyrolysis spectrometry

(Continued on reverse)

20. DISTRIBUTION/AVAILABILITY OF ABSTRACT	21 ABSTRACT SECURITY CLASSIFICATION
☒ UNCLASSIFIED/UNLIMITED ☐ SAME AS RPT ☐ DTIC USERS	UNCLASSIFIED

22a. NAME OF RESPONSIBLE INDIVIDUAL	22b TELEPHONE (Include Area Code)	22c OFFICE SYMBOL
SANDRA J. JOHNSON	(301) 671-2914	SMCCR-SPS-T

DD Form 1473, JUN 86 *Previous editions are obsolete.*

6b. Office Symbol (continued)

SMCCR-RSC-C
SMCCR-PMP
SMCCR-SPS-T

12. Personal Author(s) (Continued)

Durst, H. Dupont, Ph.D. and Hallowell, Susan F.

Prepared by: Pobedinsky, Denise

Edited by: Neumann, Cecilia B. and Reeves, Patricia J.

19. Abstract (Continued)

c. Toxicological tests

d. Optical fiber waveguide

e. Toxicity estimates

f. Improved methods of agent detection/decontamination

g. Artificial intelligence

h. Regenerative adsorbents

TABLE OF CONTENTS

BLANK PAGE

CHEMICAL RESEARCH, DEVELOPMENT AND ENGINEERING CENTER

INDEPENDENT RESEARCH PROGRAM

ANNUAL REPORT FY88

INTRODUCTION

The U.S. Army Chemical Research, Development and Engineering Center (CRDEC) continues to place a high degree of importance on the Independent Research Program. This program provides a source of funding for novel, innovative, and high-risk ideas and serves as a source of feedstock for significant change in the core programs. The value of the programs, in the generation of new ideas, professional development, and employee morale, far outweighs its percentage of the total budget.

At CRDEC, a call for Independent Research Proposals is issued in July of each year, although we encourage and receive proposals at any time. These are screened first by the directors for individual review and discussion, and then evaluated by the Associate Technical Director for Technology and a directorate level peer group. The Associate Technical Director for Technology gives me his recommendations and a tentative order of merit ranking. I review these recommendations, discuss any questions I have with the investigators, and publish my approval decision. My acceptance of a proposal then becomes a direct contract between the principal investigator and the Technical Director. The principal investigators have direct access to me on matters concerning IRP. At mid-fiscal year, the Associate Technical Director for Technology reviews each ongoing effort with the investigator and gives me his evaluation of progress. Finally, we conduct a formal year-end review that leads to this report. Any effort proposed for a second year of Independent Research funding must again go through the competitive process.

In FY88, our emphasis on encouraging basic engineering proposals along with basic science continued. With the continued emphasis on placing large development contracts for our engineering development projects, it is more important than ever to foster innovative engineering research within the Army laboratory/center structure. I feel the Independent Research program can provide the mechanism for fostering such work. To that end, I have tried to achieve a balance in our projects selected for funding. The projects selected cover a wide range of technologies, some very fundamental and others somewhat applied. All projects within the Independent Research Program reflect CRDEC's objectives and strongly emphasize the emerging technologies and chronic problem areas of the Tech Base Investment Strategy.

DISTRIBUTION OF IRP FUNDING BY TECH BASE INVESTMENT STRATEGY

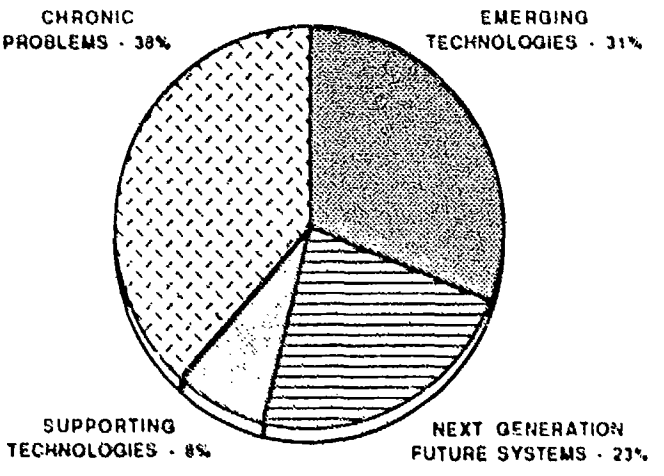

The 13 efforts in the FY88 program were selected from 60 proposals. All 13 programs were reviewed and recommended for continuation at the mid-year review. This year two projects were rated outstanding, one for scientific research and the other for engineering research. These are highlighted in the report and each of the investigators will be presented with a plaque in recognition of their efforts. Ranking and selection of the outstanding projects are based on several factors: (1) innovativeness, (2) scientific achievement, (3) relevance to CRDEC's mission, and (4) improvement of the Center's capabilities.

A valuable by-product of these efforts is the publication of results in the open literature. An outstanding example of this effort is Susan Haliowell's project entitled "An Enzyme Amplified Receptor Based Assay (ERA): New Approaches for Drug and Toxin Detection." This program produced four publications in FY88 and was highlighted in a major article by Professor Gary A. Rechnitz, Unidel Professor of Chemistry and Biotechnology, University of Delaware, in Chemical and Engineering News (September 5, 1988 issue, pp 24-36). Dialogue between Independent Research investigators and their counterparts in the scientific community have resulted in the enhancement of the Chemical Research, Development and Engineering Center's position as a center of scientific excellence.

The Independent Research review process provides a means of direct communication between the director level and the bench, with benefits to both. The feedback from the bench level on problems and quality of the staff is invaluable to the director. The directorate attention given to the Independent Research participants is a boost to both employee morale and professional self-esteem.

DISTRIBUTION OF TECH BASE FUNDING BY TECHNICAL AREA (FY88 = 48.5M)

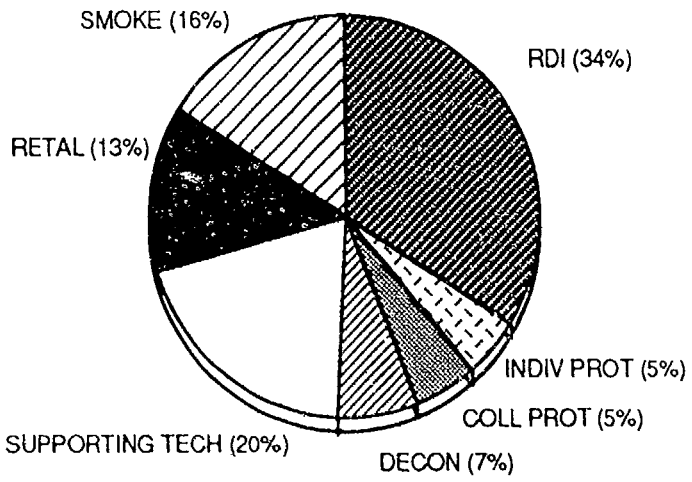

The quality of the CRDEC's Independent Research efforts continues to improve and contribute significantly to the core efforts of the Center. At the beginning of the year it appeared that Department of the Army (DA) would reinstitute the Independent Research program for FY88. It was a blow to the program when DA was not able to because of budget constraints. Because of my feeling on the critical nature of this program and its benefit to both CRDEC and the ARMY, I provided internal funds in this extremely tight budget year to continue an Independent Research Program. I think that it was a wise decision and will benefit the Army. We evaluated 66 proposals for FY89 under the Independent Research Program; only 11 of these were funded because of budgetary constraints. I hope that in the future DA will identify funds to continue and expand the program so that more basic research is provided to the U.S. Army technical data base. I wish to assure all those CRDEC researchers and engineers who submitted unsuccessful proposals that most were rated very high in scientific content and would have been funded in previous years. I hope that you will all continue your interest in the program and submit proposals again next year.

JOSEPH J. VERVIER
Acting Technical Director

MOST OUTSTANDING INDEPENDENT RESEARCH PROGRAM EFFORTS OF 1988

BLANK PAGE

LISTING OF PROJECT REPORTS

BLANK PAGE

Joseph E. Matta, CRDEC

A METHOD OF LIGAMENT STRETCHING AT HIGH EXTENSION RATES

A novel free fall extensional device was developed, and its usefulness in measuring the elongational viscosity of both Newtonian and viscoelastic liquids was demonstrated. A small liquid quantity is inserted between the ends of two cylinders that are vertically oriented one above the other. The upper cylinder is held fixed while the lower cylinder, initially at rest, is allowed to fall and stretch the adhering sample. Time sequence photos of the stretching process are used to deduce the liquid deformation rate and ligament stress. The elongational viscosity is then determined from the stress/deformation rate ratio. Since only a small liquid quantity is required for testing and the apparatus can conveniently fit into a glove box, the elongational characterization of toxic chemical agents are now possible.

INTRODUCTION

Aerodynamic forces are often used to atomize liquids for various applications. However, when Newtonian liquids are subjected to relatively high air velocities, small particles normally result. To increase the drop size of the atomized fluid, polymers are often added. With this addition of polymer, non-Newtonian viscoelastic solutions are produced. Although the exact mechanisms of atomization are not well known, experimental studies[1-3] indicate that extensional rheological properties play a critical role in the breakup process and significantly influence the resultant drop sizes. Some theoretical arguments[4,5] indicate that nonlinear viscoelastic effects tend to stabilize viscoelastic ligaments, resulting in the formation of larger drops than those produced from a Newtonian fluid of similar viscosity. Thus, in order to develop a valid predictive drop size capability for viscoelastic breakup, an understanding of the extensional flow behavior of the fluid is required.

In steady extensional flow, the elongational viscosity, η_e, is the material function used to characterize the fluid. Elongational viscosity measurements on viscous polymer melts are normally made using a tensile testing machine[6] on which a rod-like sample is suspended in a silicone oil bath (to compensate gravity by buoyancy) and then stretched at a constant tensile stress or constant strain rate. However, polymer solutions typically have shear viscosities far too low to form a stable rod-like configuration. Other methods of characterizing the extensional flow behavior of a solution exist (e.g. tubeless syphon, impinging jets, and spin rheometer).[6] These methods, however, are not very suitable for use with toxic fluids since large liquid quantities are required. Also, since these methods all involve pre-shearing of the liquid, which is known to significantly affect the fluid rheology, the measurements are questionable. Extensional measurements of polymeric solutions are also possible using a falling drop experiment. Here a liquid sample is extruded vertically downward from a capillary until the drop forming at the capillary tip is no longer supported by surface tension. The falling drop stretches the connecting ligament. This method is limited since it is not possible to vary the extension rate to insure that liquid does not flow into the drop during the stretching process. In addition, it is not possible to precisely initiate the moment of stretching since this is controlled largely by the surface tension of the liquid.

Since no suitable methods exist to investigate the stretching behavior of toxic fluids at high rates of extension, a novel free fall stretching apparatus was developed. The device and its use with Newtonian and viscoelastic liquids is discussed here.

SIMPLE EXTENSION

Consider the flow established in a ligament being stretched by a falling cylinder as shown in Figure 1. Simple elongational flow occurs within the ligament of length L at time t if the rate of deformation tensor Λ is written as:

$$\Delta = \dot{\varepsilon} \begin{pmatrix} 2 & 0 & 0 \\ 0 & -1 & 0 \\ 0 & 0 & -1 \end{pmatrix} \qquad (1)$$

and the elongation rate $\dot{\varepsilon}$ is defined as $L^{-1}\, dL/dt$. From the conservation equation, it follows that one can also write the elongation rate as:

$$\dot{\varepsilon} = \frac{-2\, V_r}{r} \qquad (2)$$

where r is the ligament radius with radial velocity V_r

Neglecting interfacial surface tension, you can easily show that, for a Newtonian fluid, the total stress T_{11} required to establish such a flow is expressed as:

$$T_{11} = 3\eta_0 \dot{\varepsilon} \qquad (3)$$

where η_0 is the Newtonian shear viscosity. Since the elongational viscosity, η_e, is defined as:

$$\eta_e = \frac{T_{11}}{\dot{\varepsilon}} \qquad (4)$$

a simple relationship exists for a Newtonian fluid between the shear and elongational viscosity, i.e. $\eta_e = 3\eta_e$ and is commonly referred to the Trouton expression.[7] However, if you include interfacial surface tension, σ, as a source of stress on the ligament, then the total stress found necessary for simple extension is:

$$T_{11} = \eta_e \dot{\varepsilon} + \frac{\sigma}{r} \qquad (5)$$

Thus, if the ligament shown in Figure 1 is subjected to a simple extensional deformation, it must follow for a Newtonian fluid that the force F_L exerted on the cylinder by the ligament is:

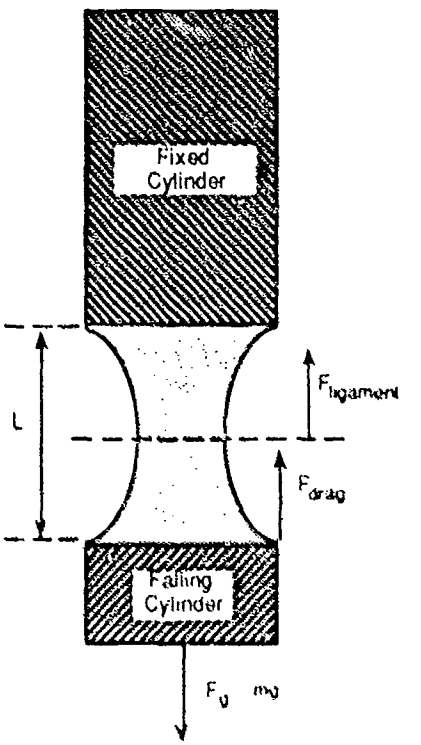

Figure 1 Force Diagram of a Ligament Stretched by a Falling Cylinder

$$F_L = T_{11}\,\pi r^2 = \eta_e \dot{\varepsilon}\,\pi r^2 - \pi\sigma r \quad (6)$$

Solving for the elongational viscosity, one obtains:

$$\eta_e = \frac{(F_L - \pi\sigma r)}{\dot{\varepsilon}\,\pi r^2} \quad (7)$$

Therefore, simple extension is assumed to occur in the ligament stretched by a falling cylinder, if you measure F_L and observe using Equation 7 that the Trouton expression is satisfied.

To measure the ligament force, F_L, acting on the falling cylinder with mass, m, Newton's second law is applied, i.e.,

$$ma = mg - F_L - F_d \quad (8)$$

where F_d is the drag force exerted on the cylinder, a is the acceleration, and g is gravitational constant. By rearranging Equation 8, one can then express the ligament force as.

$$F_L = m(g - a) - F_d \quad (9)$$

EXPERIMENTAL METHODS

To generate an elongational flow, a novel free fall extensional device was developed (Figure 2). A small quantity of liquid (~30 mg) is inserted between the ends of two cylinders that are 6.35 mm in diameter that are vertically oriented one above the other. The upper cylinder is held fixed, while the lower cylinder initially rests on top of an air piston. When activated, the piston quickly retracts downward, allowing the cylinder to fall and stretch the liquid sample adhering between the two cylinder end surfaces. High speed photographs (~1000 frames/sec) of the stretching process and the falling cylinder are used to deduce the liquid

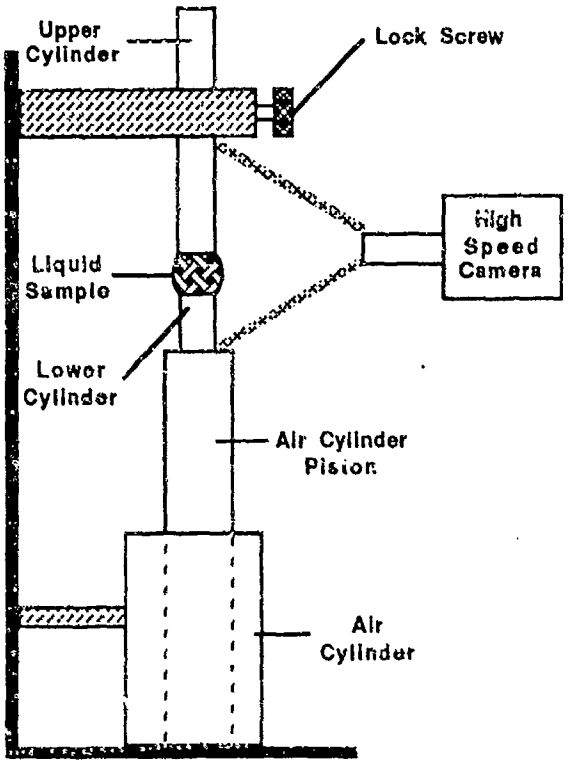

Figure 2. Schematic of Falling Cylinder Apparatus

deformation rate to determine the ligament stress, repectively. The elongational viscosity is then determined from the stress and deformation rate ratio (Equation 4).

Preliminary trials without liquid were conducted to determine the accuracy of the experiment and the significance of air drag on the free falling cylinder. Figure 3 is a plot of the measured fall velocity versus time for an 0.81-g cylinder. From the slope of the linear least square, a constant acceleration of 960 cm/sec^2 is measured. Similar free fall trials using 2.15-g and 3.11-g cylinders without liquid all resulted in constant acceleration within 2% of the gravitational constant of 980 cm/sec^2. Thus, even if air drag is neglected, the fall acceleration is measured with 2% accuracy.

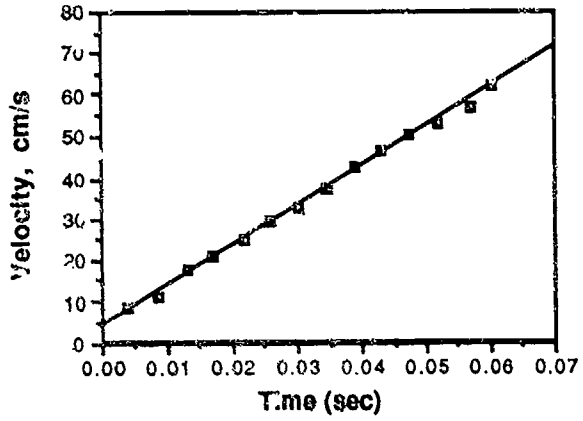

Figure 3. Velocity versus Time Plot for a Free Falling (0.81gm) Cylinder - No Liquid

NEWTONIAN RESULTS

Figure 4 is an example of a few selected frames taken of a standard ASTM oil (S2000 Canon Instrument, Co.) being stretched by an 0.81-g cylinder that resulted in an elongation rate ranging from 45 to 56 sec^{-1}. The time history of the measured cylinder fall velocity is shown in Figure 5. Table 1 provides a summary of the measured cylinder acceleration, ligament radius and elongation rate, and the measured elongational viscosity obtained using Equation 7.

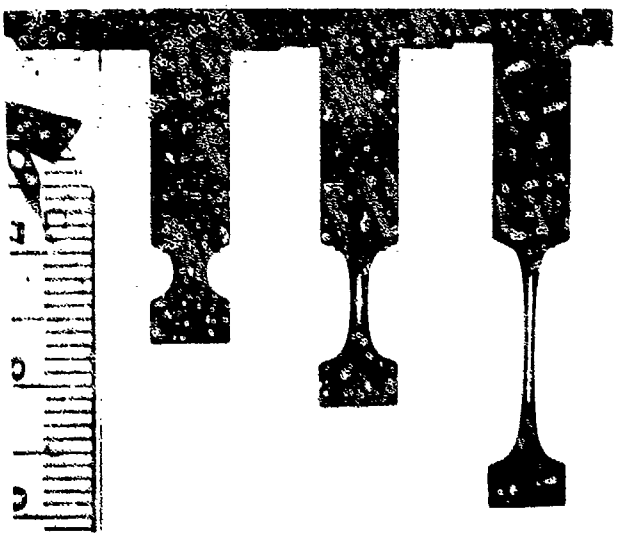

Figure 4. Time Photo of ASTM Oil Stretched by (0.81gm) Cylinder

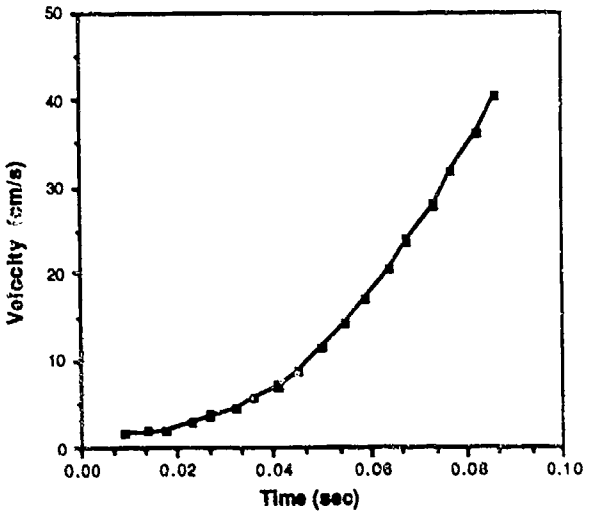

Figure 5. Fall Velocity versus Time Plot for a 33 Poise Newtonian Oil Stretched by a (0.81 gm) Cylinder

Table 1. Results For a 33 Poise Newtonian Oil Stretched by a 0.81 gm Cylinder

Time (s)	a (cm/s^2)	r (cm)	e (s^{-1})	η_e (poise)
.036	291	.203	34.4	123.6
.041	366	.186	39.3	114.3
.046	467	.169	45.1	100.8
.050	575	.151	47.1	95.4
.055	636	.134	51.0	94.8
.059	701	.122	52.3	90.3
.064	764	.107	54.6	86.1
.068	812	093	57.6	83.1
.07[illegible]	853	.081	56.3	84 3
.07[illegible]	870	.073	58.4	87.3
.082	897	.066	50.1	92.7

The reported accelerations were graphically determined from slopes drawn to the velocity versus time curve (Figure 4). Although not shown, the elongation rate was similarly determined from the corresponding ligament radius versus time curve. Once the cylinder had fallen about 2 mm that occurred in about 0.05 sec, good agreement between the measured elongational viscosity and the Trouton prediction of 99 poise was observed.

Even better agreement was observed for the five other Newtonian trials conducted (Table 2). The reported elongational viscosities are the average values measured after the cylinder has fallen 2 mm. Prior to the 2-mm displacement, the measured elongational viscosities were always greater than that predicted for simple extensional flow, indicating that the initial deformation is not merely simple extensional flow. The two trials performed with the heavier 2.15-g cylinder demonstrate how it is possible to increase the deformation rate of the stretching process.

Table 2. Newtonian Liquid Test Results.

Fluid	Temp. (°F)	Cyl. Mass (gm)	Elong. Rate (s^{-1})	η_e (poise)	$3\eta_0$ (poise)
ASTM Oil S2000	85	0.81	45-58	89	99
ASTM Oil S2000	77	2.15	65-68	146	150
ASTM Oil S600	85	0.81	73-90	29	27
Silicone Oil	85	0.81	56-70	104	99
Silicone Oil	85	2.15	68-77	99	99
Glycerol	83	0.81	92-105	12	12

VISCOELASTIC RESULTS

A 7.6-g/dL solution of K-124 diethylmalonate (DEM) was tested using the free-falling cylinder device. K-125 is a copolymer of 80% polymethyl methacrylate and 20% poly (ethyl/butyl acrylate) with a molecular weight average of about 2 million. The shear viscosity and first normal stress difference was measured as a function of shear rate with a cone and plate viscometer (Table 3).

Table 3. Measured Shear Viscosity and First Normal Stress Difference for 7.6 g/dL Solution of K-125 in DEM

Shear Rate (s^{-1})	Viscosity (poise)	Normal Stress ($dyne/cm^2$)
.27	48.3	-
.54	47.2	-
1.09	47.4	-
2.15	43.0	-
4.29	37.9	-
8.56	32.0	350
17.08	27.5	800
34.07	22.5	1500
67.98	16.2	2900
135.64	11.9	6100
270.64	8.8	10900

Figure 6 is a plot of the fall velocity versus time using an 0.81- and 2.15-g cylinders. For the heavier cylinder, the initial 2-mm displacement occurred in about 0.02 seconds, while for the 0.81-g cylinder, it took about 0.05 seconds to fall the same distance. For both trials, shortly after the 2-mm distance, a constant fall acceleration was measured.

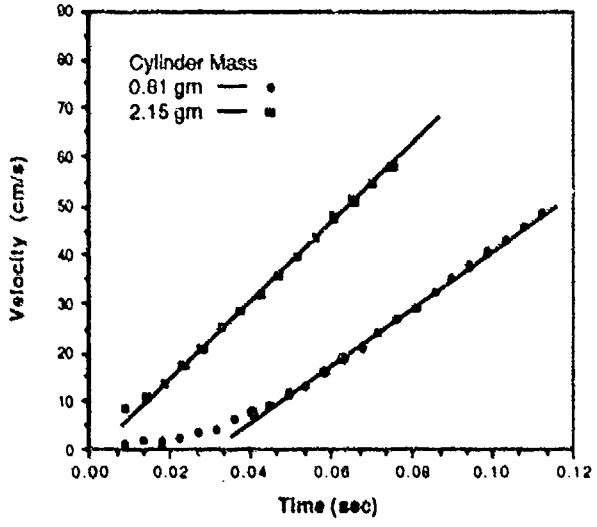

Figure 6. Fall Velocity versus Time for a K125/DEM Solution (7.6 g/dL) Stretched by a 0.81 and 2.15 gm Cylinder

Figure 7 is a ln-ln plot, the ligament radius versus time for the two viscoelastic trials. A radius of about 0.13 cm corresponds to a 2-mm displacement of the falling cylinder. As observed by the good linear fit to the data, the radial time dependence is well approximated by a power law relationship. With this relationship, one can easily show that the elongation rate for both trials varies inversely with time.

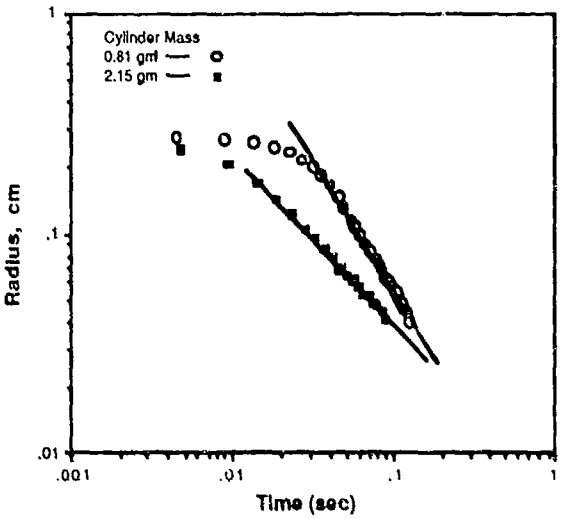

Figure 7. A Ln-Ln Plot of Radius versus Time for a Solution of K125/DEM Solution (7.6 g/dL) Stretched by a 0.81 and 2.15 gm Cylinder

Figures 8 and 9 show the measured elongational viscosities and deformation rates plotted versus time for the trials with 0.81-g and 2.15-g cylinders, respectively. The data clearly indicates that the elongational viscosity is much greater than that predicted for a Newtonian liquid. In addition, a comparison of the two figures shows that the rate at which the viscosity increases with time depends upon the rate at which the ligament is stressed. When the ligament is stressed at a higher rate by using the heavier cylinder, the elongational viscosity increases more rapidly with time.

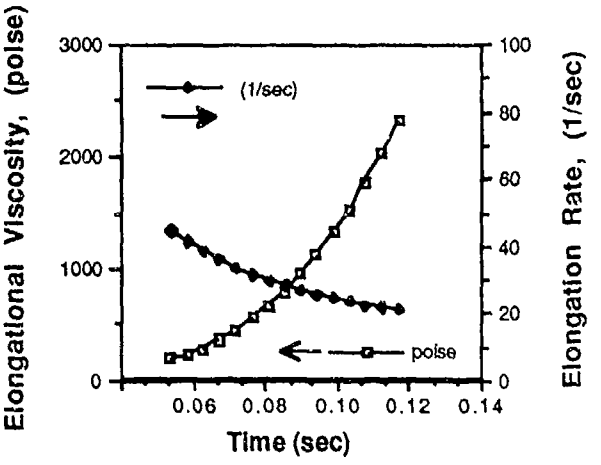

Figure 8. Elongational Viscosity and Deformation Rate Measured for a K125/DEM Solution (7.6 g/dL) Using a 0.81 gm Cylinder

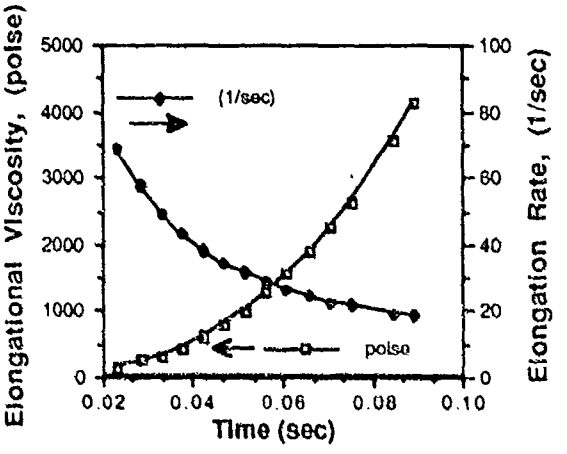

Figure 9. Elongational Viscosity and Deformation Rate Measured for a K125/DEM Solution (7.6 g/dL) Using a 2.15 gm Cylinder

CONCLUSION

A novel liquid-stretching device was successfully developed, and its usefulness in generating simple extensional flow fields with Newtonian liquids to measure the extensional viscosity was demonstrated. Viscoelastic liquids were tested with the device, and it is indicated that the elongational viscosity increases with time and is significantly greater than that of a comparable

viscous Newtonian liquid. Since small liquid quantities are required for testing and the apparatus can fit conveniently into a glove box, the elongational characterization of toxic chemical agents are now possible.

Dr. Matta received a B.S. in physics from St. Joseph's University, Philadelphia, PA, in 1970 and a Ph.D. in physics from Lehigh University, PA, in 1974. He is presently a research physicist in the Research Directorate at CRDEC.

LITERATURE CITED

1. J.E. Matta and R.P. Tytus, "Viscoelastic Breakup in a High Velocity Airstream," *J. Appl. Polymer Sci.* Vol. 27, pp 397-405 (**1982**).

2. J.E. Matta, R.P. Tytus and J.L. Harris, "Aerodynamic Atomization of Polymeric Solutions," *Chem. Eng. Com.* Vol. 19, pp 191-204 (**1983**).

3. K. C. Chao, C. A. Child, E. A. Gren, and M. C. Williams, "The Anti-Misting Action of Polymer Additives in Jet Fuels," 53rd Annual Meeting of the Society of Rheology, KY, Oct 11-15, (**1981**).

4. M. Goldin, J. Yerushalmi, R. Pfeffer, and R. Shinnar, "The Stability of Viscoelastic Capillary Jets," *J. Fluid Mech.* Vol. 38, p 689 (**1969**).

5. S.L. Goren and M. Gottlieb, "Surface-Tension-Driven Breakup of Viscoelastic Threads," *J. Fluid Mech.* Vol. 120, pp 245-266 (**1982**).

6. C.J.S. Petrie, Elongational Flows, Pitman Publishing Limited, London, England, **1979**.

7. F.T. Trouton, *Proc. Roy. Soc.* Vol. A77, p 426 (**1906**).

BLANK PAGE

William M. Lagna and Ronny C. Robbins, CRDEC

Infrared Radiative Pyrolysis Mass Spectrometry of Biological Materials

Pyrolysis mass spectrometry has been utilized as an analytical technique for the profiling of biological materials that are well beyond the mass range associated with traditional mass spectrometry. The biomaterials, which include fungi, pollen, bacteria, and viruses, are pyrolyzed for the release of characteristic compounds or groups of compounds. These chemical signatures can be used as the basis for identification of the compounds. A quartz pyrolysis apparatus based on radiative infrared heating has been developed for the direct analysis of biological materials. As an extension to this technology, the pyrolyzer has been integrated with an aerosol sampler and quadrupole ion storage mass spectrometer to form a compact system for characterization of airborne biological particulates.

INTRODUCTION

A single apparatus capable of early warning in the event of CB deployment is currently being developed as the CB Mass Spectrometer. Biological agents, however, are beyond the mass range of conventional mass spectrometers and can not be characterized directly. Pyrolytic treatment of the biological agent prior to mass analysis yields a characteristic spectrum over a limited mass range[1-4]. This signature can then be correlated to the specific type of bioagent. Current pyrolytic MS approaches employ laser, heated filament, or Curie point pyrolysis. These approaches rely on consistent sample distribution on thin filaments or surfaces to achieve reproducible results. These specific sample requirements necessitate the use of sophisticated sampling devices that must operate in a variety of climatic and atmospheric conditions. The sampling times required to accumulate sufficient material for analysis results in delayed agent detection.

Recently, a radiative pyrolysis device based on infrared emission through quartz sampling chambers has been integrated with a mass spectrometer as a biological sample processing unit (Figure 1). The radiative nature of the process allows the sample to be pyrolysed directly. The

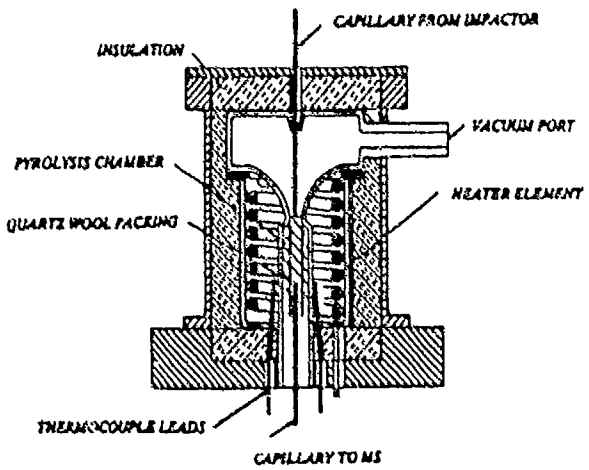

Figure 1. CB Mass Spectrometer Cell

quartz offers an unreactive pyrolysis surface that is transparent in the infrared region. Results using bee pollen, brewer's yeast and selected bacteria demonstrated reproducible and visually differentiable spectra. As an extension of this technology, the device has been adapted for interface with an aerosol sampler to form a compact detection system with real-time aerosol characterization capability.

EXPERIMENTAL METHODS

A review of available sampling technologies suggested the use of virtual impaction for dynamic acquisition and particle enrichment of the aerosol[5]. Direct filtration and jet separation were also considered as alternative approaches to sample acquisition. However, the time required to accumulate sufficient sample for analysis by the direct filtration method precludes application in a real-time detection system. Jet separation, in which the aerosol is selectively sampled through a very high-pressure differential, is not easily adaptable to the region of atmospheric pressure associated with current ion trap mass spectrometers. Jet separation could be useful, however, in applications employing conventional mass filters equipped with large vacuum pumping systems.

A revised pyrolyser was designed based on commercially available components (Figure 2). The new device was constructed with provisions for batch sample introduction, interface to an aerosol sampling device, or direct sampling of airborne biomaterials within the pyrolyser volume. A programmable temperature controller is used for either isothermal or temperature-ramped heating and is programmed through the serial communications adapter of the data system of the mass analyzer. A section of quartz tubing is used to construct the pyrolysis cell. Quartz wool is placed within the cell and acts as the pyrolysis surface for batch samples, or as a filter when the device is interfaced with an aerosol sampler. The cell is wound with nichrome wire and mounted within a larger quartz tube. A four-way tee (Crawford Fitting Company, Solon, Ohio) is used to connect the unit to the capillary inlet of the gas chromatograph or mass spectrometer. Glass-filled teflon or polyimide ferrules must be used to avoid damage to the quartz tubes. The heater and thermocouple leads are passed through the connector with a feed through designed for such purposes, and a small vacuum pump is connected to the tee. The unit can be placed within the oven of a gas chromatograph or insulated for stand-alone applications. A three-way tee on the opposite end can be used as an inlet for helium, as an interface to the capillary output line of an aerosol sampler, or deleted for oxidative pyrolysis.

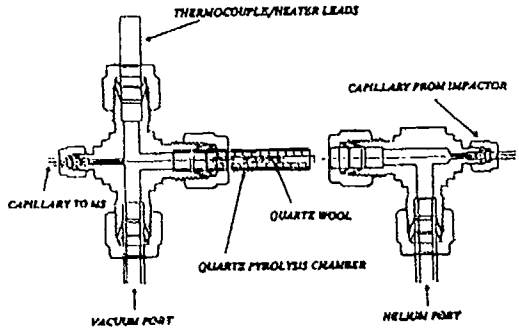

Figure 2. Revised Pyrolysis Device

The pyrolyser was interfaced to the three-stage virtual impactor from the CB Mass Spectrometer breadboard model (Bruker Franzen Analytik, GmbH, Bremen, Germany) to demonstrate feasibility. The impactor has an effective particle size range of 2-11 μ, an inlet air flow of 10 L/sec, and an outlet flow of 1 mL/sec. Foreground samples were acquired for periods between 20 and 120 secs, followed by temperature-programmed pyrolysis. Background samples were also acquired over periods of 2 to 8 hrs. Repeated operation of the pyrolyser, however, resulted in an increasing background signal. The background signal intensified after each analysis until it effectively masked the signature of the sample. This background signal was attributed to the presence of incompletely pyrolysed contaminants from earlier analyses. Also in these tests, pyrolysis occurs in an oxidizing atmosphere and the nature of the products differs substantially from the products observed from pyrolysis in an inert atmosphere. The oxidative degradation products

were characterized by lower molecular weights and therefore contained less information related to their biochemical origin.

RESULTS

The run-to-run reproducibility of the method was high however, day-to-day reproducibility was poor. This variance might be attributed to the effects of humidity on the pyrolytic process. The analyses were limited to comparisons of reproducibility no further effort was made to interpret the data.

The revised pyrolyser cell can also be used for sample acquisition when connected to a small vacuum pump. A prefilter would be used to limit the size of the particulates collected during acquisition. Collection times would range between 2 to 24 hrs without the benefit of particulate concentration.

To overcome the problems associated with the revised pyrolyser, a disposable pyrolyser cell was constructed (Figure 3). In this design, a new pyrocell is used for each analysis. The pyrocell is a quartz tube, packed with quartz wool, and wound with heating filament, which terminates on electrical contact bands at either end. Positioning guides from the outlet of the virtual impactor and the inlet to the mass analyzer act as electrodes to close the heating loop. The thermocouple has been eliminated in favor of calibrated heating by controlling the current flow between the electrodes.

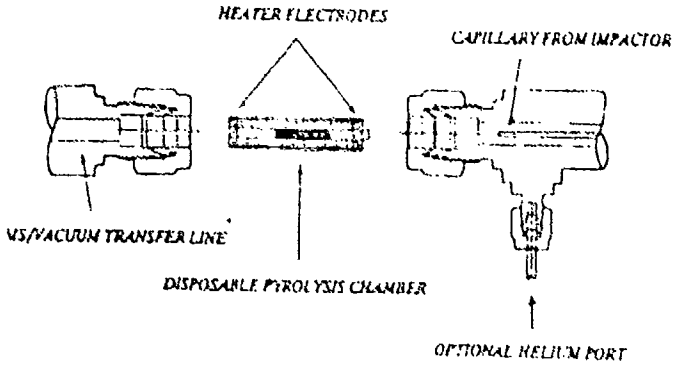

Figure 3. Disposable Pyrolyser

Analyses were performed on batch-introduced samples of inactivated Rift Valley Fever virus vaccine (The Salk Institute) and controls under a helium atmosphere. Isothermal heating resulted in reproducible thermal degradation of the sample with some separation of pyrolysates (Figure 4). It was anticipated that the difference spectra (sample/control) would represent the reconstructed signature of the virus. However, only small differences were observed between the normal and vaccine analyses. In the unlikely event of aerial dissemination of viral agents, it is anticipated that the signal from the dispersion medium would mask the signal from the infectious agent. These results suggest that direct identification of viral agents by pyrolysis mass spectrometry may not be possible due to the low signal-to-noise (background) ratio.

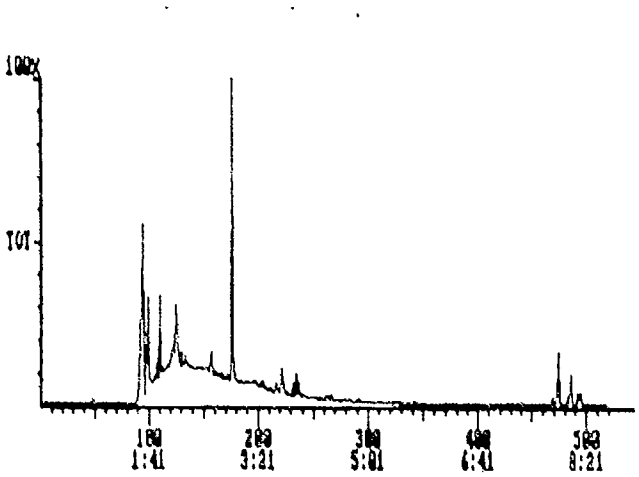

Figure 4. Intensity vs. Time Chromatogram of Rift Valley Fever Pyrolysate

CONCLUSION

This project has demonstrated the feasibility of integrating an aerosol sampler, pyrolysis unit, and mass spectrometer for characterization of airborne biological materials. The system eliminates the need for a separate aerosol sampling device and extends pyrolysis applications to include dynamic aerosol sampling. The technology has been incorporated into the CB mass spectrometer program and has additional applications in the environmental, process, and medical fields.

LITERATURE CITED

1. K.J. Voorhees, Analytical Pyrolysis: Techniques and Applications, Butterworths, London, England, 1985.

2. W.J. Irwin, Analytical Pyrolysis: A Comprehensive Guide , Marcel Dekker, Inc., New York, N.Y. 1982.

3. H.L.C. Meuzelaar, W. Windig, A.M. Harper, S.M. Huff, W.H. McClennan and J.M. Richards, "Pyrolysis Mass Spectrometry of Complex Organic Materials," *Science* Vol. 22, p 268 (1984)

4. J.M. Richards, H.T. Stolk, W.H. McClennan, and H.L.C. Meuzelaar, Development of a Curie Point Pyrolysis Inlet for the Finnigan Ion Trap Detector , 34th Annual Conference on Mass Spectrometry and Allied Topics, Cincinnati, OH, June 13, 1986.

5. Benjamin Liu, and W.M. Farmer, Aerosol Sampling Subsystems, A Panel Report, A. Deepak Publishing, Hampton, Virginia, March 1987.

Dr. Lagna received a B.S. degree in 1977 from Washington and Lee University, Lexington, VA, and an M.S. degree in 1981 from the University of Maryland. In 1985 he earned a Ph.D. in analytical and medicinal chemistry from the University of Maryland. He is a chemist in the Detection Technology Division, Detection Directorate, and the Contracting Officer's Representative on the exploratory development contract for the CB mass spectrometer.

Dr. Robbins graduated in 1974 with a B.S. degree, majoring in mathematics, chemistry, and physics, from Dallas Baptist College, Dallas, TX. In 1978, he received an M.S. degree in physical chemistry from Baylor University, Waco, TX, and in 1983 a Ph.D. degree in radiation chemistry from Texas Woman's University, Denton, TX. He is a chemist working in the area of mass spectrometric detection of CB agents with the Detection Technology Division, Detection Directorate, CRDEC.

Susan F. Hallowell, CRDEC, and Garry A. Rechnitz, University of Delaware

An Enzyme Amplified Receptor Based Assay (ERA): New Approaches for Drug and Toxin Detection

A new assay is described based upon recognition of drugs or toxins by receptors. This assay is unique by virtue of the combination of molecular recognition by a receptor moiety and enzyme amplification of this binding event. A brief theoretical basis of this procedure is given and illustrated with the acetylcholine receptor system. This technique is demonstrated for three drugs (PCP, chlorpromazine, and imipramine) and one toxin (snake venom from *Bungarus multicintus*).

INTRODUCTION

The detection of chemicals and toxins in combat, in the environment, or in body fluids has required analytical procedures based upon some knowledge of the identity of the species to be detected. A detection strategy based upon the pharmacological effect of the drugs, toxins, or viruses resulting from the molecular recognition of these agents by the physiological targets known generically as receptors would provide a vastly superior approach for the detection of these compounds.

Receptors are macromolecular binding proteins that are vital for cellular function and can recognize and respond to agents at extremely low concentrations. Since threat potential and pharmacologic potency are directly correlatable to receptor affinity, receptors are by nature extremely efficient detectors. Radioreceptor assay (RRA) exploits this phenomenon and has been routinely utilized by pharmacologists to determine pharmacological potency of compounds. Although the use of antibody/antigen and biocatalyst-based biosensor systems has emerged in the last 15 years, the use of isolated receptors as the molecular recognition element in a detector system has only lately been proposed.[1] This concept appears to be very viable. Valdes et al. have recently demonstrated an acetylcholine receptor-based biosensor.[2] Using a hydraulic lift, a capacitive sensor was slowly withdrawn from a solution containing phospholipids to form a monolayer. The sensor was then immersed in another trough containing phospholipid vesicles enriched in acetylcholine receptor protein, such that a bilayer impregnated with receptors layered on the interdigitated surface of the capactive sensor was formed. The receptor-based capacitive biosensor showed the response of the acetylcholine receptor to the binding of acetylcholine and the dramatic modulation of this binding event by the presence of toxins that are receptor antagonists. This system has the unique characteristic of pharmacological recognition of toxins at the level of toxicity, unlike immunogenic systems.

Many successful bioassays and biosensor systems have been developed that have employed antibodies, antigens, isolated enzyme, enzyme systems, microorganisms, and plant and animal tissue as the recognition element. These have been demonstrated in conjunction with a variety of transducers that provide the signal-generating element for biosensors, including electrochemical sensors (potentiometric, amperometric or conductimetric), optical sensors (fiber optics, surfacer plasmon resonance, total internal reflection fluorescence), field effect transistors, thermistors, and piezoelectric

crystals.[3,4,5] In theory, many of these transduction systems could be used in conjunction with molecular recognition by a receptor protein, thus providing us with a variety of strategies by which transduction of the receptor-toxin binding phenomenon could be measured. Indeed, researchers are beginning to explore these strategies for the fabrication of receptor-based sensors. A new type of acetylcholine sensor was recently described using an Ion Sensitive Field Effect transistor (ISFET) with an acetylcholine receptor.[6]

The focus of our research was to develop a receptor-based assay, preferably a kit, as a screen for drugs and toxins that was rugged and would yield analytical results at levels of pharmacological toxicity that could be obtained in a minimally equipped laboratory. A receptor-based assay that would also be suitable for transition to a biosensor configuration for potential battlefield applications was desirable. One technique that looked like it might be ideal was an enzyme amplification scheme. Using antibody recognition, the Enzyme Multiplied Immunoassay Technique (EMIT), along with the Enzyme Linked Immunosorbent Technique (ELISA), has been widely commercialized for screening urine or plasma for prescribed drugs or illicit substances of abuse. These immunoassays are used mainly as diagnostic tools for large-scale screening of many specimens at reasonable cost and with minimum training of personnel. The general approach in these techniques required the addition of complementary antibodies that will selectively bind the drug of interest depending on its equilibrium affinity constants. The elements in an EMIT assay are the compound to be measured, enzyme-labeled molecules of the compound, a specific antibody that binds the compound, and a specific enzyme chromogenic substance that forms color when converted by the enzyme conjugate. A key feature of this assay is that one of the reagents, the enzyme-labeled ligand, catalytically amplifies the antibody-antigen binding reaction by a factor related to the turnover number of the enzyme, such that relatively insensitive detectors (spectrophotometers or colorimeters) can be used to monitor nanomolar quantities of the analyte. We propose a new technique, Enzyme-Amplified Receptor Assay (ERA), which uses enzyme amplification in conjunction with receptor recognition for drugs or toxins.[7] We used the acetylcholine receptor system as our model system. One initial concern was whether an enzyme-labeled ligand could physically bind to the receptor site. The enzyme-labeled ligand is a large molecule with a molecular weight exceeding 100,000. This protein is required to bind to the ionic channel of the acetylcholine receptor, which is hypothesized to be located in the pore structure of the activated receptor. It was unknown whether steric hindrance would excluded the desired binding phenomena or whether a commercially available enzyme-labeled ligand made for antibody recognition would have the appropriate molecular conformation for receptor recognition. In a preliminary study, we were able to describe the first successful demonstration of receptor recognition in conjunction with enzyme amplification.[8] Our primary objective this year was to show the analytical utility of this approach by examining the theoretical basis for sensitivity and selectivity of the assay and demonstrating an assay for some compounds of interest for a system that had been formally optimized for performance, again using the acetylcholine receptor as a model system.

The acetylcholine (nicotinic) receptor is the best characterized neuroreceptor and was the one to be identified as a molecular entity that could be isolated, purified, and reconstituted into artificial membrane systems with quantitative retention of physiological properties. Generally speaking, researchers refer to two different sites on the receptor protein. The receptor-active site binds the chemical messenger acetylcholine, or other agonist or antagonist compounds, in a voltage-independent manner. The "allosteric" or "ionic channel" site bind several drugs and toxins whose action is voltage independent.[9,10] Examples of radiolabeled probes that have been used to identify the active site are acetylcholine,[11] alpha-bungarotoxin,[12] and d-tubocurarine.[13] Those used to identify the channel sites are perhydrohistrionicotoxin,[14] PCP,[15] trimethisoquin,[16] meproadiphen,[13] and imipramine.[17] The binding of these compounds

to the allosteric channel-binding site is affected by the presence of agonist compounds due to favorable ligand-induced conformational changes caused by the latter. This intramolecular communication phenomenon lead us to believe that we could use either an enzyme labeled with a channel compound to detect the presence of drugs or toxins to this site and the acetylcholine site, or an enzyme labeled with a drug or toxin that targets the acetylcholine site and monitors both sites. We chose to use an enzyme labeled with a compound that targets the allosteric channel site, since there were two suitable candidates commercially available. However, the chemical conjugation procedure of binding a drug or toxin is relatively straight forward and can readily be accomplished in an ordinary laboratory. Therefore, within certain constraints of the experiment, the potential exists to develop any enzyme-toxin/drug conjugate that can be tailored to any receptor/transducer system. For instance, a toxin known to bind to a sodium channel could be conjugated to an enzyme known to produce ammonia, whose activity could then be monitored with an ammonia electrode.

In our current work, we chose to study drugs with high affinities for the channel site: PCP, a potent hallucinogenic substance that is an extremely popular illicit drug with the street name "angel dust;" chlorpromazine, a therapeutic antipsychotic agent; and imipramine, a tricyclic antidepressant. These compounds all possess affinities for the channel site above 10^6/M. We also tested crude snake venom from *Bungarus multicintus*, which targets the acetylcholine site on the receptor as the pharmacological site of toxicity.

Our program this year was a two-phase effort. Phase I was an optimization study. We did several computer simulations of response surfaces by solving the equilibrium equations while varying the concentrations of the reagents (enzyme, ligand, receptor) and the relevant affinity constants. (Ka for the analyte and Ka* for the enzyme-labeled ligand.) This provided the basic guidance for the general case of any receptor-ligand system and aided the experimental design of our model system. We then optimized our model system with respect to parameters that would be unique for a chosen receptor-enzyme-ligand system. This included parameters such as ionic strength and buffer media, receptor concentration, enzyme concentration, incubation time, concentration of activator compound (carbamylcholine), and the choice of enzyme-labeled ligand. Phase II was the demonstration of the analytical utility of the ERA procedure, by the measurement of drugs and toxic compounds, and the establishment of the accuracy and precision of the method.

METHODS

Preparation of Synthetic Data

Theoretical response curves were prepared using a VAX with the program written in Fortran. Using the appropriate equilibrium expressions, parameters were varied to determine the concentrations of reagents that would yield the best responses. This included the concentration of the total amount of enzyme -labeled ligand (At*), the total amount of receptor (Rt), the total amount of analyte (At), the affinity constant of the ligand used to labeled the enzyme (Ka*) and the affinity constant of the target analyte. The optimal response regions are a function of the ratio of bound enzyme-labeled ligand to the total amount of enzyme-labeled ligand (Af*/A*t). This ratio is what is effectively observed experimentally. Two sets of data were generated. One set determined the conditions of optimization of the direct binding of enzyme-labeled ligand to receptor, while the other determined the conditions of optimization for the response curve in the presence of analyte. The later data indicated how the dynamic range of the assay could be modulated by varying the relevant experimental parameters. Synthetic data was also collected that indicated the effects of varying only one parameter in a given experiment (such as receptor concentration in the presence of a fixed quantity of enzyme.) This data was compared to experimentally derived results.

Reagents

Imipramine (IMP), chlorpromazine (CHL), snake venom (SV), nicotinamide adenine dinucleotide (NAD), glucose 6-phosphate (G6P), glucose-6-phosphate dehydrogenase (G6PD, *L.*

mesenteroides), and snake venom from *Bungarus multicinctus* were all purchased from Sigma and used without further purification. The phencyclidine (PCP) was obtained from the Biotechnology Division. The glucose-6-phosphate dehydrogenase labeled with PCP or DES were both purchased from Syva Co. (Palo Alto, CA) as a part of EMIT kits and were reconstituted with water and allowed to equilibrate at room temperature (20 to 25 °C) for at least 1 hr prior to use. No information was available on the enzyme activity of the DES or PCP concentration of this conjugate. (Under assay conditions comparable to unconjugated enzyme, the G6PD-DES was estimated to be about 1.2 units/mL, while the G6PD-PCP was estimated to be about 1 unit/mL.)

Preparation of Acetylcholine Receptor

Torpedo californica was purchased from Pacific Biomarine (Inglewood, CA) and *Torpedo nobiliana* was purchased from Biofish (Boston MA); it was stored at -70 °C. The preparation of acetylcholine receptor was performed at low temperature (0- 4 ° C). Torpedo (20 g) was first chopped, then homogenized, in 40 mL of Torpedo buffer consisting of 154 mM NaCl, 50mM Tris, 5 mM of Na_2HPO_4, and 1mM EDTA (all from Fisher Scientific) at pH 7.4 for 1 min. The homogenate was allowed to stand for 2 min and was again homogenized for 1 min. The mixture was centrifuged at 2,500 rpm for 10 min, and supernatant was filtered in two layers of cheesecloth. The remaining pellet was again homogenized, centrifuged, and filtered as described above. The combined filtered supernatant was centrifuged at 10,000 rpm for 1 hr at 4 °C. After separating the filtrate, the final pellet was suspended in 4 mL of Tris buffer consisting of 154 mM NaCl, 50mM Tris, and 1 mM EDTA adjusted to pH 7.4 at an average protein concentration of 6-10 mg/mL. This procedure yields receptors prepared as vesicles. The acetylcholine receptors were assayed with respect to total protein concentration by the method of Bradford.[18]

Optimization Study

Various experiments were conducted in which the concentration of one parameter was varied, while the others remained fixed. The parameters examined included the receptor concentration, the enzyme-ligand concentration, the concentration of carbamylcholine, or the incubation time. The basic procedure was to introduce a fixed volume of each species with the concentration of the reagent under consideration varied over a range that would produce a significant effect. Typical volumes of reagents were 8 µL of carbamylcholine, 150 µL of receptor protein, 15 µL of G6PD-ligand, and 7 µL of buffer. The pH was usually at 7.4. All the reagents were placed in a 1.5 mL-microcentrifuge tube.

CALIBRATION CURVES BY ERA

Standard solutions of imipramine, chlorpromazine, and PCP were prepared using Torpedo buffer without Na_2HPO_4. Concentrations typically ranged from 0.2 µM to 10 µM, that resulted in final concentrations of analytes in the reaction vials of about 4 to 400 nM. The snake venom standard was prepared in methanol and was blown to dryness in the reaction vial prior to use. Buffer (8 µL) was then introduced to resuspend the toxin before the addition of the other reagents. A 7 µL quantity of 1 mM carbamylcholine was first added to vials containing 150 µL of receptor protein or Torpedo buffer (as blank) and were allowed to stand for 2 min. Standard solutions of analytes (8 µL) were then introduced, and the mixtures were mixed thoroughly. After allowing these mixtures containing the drug and receptor to preincubate for about 5 min (60 min for snake venom), 15 µL aliquots of G6PD-DES enzyme were added. All vials were then incubated for a minimum of 30 min.

Analysis of Samples

After an incubation period, the vials were centrifuged at 8,000 rpm for 10 min at 4 °C. Then, 50 µL of the supernatant from each vial were added to 750 µL of substrate containing 1mM G6P

and NAD in a quartz cuvette, and this was immediately followed by measurement of enzyme activity.

Instruments

Centrifugation was carried out with an IET-HT Centrifuge at 4 °C. Acetylcholine receptors were homogenized using a Polytron (Brinkman Instruments) setting of 5 (50% power). Reactions were carried out in 1.5-mL microcentrifuge tubes at room temperature (22 °C). Enzymatic activity of the G6PD ligand conjugate was monitored in quartz cuvettes with the spectrophotometer at 340 nM. Measurements were made with a Hitachi model 100-60 spectrophotometer. Responses were followed on a Heath strip chart recorder and inital rates calculated manually from recorder tracings.

Preparation of Data

In most experiments, the data was normalized to indicate the percentage of initial enzyme activity remaining (or the percentage inhibition of enzyme activity) as a function of the parameter being studied. This treatment seemed to factor out the small fluctuations in the receptor activity from preparation to preparation and allowed the comparison of run-to-run data.

RESULTS

Computer Modeling of the ERA

Guidelines were established for the use of the ERA procedure for the general case for any receptor-ligand system. Various contour maps were prepared indicating regions of inhibition of enzyme activity, varying the receptor, enzyme-labeled concentration, with a given affinity constant. From maps such as these, one-dimensional information (varying only one parameter, e.g. either the concentration of enzyme or the concentration of receptor) can be derived about the theoretical shape of a binding curve. From contour maps it was also determined that the enzym- labeled ligand (the signal-creating species) should contain a ligand with a high affinity (large Ka*) for the receptor. Practical considerations in this experiment mandate that the absolute lowest concentration of the enzyme that can be assayed using the analytical system should be determined before proceeding with experimental work. We also found that the receptor and enzyme-labeled ligand concentrations should be in a range in which significant inhibition of the original enzyme activity can be measured. Generally speaking, this condition is achieved using a high receptor concentration [Rt] and a low enzyme-ligand concentration [A*t].

The final consideration in optimization strategy is the range of the analytical curve. This is modulated by the ratio of the total receptor concentration to the enzyme-labeled ligand concentraion [Rt]/[A*t]. The ratio of [Rt]/[A*t] appears optimal at about 10. It was interesting to note that the anaytical range of the analyte of interest [A] is established based upon the Ka of the ligand to the receptor system. For instance, compounds with a high affinity for the receptor protein have analytical ranges at much lower concentrations than those with low affinities. This provides a theoretical basis for the notion that receptor recognition will be at the level of the pharmacological effectiveness.

Optimization of the Acetylcholine System

The general scheme for the ERA technique as it applies here is:

$$\text{AChR} + \text{Analyte} \rightleftharpoons \text{AChR:Analyte} \quad [1]$$

$$\text{AChR} + \text{Analyte} + \text{G6PD-ligand} \rightleftharpoons \text{AChR:Analyte} + \text{AchR:G6PD-ligand} \quad [2]$$

Equation 3 shows the overall reactions involved in the analytical method.

$$\text{G6P} + \text{NAD}^+ + \text{analyte} + \text{AchR} \longrightarrow \text{6-phosphoglucono-d-lactone} + \text{NADH} + \text{H}^+ + \text{AchR:analyte} + \text{G6PD-ligand:AchR (inactive)} + \text{G6PD-ligand (active)} \quad [3]$$

As previous determined, the binding of a specific drug or toxin is mainly dependent on the affinity equilibria in the first reaction. The assay employs commercially available G6PD, which has a ligand attached to it known to bind to the channel site. Since the ligand has been covalently attached in close proximity to the active site of catalytic action, the binding of the ligand to the receptor will result in the inactivation of the enzyme, as shown in equation 3, while the unbound enzyme-labeled ligand remains active and is still available to convert substrate to product. In the presence of the enzyme-labeled ligand and free analyte, a competition for binding sites between the free drug and the enzyme labeled ligand results in a constant product ratio. With no analyte, the enzyme marker's activity is inhibited by its binding to the receptor protein. (The enzyme is "turned off" quantitatively as determined by the protein concentration.) The activity of the enzyme increases analytically as the analyte (drug or toxin) competes for the same binding site on the receptor protein as the marker enzyme. Therefore, the binding event of the analyte to the receptor (typically at the nanomolar level) is catalytically amplified by a factor of about 100,000, the turnover number of the enzyme. Using constant amounts of AchR and G6PD-ligand, quantitation of free drug can then be performed in the presence of the substrate using a calibration curve. The activity of the enzyme is measured by monitoring the conversion of substrate (NAD) to product ($NADH^+$) using a conventional detector, in this case, an ordinary spectrophotometer set at 340 nm. The rate of formation of NADH is proportional to the amount of enzyme (or to the free drug) present.

Choice of Enyzme-Labeled Ligand

Two enzyme-labeled ligands were commerically available that were suitable candidates. They met the criterion established by the modeling experiment that required affinity constants of at least 10^6/M . Both were the G6PD enzyme; one was labeled with phencyclidine (with an Ka* of about .1 to 3.3 X 10^7/M) and the other was labeled with desipramine (with a Ka* of about .1 to 1.25 X 10^7/M.) Although much of the initial work was done with the G6PD-PCP conjugate, a comparison indicated that the G6PD-DES showed greater inhibition characteristics when the two enzyme-conjugates were used at the same concentration with respect to enzymatic activity. It is unclear why this is true, and the manufacturer could not release information pertaining to the ratio of ligand to enzyme, or details of the conjugation procedure. But we believe that this effect was due to some aspect of the conjugating procedure that produced this difference in receptor recognition, or enzyme activity modulation, caused by receptor-enzyme binding. The G6PD-DES was used in all subsequent studies.

Effect of Varying Receptor Concentration

The theoretical calculations indicated that conditions of optimal binding of enzyme-labeled ligand to receptor would occur with higher concentrations of receptor protein. Figure 1A shows a theoretical binding curve for a receptor-ligand-labeled enzyme system with an affinity constant of 4 X 10^6. The enzyme-ligand concentration has been fixed at 1.6 X 10^{-7}M, while the receptor concentration is varied from 10^{-9} to 10^{-6}M. In practice, when this is done, the

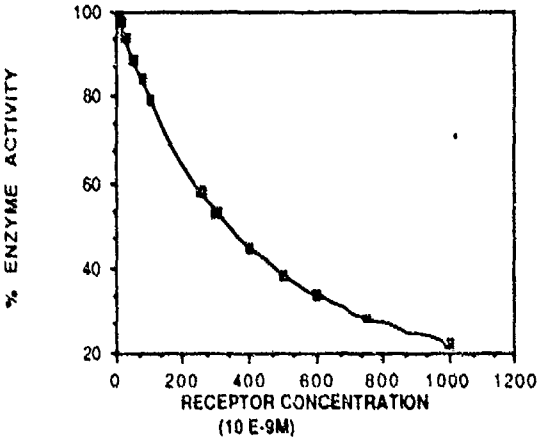

Figure 1A. A Theoretical Binding Curve for a Receptor-Ligand-Labeled Enzyme System with an Affinity Constant of 4 X 10^6. Receptor Concentration is Varied from 10^{-9} to 3 X 10^{-6}M and the Enzyme Concentration is Fixed at 1.6 X 10^{-7}M.

receptor is characterized in terms of protein mass rather than molar concentration of binding sites. (Receptor concentration was varied from 0 to approximately 7.8 mg/mL of protein, with the enzyme activity fixed at 0.10 units/mL.) The predicted response curve was observed as shown in Figure 1B.

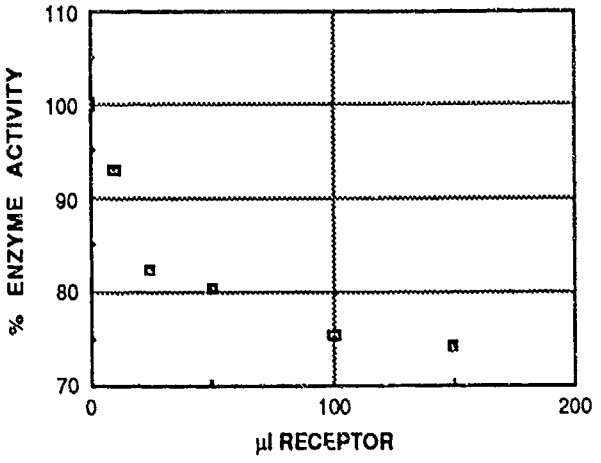

Figure 1B. Experimental Data Collected on the Effects of Varying Receptor Concentration With a Fixed Amount of Enzyme Labeled Ligand

Effect of Varying Enzyme Concentration

The theoretical calculations indicated that conditions of optimal binding of enzyme-labeled ligand to receptor would occur with lower concentrations of enzyme-labeled ligand, with the absolute lower limit determined by the ability of the analytical method to monitor low concentrations of enzyme. A computer-generated binding curve, in which the receptor concentration was fixed $2.5X10^{-7}$ M and the enzyme concentration was varied from 10^{-9} to $3X10^{-6}$ M is shown in Figure 2A. An experiment was performed in which the receptor concentration was fixed at about 7mg/mL of protein, and the enzyme concentration was varied from .02 units/mL to .5 units/mL. The results are shown in Figure 2B. The response curve closely followed that predicted by the modeling study.

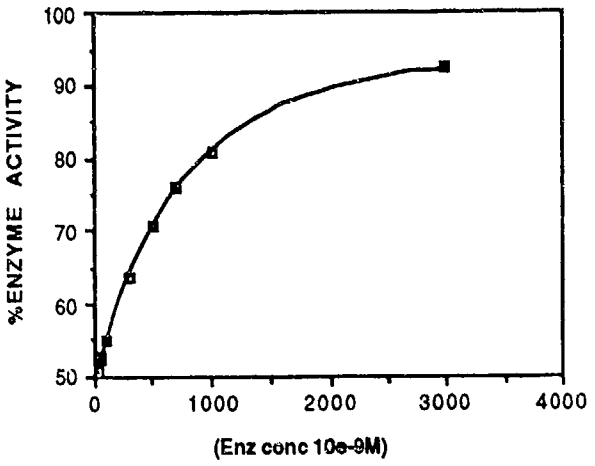

Figure 2A. A Computer-Generated Binding Curve. The receptor concentration was fixed at 2.5×10^{-7}M and the enzyme concentration was varied from 10^{-9} to 3×10^{-6}M.

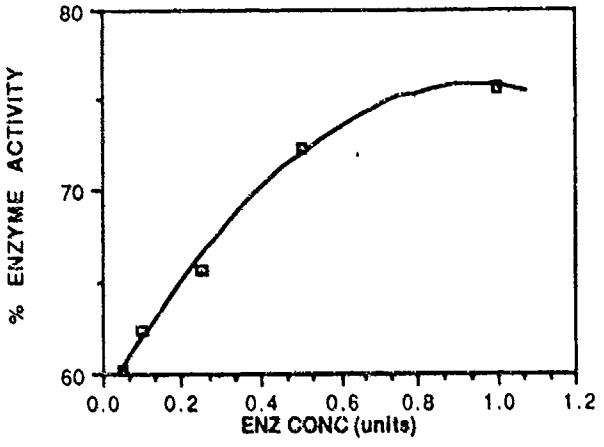

Figure 2B. Effect of Varying Enzyme Concentration. The receptor concentration was fixed at about 7 mg/mL of protein, and the enzyme concentration was varied from 0.02 units/mL to 0.5 units/mL.

Effect of Activator Compound

The existence of three distinct states of the acetycholine receptor as related to the concentration of activator compound and exposure time with the receptor has been

postulated.[19] These states are nominally described as resting (inactivated), activated, and desensitized. Channel-binding compounds bind best to receptors that are activated; the presence of activator compound appears to increase the affinity of the channel-binding compound to the site. The relationship between observed binding of G6PD-PCP to the acetylcholine receptors and varying quantities of activator compound was determined using carbamylcholine as the physiological activator. An experiment was conducted to determine the optimum concentration range of carbamylcholine necessary to fully activate the binding of the channel compounds without desensitizing the tissue. The results are shown in Figure 3.

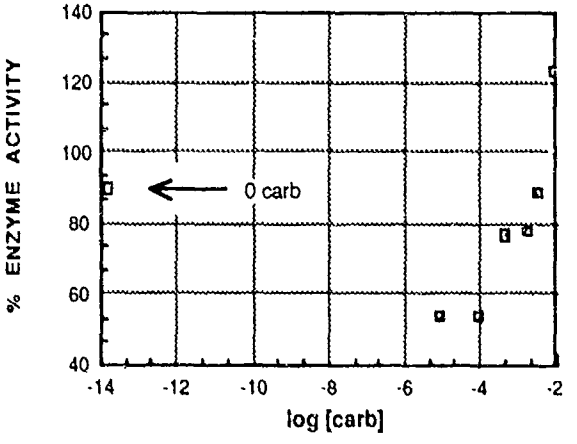

Figure 3. Effect of Activator Compound on Binding of Receptor to G6PD-PCP. Graph displays apparent activity of enzyme in the presence of increasing amounts of carbamylcholine.

In the absence of carbamylcholine, some binding of G6PD-PCP to the receptor occurred as evidenced by the 10% reduction in enzyme activity. Concentrations of activator up to 0.1mM seemed to cause optimum binding, since the activity of the enzyme appeared to decrease to the 50% level. However, above this level, the binding reaction was hindered, presumably due to receptor desensitization. At 200 mM of carbamylcholine, the enzyme activity appeared to be 20% higher than the control run with no receptor protein, probably due to the fact that the receptor protein itself is water insoluble and occupies some percentage of the total volume in the microcentrifuge tubes. This effectively concentrated the enzyme into a smaller volume. This study was repeated with G6PD-DES and results were in close agreement with the G6PD-PCP study. Although this dose-dependent behavior of torpedo membrane toward the receptor agonist has been studied extensively, it is advantageous to use such response as a means of confirming the receptor activity, since this is a unique characteristic of this receptor system.

Effect of Buffer Type

The effect of buffer type on assay performance was examined with three different types. Receptor function is known to be highly dependent on the ionic strength and media of the immediate environment. Also, it was known that the enzyme activity could be affected by buffer type. The torpedo buffer and a 50 mM tris buffer with 154 mM NaCl and 1 mM EDTA (pH7.4) were prepared as described earlier. A tris buffer was prepared from .055 M Tris-HCl at (pH 8.0 with 0.05% sodium azide stabilizer.) Receptors were prepared as usual and resuspended into one of the three buffers. Using blanks prepared without receptors, the amount of inhibition of enzyme activity was measured. The standard deviation of each experiment was determined from four measurements, and the relative standard deviation was calculated. The results are shown in Figure 4. The torpedo buffer without phosphate presented the most favorable conditions for receptor-ligand binding, as indicated by the higher percentage of enzyme inhibition due to enzyme-ligand-receptor binding.

Effect of Incubation Time

Antigen-antibody reactions can require incubation times of 30 min or more for full equilibration. Therefore, it seemed plausible that the receptor-drug interaction might require some time for full equilibration of the reaction. An experiment was conducted in which several samples were prepared under the same conditions

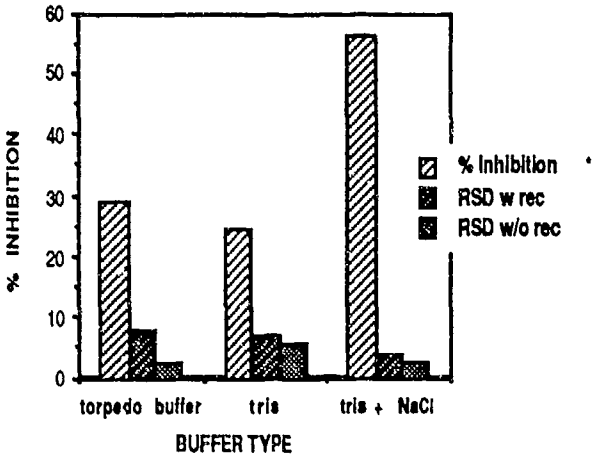

Figure 4. Effect of Buffer Conposition of Apparent Binding of Enzyme-Labeled Ligand to Receptor Protein as Indicated by Percent Enzyme Inhibition

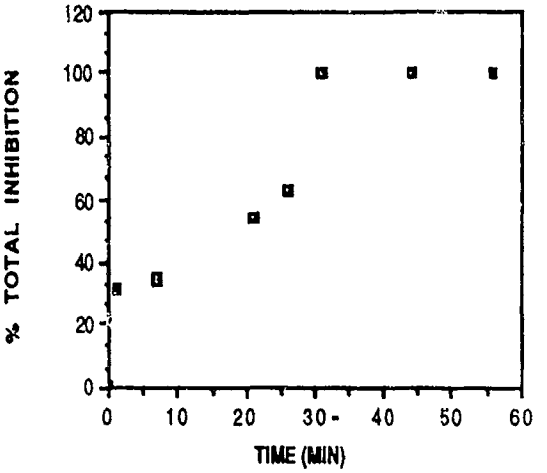

Figure 5. Dependence of Enzyme Activity on Incubation Time

and allowed to incubate for various amounts of time prior to centrifugation and assay. One modification was that centrifugation was performed for 5 min rather than the usual 10-min interval. The total amount of time for incubation was defined as that time elapsed prior to centrifugation. Incubation was completed after 30 min as determined by no further change in the enzymatic activity (Figure 5), and this period was used for all subsequent experiments. It should be noted that the solutions were fairly high in receptor concentration, and constant stirring was not used. It is believed that this incubation time can be reduced if lower concentrations of receptor are used in conjunction with continuous stirring or shaking after introduction of all reagents.

Calibration Curves of Channel-Binding Compounds

Using the optimized reagent concentrations, three channel-binding compounds (PCP, imipramine, and chlorpromazine) with similar affinity constants were measured using the ERA technique. Since ERA and Emit methods are based on competition between free drug and enzyme-labeled drug for binding sites, the measured enzyme activity is proportionally related to concentration of the drug in the sample. A shape of a theoretically derived response curve for an analyte with an affinity of 10^5/M and 10^6/M is shown in Figure 6A. This can be compared to an actual response curve generated for the analyte PCP (Figure 6B). Although we were uncertain as to the actual ratio of total receptor to enzyme-labeled ligand, the actual and predicted curves are very similar.

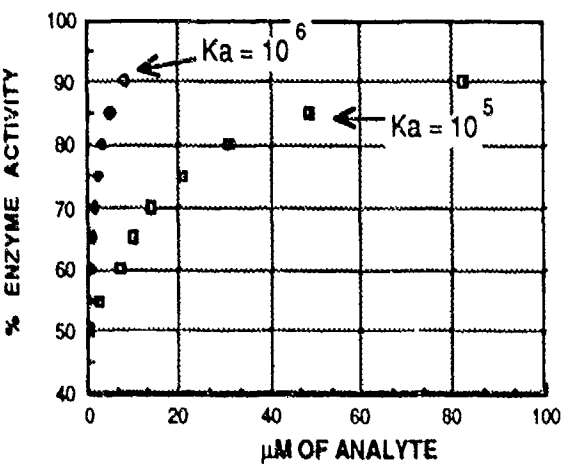

Figure 6A. ERA Theoretically Derived Response Curves for Analytes with Affinities of 10^5/M and 10^6/M. The ratio [Rt]/[R*t] has been fixed at 10.

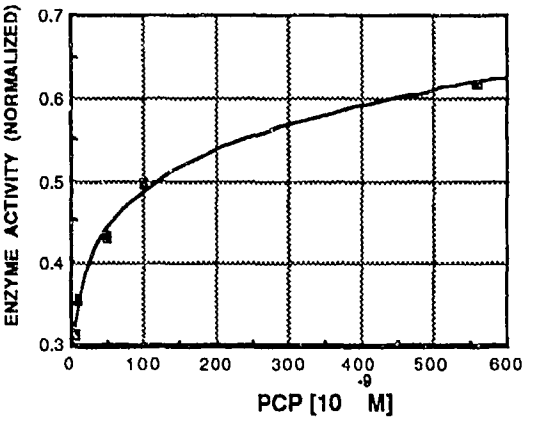

Figure 6B. Response Curve for the Analyte PCP

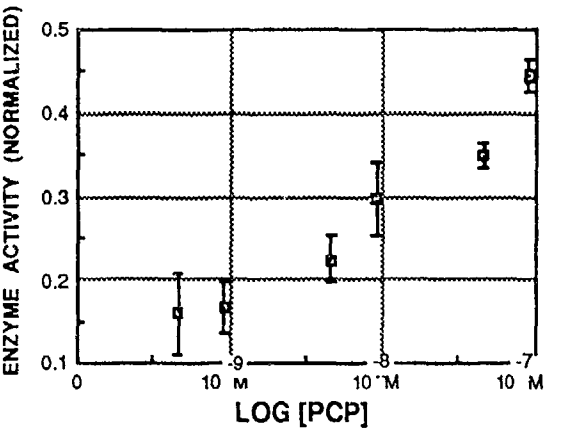

Figure 7. ERA Regression Curve for PCP Concentrations are Log Transformed

To use response curves for quantitation, we found that those prepared showing the regressing normalized enzyme activity against a log transformation of analyte concentration gave suitable correlation coefficients (> .95).

We also compared the performance of the ERA assay to a commercially available immunoassay (EMIT) screen for the analyte PCP. Samples were prepared in a urine matrix and analyzed using the two different methods. EMIT was used exactly as stated in the instructions, except that measurements were taken manually. A standard curve for PCP used in the ERA assay is shown in Figure 7. The precision and accuracy of these two techniques are compared in Table 1. The ERA technique appears to be at least as accurate as the EMIT method, with somewhat better precision.

The response of the other binding compounds, chlorpromazine and imipramine, was very similar to that of PCP with respect to slope and intercept. The imipramine showed somewhat better response characteristics, which might be anticipated since it is structural analog to the ligand used to label the enzyme probe used.

Calibration Curve of Snake Venom

Figure 8 shows a response curve for crude venom from *Bungarus multicintus;* the response to snake venom was linear rather than logarithmic over a narrow concentration range. This plot represents our first work with antagonist compounds, and more work is needed to fully characterize the response. Table 2 summarizes regression curve parameters for some of the drugs and toxins we tested this year.

TABLE 1: COMPARISON OF ERA AND EMIT PCP ASSAY IN URINE MATRIX: PRECISION AND ACCURACY

	ACCURACY		PRECISION	
Target concentration	FOUND CONC(ERA)	FOUND CONC(EMIT)	STANDARD DEVIATION (ERA)	(EMIT)
(nanomolar)				
4.9	5.25	3.88	8.78	6.77
49	41.5	82.6	31.8	174
490	526	374	720	6730
Correlation Coefficient (R)			0.998	0.983

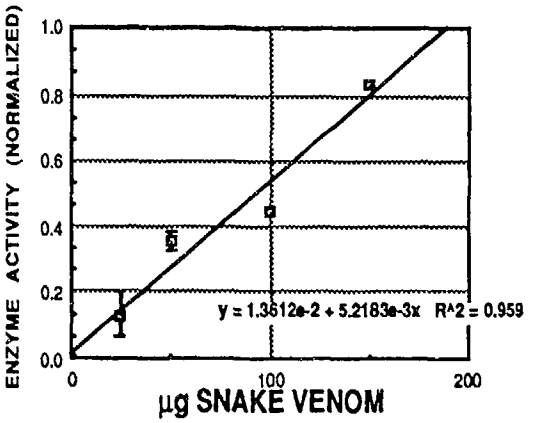

Figure 8. ERA Regression Curve for Crude Venom from *Bungarus multicintus*

DISCUSSION

The data given here represent a demonstration of the feasibility of using enzyme amplification in conjunction with receptor recognition to develop clinical assays for drugs. We still have some unresolved technical issues that must be addressed before this technique can be routinely used. It would be highly desirable to reduce the response times. We believe the long incubation time is induced because of the long equilibration time between receptor and drug due to lack of mixing and high concentrations. If receptor concentrations can be reduced experimentally, a reduction in the minimum 30-min incubation time may follow as a matter of course. It may be that an immobilzation procedure of the receptor onto a plate or film will show the optimum response characteristics. Another concideration is the analytical range of this technique. We may be operating close to the limits of this technique as presently configured, since some of the lots of torpedo fish we received did not display significant activity to be used with our ERA method. Current plans include switching our detection technique to an amperometric detection which is at least one order of magnitude more sensitive that our current colorimetric method. We also need to address the response characteristics of toxins that are acetylcholine antagonist compounds. This work is planned for early next year. Future engneering efforts may yield a variety of ways to physically deploy this assay. It should be technically feasible to engineer it into the development of enzyme-receptor field "tickets" that change color in the presence of toxins, or into microtiter plates for drug and toxin screens.

LITERATURE CITED

1. United States Army Receptor Technical Program Plan,Adjunct to the RDI Master Plan, CRDEC, (**1986**).

2. James, J. Valdes, Joseph G. Wall, Jr. James P. Chambers, and Mohyee E. Eldefrawi, *Johns Hopkins APL Tech Digest*, Vol. 9, p 1, (**1988**).

3. Garry A. Rechnitz, *Chemical & Engineering News*, Vol. 66 (36), (**1988**).

4. A. P. F.Turner, I. Karube, G.S. Wilson, eds., *Biosensors: Fundamental and Applications*, Oxford University Press, Oxford, England, (**1987**).

TABLE 2: ERA REGRESSION CURVE PARAMETERS FOR DRUGS,TOXIN

	PCP	CHLORPROMAZINE	SNAKE VENOM	IMPRAMINE
slope (Normalized activity/Log C)	0.146	0.135	0.0052	0.3005
correlation coefficient (R)	0.989	0.987	0.979	0.988
Intercept	0.184	0.112	0.014	2.62
lowest standard	6e-9 M	4e-9 M	25 µg	4 e-9 M

* Concentrations are not log transformed

5. Garry A. Rechnitz, "Biosensors: An Overview," *Clin. Lab. Anal.*, Vol. 1, pp 308-312 (**1987**).

6. M. Gotoh, E. Tamiya, M. Momoi, Y. Kagawa, I. Karube, "Acetylcholine Sensor based on Ion Sensitivie Field Effect Transistor and Acetylcholine Receptor," *Anal Ltr*, Vol. 20 (6), pp 857-870 (**1987**).

7. S. F. Hallowell and G. A. Rechnitz, UD Patent Application 12-88, Enzyme-Amplified Receptor Assay (ERA), **1988**.

8. S. F. Hallowell, G. A. Rechnitz, "Enzyme-Amplified Receptor Assy (ERA): A Novel Aproach to Drug Detection," *Anal Ltr* Vol. 20 (12), pp 1929-1949 (**1987**).

9. E. X. Albuquereque, M. Adler, C. E. Spivak, and L. Aguayo, *Ann. N.Y. Acad. Sci.* Vol. 358, pp 204-238 (**1980**).

10. M. E. Eldefrawi, A. G. Britten, and A. T. Eldefrawi, "Coupling Between the Nicontinic Acetylcholine Receptor Site and Its Ionic Channel Site. *N. Y. Acad. Sci.* Vol. 358, pp 239-252 (**1980**).

11. M. E. Eldefrawi, A. G. Britten, and A. T. Eldefrawi, *Science* (Wash. D.C.) Vol. 173, p 338 (**1971**).

12. R. Miledi, P. Molinoff, and L.T. Potter, *Nature* (Lond.) Vol. 229, p 554 (**1971**).

13. R. R. Neubig, E. K. Krodel, N. D. Boyd, and J.B. Cohen, *Proc. Natl. Acad. Sci.* U.S.A. Vol. 76, p 690 (**1979**).

14. R.S. Aronstam, A. T. Eldefrawi, I. N. Pessah, J. W. Daly, E. X. Albuquereque, and M. E. Eldefrawi, *J. Biol. Chem.* Vol. 256, p 2842 (**1981**).

15. M.E. Eldefrawi, A.T. Eldefrawi, R.S. Aronstam, M.A. Maleque, J.E. Warnick, and E.X. Albuquereque, *Proc. Natl. Acad. Sci.*, U.S.A. Vol.77, p 7458 (**1980**).

16. R. Oswald,A. Sobel, G. Waksman, B. Roques, and J.P. Changeux. *F.E.B.S. Lett.* Vol. 111, p 29 (**1980**).

17. M. E. Eldefrawi, J. E. Warnick, G.G. Schofield, E. X. Albuquereque, and A. T. Eldefrawi, *Biochem. Pharmacol.* Vol. 30, p 1391 (**1981**).

18. M. Bradford, *Anal. Biochem.* Vol. 72, p 248(**1976**).

19. F. Dreyer, *Br. J. Anaesth*. Vol. 54, p 115 (**1982**).

Susan Fowler Hallowell has been a research chemist in the Analytical Division, Research Directorate for 7 years. She received a B.A. degree from Western Maryland College , Westminster, MD, in 1974. She is completing her Ph.D. in Analytical Chemistry at the University of Delaware, and is a member of the Biosensor Research Laboratory, Department of Chemistry and Biochemistry, under the direction of Garry A. Rechnitz, Unidel Professor of Chemistry. Her research interests center around the development of analytical methods for the quantitative or semiquantitative analysis of agents, drugs, or toxins in biological or environmental samples. She is a member of the American Chemical Society and Sigma Xi.

Garry A. Rechnitz is Unidel Professor of Chemistry and Biotechnology at the University of Delaware. He received a B.S. degree in chemistry from the University of Michigan in 1958 and a Ph.D. degree from the University of Illinois in 1961. He taught chemistry at the University of Pennsylvania from 1961 to 1966 and then at the State University of New York, Buffalo, until he joined the faculty at the University of Delaware in 1977. During a sabbatical leave in 1987 he was visiting professor of pathology at Scripps Clinic and Research Foundation, La Jolla, CA. Rechnitz's research in bioanalytical chemistry and on sensors has resulted in more than 275 publications and has provided research experience for more than 120 graduate and postdoctoral students.

BLANK PAGE

Cynthia A. Ladouceur, CRDEC

Development of a Highly-Sensitive Microcalorimetric Immunoassay and a Thermal Imaging Immunoassay for the Detection of Small or Large Molecular Weight Substances

An infrared imager was used to determine whether or not it is possible to 'visualize' the heat liberated from antigen-antibody binding events. Based on the preliminary experimental results, it appears that this may be a useful tool for the detection of antigen-antibody reactions. This, in turn, could result in the development of a new immunodiagnostic test for the detection of a variety of small and large molecular weight substances in solid samples such as hair and feathers.

INTRODUCTION

Currently, a battery of immunologic assays are available for use in analytical laboratories. All of these assays involve the binding of antigens to specific antibodies. Examples of these assays are the radioimmunoassay, enzyme-linked immunosorbent assay, fluorescent immunoassay, hemagglutination inhibition immunoassay, and free radical assay technique. Since labels such as radioisotopes, enzymes, fluorophores, red blood cells, and stable free radicals are employed in these immunoassays, the limiting factor in determining the sensitivity of the assay is the ability to detect the label.[1,2]

Several studies have shown that heat is a byproduct of the binding of an antigen to a specific antibody, and this heat can be detected with a flow calorimeter.[3-9] The heat liberated within the reaction vessel of the calorimeter flows by conduction from the vessel through a thermopile to a thermostated heat sink. The temperature gradient across the thermopile produces an output voltage (Peltier effect) ...at can be amplified and recorded. Commericial systems are available with limits of detectability of 0.15 microwatts (3.58×10^{-8} cal/sec). The detectability limits on the molar concentration of the substance to be tested for depends upon the reaction kinetics and the enthalpy of reaction. A typical enthalphy of reaction might be 10 K-cal/mole, and this would allow one to detect 3.6×10^{-4} moles/sec of reactant. The concentration detectability limit depends upon the specific rate constant for the reaction.

Thermography (a term derived from 'thermo' meaning heat and 'graphy' meaning the process of recording) can be used to detect and measure variations in heat emitted by different regions on a surface. An infrared imager and associated support equipment can be used to detect these variations in heat and transform them into electronic signals that can be recorded photographically (i.e., on video tape). Simultaneous infrared imaging and thermal analysis in both the 3-5 and 8-12 μm spectral bands can be accomplished with this equipment. Applications for this technoloy include the detection of vehicles (i.e., tanks and aircraft), humans, and animals. In the case of the latter two, car manufacturers are developing infrared imaging systems for night vision (i.e., detecting people or deer in a car's path). Hospital laboratories have used thermography for diagnosing abnormal or disease conditions in human tissues.

This paper reports on the use of thermography or thermal imaging with an infrared imager for the detection of antigen-antibody reactions.

MATERIALS AND METHODS

Initially, a microcalorimeter was to be used to measure the heat produced when a particular antigen combines with a specific antibody. A market survey was conducted to compare calorimeters to determine which one would be suitable for this study and for future, related studies that will enhance the Army's chemical-biological detection capabilities. A list of suitable candidates was narrowed down to the following: (a) Hart Model 7708 DSC (differential scanning calorimeter), (b) Setaram Micro-DSC Batch and Flow Calorimeter, (c) LKB Thermal Activity Monitor, and (d) Perkin-Elmer DSC-7. After a careful review of the specifications and capabilities of each calorimeter and demonstrations of the equipment in actual use, the Hart Model 7708 DSC was selected. As a result of the many delays encountered in its procurement, the microcalorimeter needed for this study was not available.

Instead, an alternate technology for heat detection was employed. A collaborative effort was set up between Dr. Cynthia A. Ladouceur and three employees of the U.S. Army Combat Systems Test Activity (CSTA), Aberdeen Proving Ground, MD. These individuals are Mr. Frank R. Carlen, Ms. Pamela N. Costianes, and Mr. William C. Burch. Several experiments were performed to determine whether or not the Inframetrics Model 210 Infrared Imager could be used for visualizing the heat liberated when an antigen-antibody binding event occurs. Initial experiments utilized commercially-available antigens and antibodies. All reactions were carried out on nitrocellulose membranes since proteins are easily adsorbed to the surface of these membranes. The thermal images were recorded on U-matic videocassettes so that changes in heat resulting from the reaction of antigen with specific antibody could be quantified and interpreted at a later date. Using look-up tables, contrast expansion, pseudocoloring , and a 256 frame-integration technique, still photographs were also taken with Polaroid 339 film. For increased clarity, each photograph was magnified.

RESULTS

Based on the initial findings, it appears that the Inframetrics Model 210 Infrared Imager can be used for the visualization of the heat liberated from antigen-antibody reactions.

Figures 1 and 2 illustrate the thermal image produced at 1 and 4 min, respectively, after an antigen (bovine serum albumin - BSA) was reacted with specific antibody (antiBSA antibody). As can be seen from the look-up tables to the right of the reaction area, this area is becoming progressively warmer as the reaction proceeds. Other photographs, taken at various stages during the antigen-antibody reactions, also illustrate this progressive warming over time.

DISCUSSION

The objective of this study was to develop a highly-sensitive analytical tool for the detection of a wide variety of substances in gas, liquid, and solid samples. Examples of the substances include threat materials, hazardous chemicals, drugs, toxins, infectious organisms, and antibodies directed against these organisms. Examples of the test samples include body fluids; hair; nails; fur; feathers; internal tissues from humans, wild or domestic animals, birds, or insects; and plant tissues.

Although many more experiments need to be done, the initial results show promise that infrared imaging can be used to detect the heat liberated from the reaction of antigen with specific antibody. This, in turn, can be used as the basis of a new immunodiagnostic test that would enable detection of small or large molecular weight substances in liquid and solid samples. The fact that the technique could be utilized for analyzing solid samples is particularly significant since few immunoassays are capable of this. In the future, this technique could be used to detect chemicals and threat agents that have been incorporated within hair, fur, or feathers. Thus, this immunoassay could have a significant impact on the verification of a chemical warfare treaty.

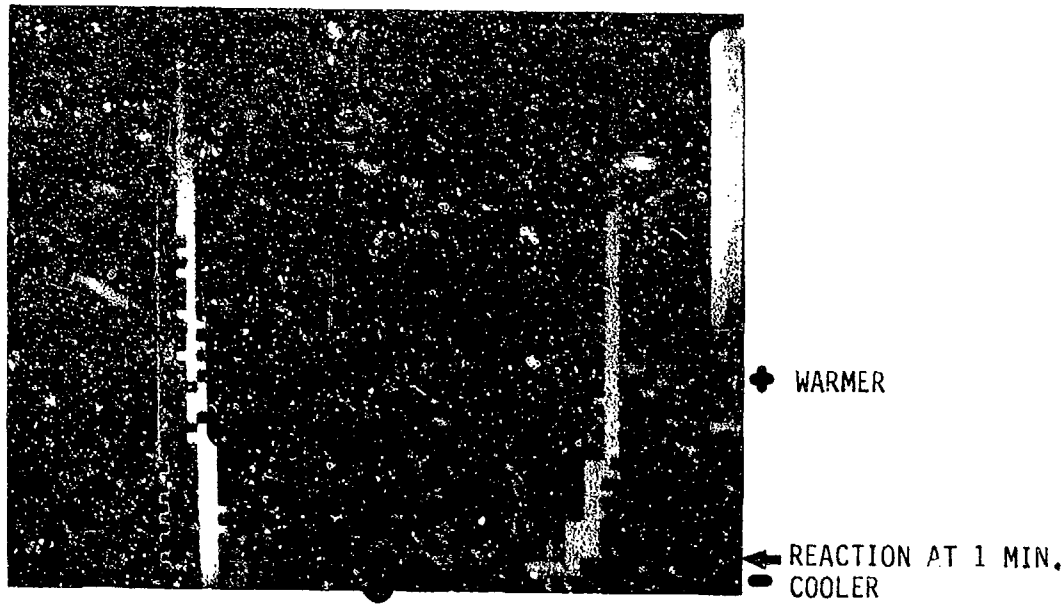

Figure 1. Photograph showing the thermal image produced one minute after an antigen (bovine serum albumin - BSA) was reacted with specific antibody (antiBSA antibody). The reaction area is framed by the large arrows. The look-up tables to the right represent a range of reaction temperatures.

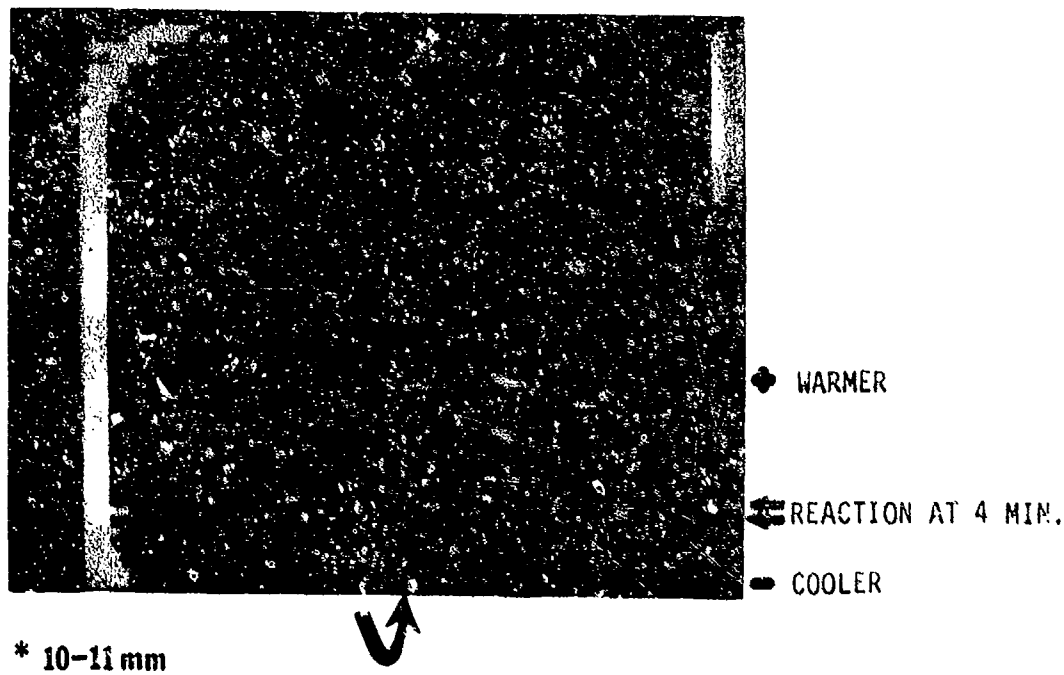

Figure 2. Photograph showing the thermal image produced four minutes after an antigen (bovine serum albumin - BSA) was reacted with specific antibody (antiBSA antibody). The reaction area is framed by the large arrows. The look-up tables to the right represent a range of reaction temperatures.

BLANK PAGE

The use of infrared imaging to 'visualize' the heat liberated from antigen-antibody binding events should also lead to a greater understanding of the variability in the strengths of antigen-antibody bonds. This technique may be useful for differentiating weak antigen-antibody bonds from strong antigen-antibody bonds. Since several immunoassays are based on the fact that different antibodies have low or high affinities for specific antigens, it would be possible to select antibodies that have the appropriate affinity to achieve maximum results from an immunoassay. Thus, the Army could use this technique in order to 'fine tune' their immunologically-based detection systems.

LITERATURE CITED

1. E. Block, "An Overview of Radioimmunoassay Testing and a Look at the Future," *Antibiotics Chemother.* Vol. 26, pp 1-9 (**1979**).

2. W. J. Brattin, and I. Sunshine, "Immunological Assays for Drugs in Biological Samples," *Am. J. Med. Tech.* Vol. 39(6), pp 223-230 (**1973**).

3. B. G. Barisas, J. M. Sturtevant, and S. J. Singer, "Thermodynamics of the Binding of Haptens to Rabbit Anti-2,4-dinitrophenyl Antibodies," *Biochem.* Vol. 10(15), pp 2816-2821 (**1971**).

4. B. G. Barisas, S. J. Singer, and J. M. Sturtevant, "Thermodynamics of the Binding of 2,4-Dinitrophenyl and 2,4,6-Trinitrophenyl Haptens to the Homologous and Heterologous Rabbit Antibodies," *Biochem.* Vol. 11(15), pp 2741-2744 (**1972**).

5. J. F. Halsey and R. L. Biltonen, "The Thermodynamics of Hapten and Antigen Binding by Rabbit Anti-Dinitrophenyl Anitbody," *Biochem.* Vol. 14(4), pp 800-804 (**1975**).

6. J. Sjoquist and I. Wadso, "A Thermochemical Study of the Reaction Between Protein A from *S. aureus* and Fragment Fc from Immunoglobulin G," *FEBS Letters* Vol. 14(4), pp 254-256 (**1971**).

7. C. C. Bigelow, B. R. Smith, and K. J. Dorrington, "Equilibrium and Kinetic Aspects of Subunit Association in Immunoglobulin G," *Biochem.* Vol. 13(22), pp 4602-4608 (**1974**).

8. K. J. Dorrington, and C. Kortan, "A Calorimetric Study of Subunit Interaction in Immunoglobulin G," *Biochem. and Biophys. Res. Comm.* Vol. 56(2), pp 529-534 (**1974**).

9. M. Monti, R. Faldt, J. Ankerst, and I. Wadso, "A New Approach to Detection of Antigen-Antibody Complexes by Microcalorimetric Measurements of Heat Production in Blood Cells," *J. Immunol. Methods* Vol. 37, pp 29-37 (**1980**).

ACKNOWLEDGMENTS

Three individuals at the Combat Systems Test Activity, Aberdeen Proving Ground participated in collecting and analyzing the data obtained with the Inframetrics Model 210 Infrared Imager. These individuals are: Mr. Frank R. Carlen, Ms. Pamela N. Costianes, and Mr. William C. Burch. Working with these people has been a pleasure. Dr. H. Douglas Ladouceur of the Naval Research Laboratory assisted in a comparison study of commercially-available microcalorimeters. His assistance is greatly appreciated.

Dr. Ladouceur received a B.S. degree in animal science from Purdue University in 1979. In 1985, she earned a Ph.D. degree in immunology and infectious diseases from The Johns Hopkins University. She is a research biologist working on the development of new immunoassays in the Biotechnology Division, Research Directorate, CRDEC.

BLANK PAGE

Thaddeus J. Novak, CRDEC

VYCOR POROUS GLASS AS AN OPTICAL-BASED FILTER LIFE INDICATOR FOR PROTECTIVE MASK FILTER ELEMENTS

A study was undertaken to identify a basis for developing a nondestructive filter life indicator small and simple enough to be used in protective masks while they are in use. Two filter life indicator concepts that utilize organic test vapors were considered. A catalytic Vycor Porous Glass (VPG) detector was used in one concept (the original) and a liquid crystal film detector was used in another (a revised version). The best VPG detector developed detects only high levels of amines and hence is not promising. Based on preliminary data, the revised concept looks promising and further study is recommended.

INTRODUCTION

This study was undertaken to identify a basis for developing a nondestructive filter life indicator sufficiently small and simple to be used in M-17 or M-40 type protective masks while they are in use. While a variety of concepts have been investigated,[1] none are appropriate for this application. The original concept investigated was based on the use of Vycor Porous Glass (VPG) as a chromogenic detector capable of indicating filter life by signaling the penetration of a carbon bed by common organic atmospheric pollutants.

This concept was revised because a newly developed catalytic detector (VPG treated with manganous chloride) required very high levels of pollutants (amines) required to trigger a detection signal. The magnitude of the deleterious effect of adsorbed water on the penetration rates of weakly adsorbed vapors in carbon beds is significant. Therefore, it was concluded that pulses of two entirely different kinds of organic vapors (both low in molecular weight, but one polar and the other nonpolar) will be needed to indicate the filter life for both strongly and weakly adsorbed CW agents. Weakly rather than strongly adsorbed organic vapors were selected for the vapor pulse(s) due to the required nondestructive nature of the test procedure.

As a consequence, we identified liquid crystal films as a class of chromogenic detectors that is vastly superior to others as an indicator of filter life. Liquid crystal detectors, which consist a of thin liquid crystal film viewed between crossed polars[2], have a unique set of attractive characteristics that coincide with our requirements. The results of research undertaken to identify catalysts that accelerate the discoloration reaction of adsorbed organics on VPG are presented. Preliminary data from penetration studies of the ASC Whetlerite carbon bed conducted with a newly developed catalytic VPG detector and also with a liquid crystal film detector are also given.

METHODS

Catalyst impregnated VPG was prepared by cutting a cleaned rod 1/8 inch in diameter (Corning Glass Works, Corning, NY) into 1/4-inch pieces and soaking each piece in a saturated aqueous solution of candidate catalyst for 15 min. The treated pieces were subsequently dried and then exposed to organic vapors in 5-mL vials. The candidate catalysts were from Strem Chemical Co. and Chem Service, Inc.

The liquid crystal film was prepared by placing ca 10 µL of liquid crystal K-15 (British Drug House, Ltd.) on a glass microscope slip 1/2 inch in diameter and smearing it with a Kim Wipe to form a uniform thin film. The carbon bed penetration studies were carried out in the apparatuses shown in Figures 1 and 2. Fresh ASC Whetlerite carbon and a sample from the same batch that had been loaded to 80% of capacity with DMMP were used. Both carbon samples were obtained from Physical Protection Directorate, CRDEC.

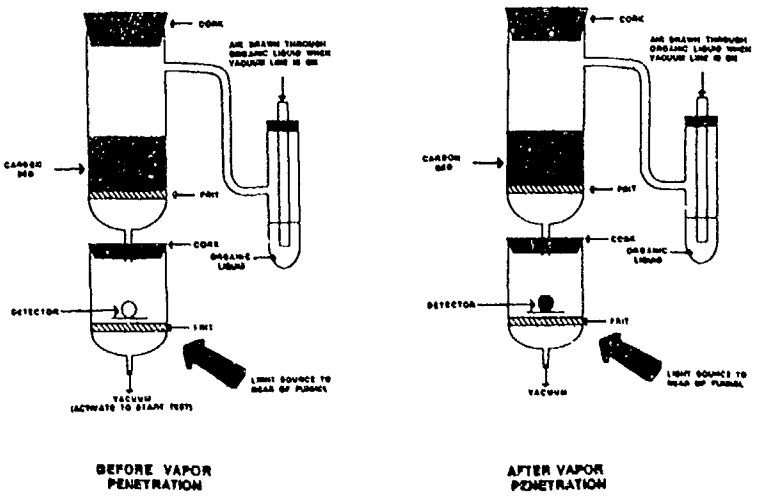

Figure 1. Apparatus for Carbon Bed Penetration Studies with Vycor Porous Glass Detector

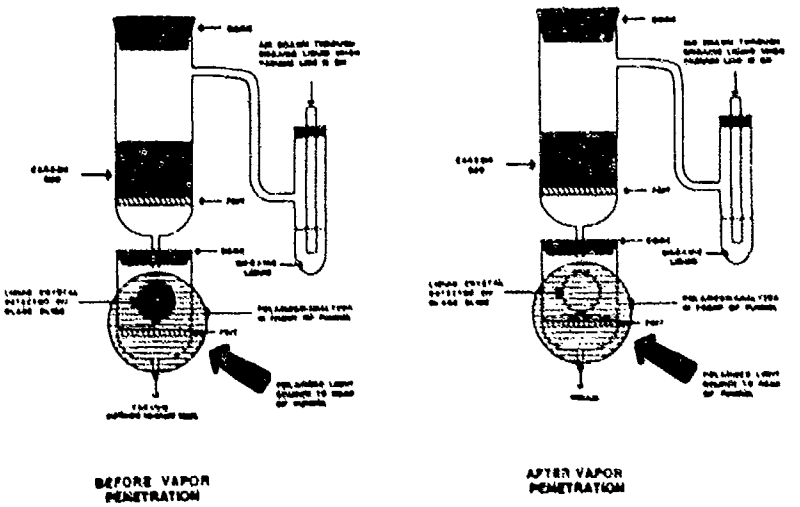

Figure 2. Apparatus for Carbon Bed Penetration Studies with Liquid Crystal Detector

DESCRIPTION OF THE ORIGINAL CONCEPT

Figure 3 depicts the original concept. A piece of VPG rod is embedded inside the carbon bed at the time of manufacture. Alternately, the VPG rod could be used in a segmented bed, which would assure mixing of the vapors that penetrated to that depth in the mask and would alleviate possible misinterpretations from the effects of nonuniformity (channeling) in the carbon bed. The VPG rod, which discolors when it adsorbs organic vapors, would be protected from contamination while the bed remained active. When organic pollutants commonly found in the atmosphere penetrated the mask and adsorbed on the VPG rod, a color change would signal that the filter should be replaced.

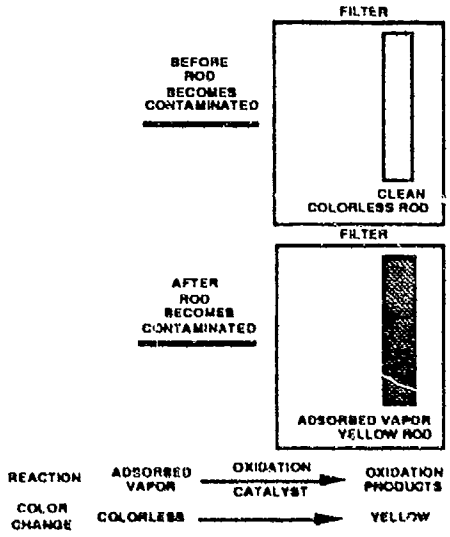

Figure 3. Vycor Porous Glass as a Residual Life Indicator for Filters

Figure 4 shows how a fiber-optic fiber could convey a chromogenic detection signal to the eyepiece of the mask where it could be viewed by the wearer. An optical fiber would convey light from a small light emitting diode (LED) to the VPG detector. Light emitted from the VPG rod would be conveyed to the eyepiece where the beam would be projected on a small screen.

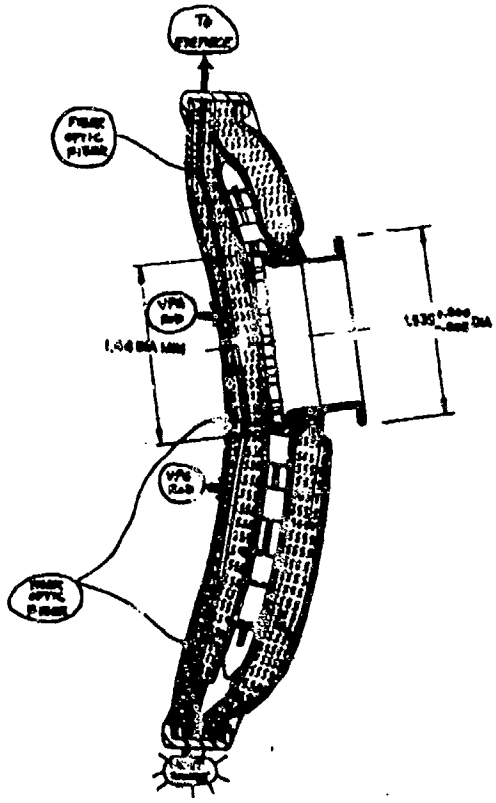

Figure 4. Vycor Porous Glass Rods Embedded Inside M13A1 Filter Element

An important characteristic of VPG that is of interest in this application is that it acts as a "light pipe." Because of this and related factors, the color change produced by contamination of the glass by organic vapors is strongest when the glass is viewed "end-on." VPG rods and rectangles (the shapes in which it is commercially made) (Figure 5) illustrate this.

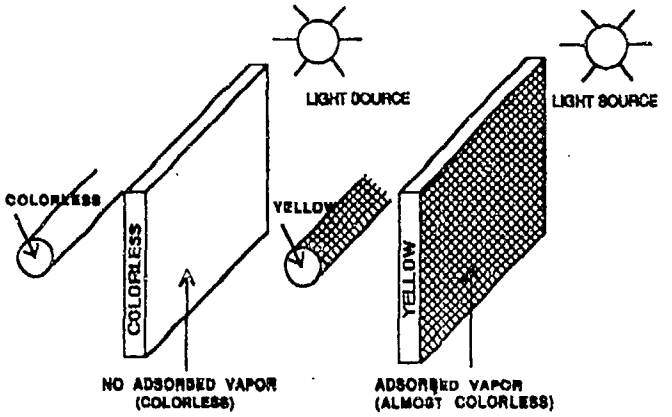

Figure 5. Effect of Adsorbed Vapors on Vycor Porous Glass

RESULTS AND DISCUSSION

Table 1 contains the vapor detection selectivity profile for cleaned VPG in the absence of catalyst. The data show that of the 26 tested, only one organic vapor produced a color change in the VPG detector within a 5-min exposure. Only two of the test vapors (piperidine and diethylamine) produced a response within a 30-min exposure. Eight of 26 vapors produced a response when exposed overnight, and 19 of 26 produced a color change after exposure to test vapors for 30 min and subsequent heating for 1 hr at 160 °C on a hot plate.

In an effort to find catalysts capable of accelerating the discoloration reactions of organic vapors adsorbed on VPG, 38 candidate catalysts (Table 2) were tested in combination with 24 organic vapors representing 18 functional group categories (Table 3). While improved detection responses were observed with seven of the candidates (Table 4), only the responses of manganous chloride were sufficiently strong and rapid to be studied further. Tests of a variety of amines (Table 5) show that the VPG/Mn detector is sensitive to amines in general. Sensitivity tests with a selected amine vapor, diethylamine, showed that vapor levels at and above 5000 ppm are detectable within 1 min; detection of smaller levels are possible but require more time.

The experimental apparatuses used to study carbon bed penetration with the VPG/Mn and liquid crystal detectors are shown in Figures 1 and 2, respectively. Organic vapors are generated by drawing a stream of air through an organic liquid. The vapors are retained on the bed according to the remaining physical adsorption capacity of the bed. When vapors penetrate, they are detected by a color change in the chromogenic detector located in the adjoining funnel. At the left of each figure, the detector is shown as it would appear before penetration, and on the right as it would when vapors break through the bed. Vapor penetration is signalled by a colorless --> brown color change in the VPG rod (Figure 1). The liquid crystal detector (Figure 2) shows a striking color change that varies depending on the type of solid support used for the liquid crystal film and the polarizers used. When the solid support is glass and circular polarizers (hand-held polariscope from Arthur H. Thomas, Inc.) are used, the color change is from bright yellow to dark purple; when linear polarizers are used, it is from yellow to black.

In Table 6 is a comparison of ASC Whetlerite bed penetration times for the VPG/Mn detector and a liquid crystal detector in tests carried out with three different organic vapors. The liquid crystal detector was made by simply smearing liquid crystal K-15 on a glass slide. Diethylamine vapor is detectable by both types of detectors; in each case it showed longer breakthrough times for the fresh bed. The liquid crystal detector, a nonspecific detector for organic vapors, can also be used with a larger variety of test vapors. When tested in combination with the liquid crystal detector, acetone and dichloromethane vapors showed longer penetration times for fresh beds than those obtained with diethylamine vapor. When viewed from a filter life indicator perspective, nonspecificity is only one of the attractive characteristics of liquid crystal vapor sensors; others are summarized in Table 7.

Table 1. Detection Selectivity for Vycor Porous Glass (no Catalyst)

TYPE/NAME (OF ADSORBED VAPOR)	OBSERVED COLOR (AFTER INDICATED TIME/TREATMENT			
	5 MIN	30 MIN	16 HR	160°C/1 HR
ACETAL/1,1-DIMETHOXYETHANE	NONE	NONE	NONE	M/TAN
ACID HALIDE/BENZOYL CHLORIDE	NONE	NONE	VW/YEL	VW/YEL
ALDEHYDE AROMATIC/BENZALDEHYDE	NONE	NONE	M/YEL	S/BROWN
ALDEHYDE AROMATIC SUB/ANISALDEHYDE	NONE	NONE	M/YEL	S/BROWN
AMIDE/N,N-DIMETHYLFORMAMIDE	NONE	NONE	NONE	VW/YEL
AMINE, MONO/PIPERIDINE	W/YEL	W/YEL	M/YEL	S/YEL
AMINE, ALIPHATIC/DIETHYLAMINE	NONE	M/YEL	S/YEL	S/YEL
AMINE, MONO, HYDROXY/ETHANOLAMINE	NONE	NONE	NONE	NONE
AMINE, POLY/DIETHYLENETRIAMINE	NONE	NONE	W/YEL	W/YEL
AMINE, AROMATIC/ANILINE	NONE	NONE	M/YEL	S/RUST
CARBONATE/DIETHYL CARBONATE	NONE	NONE	NONE	W/YEL
ESTER MONO/ETHYL ACETATE	NONE	NONE	NONE	NONE
ESTER AROMATIC/BENZYL ACETATE	NONE	NONE	NONE	NONE
ETHER/BUTYL ETHER	NONE	NONE	NONE	W/YEL
ETHER/ PROPYLENE OXIDE	NONE	NONE	NONE	NONE
ETHER, AROMATIC/ANISOLE	NONE	NONE	NONE	VW/YEL
HALOGEN CPND AROMATIC/BENZYL CHLORIDE	NONE	NONE	NONE	M/BROWN
HETEROCYCLIC CPND/4-PICOLINE	NONE	NONE	W/YEL	W/YEL
KETONE MONO/METHYL ETHYL DETONE	NONE	NONE	NONE	W/YEL
KETONE DI/ACETYLACETONE	NONE	NONE	NONE	W/YEL
KETONE AROMATIC/ACETOPHENONE	NONE	NONE	NONE	M/YEL
LACTONE/BUTYROLACTONE	NONE	NONE	NONE	NONE
NITRILE/ACETONITRILE	NONE	NONE	NONE	NONE
SULFATE/ETHYL CHLOROSULFATE	NONE	NONE	NONE	NONE
HALIDE/BENZYNE SULFONYL CHLORIDE	NONE	NONE	NONE	NONE
UNSATURATED MONOMER/METHYL ACRYLATE	NONE	NONE	NONE	M/YEL
NUMBER WHICH BECAME COLORED	1/26	2/26	8/26	19/26

CODE: W-WEAK; M-MODERATE; S-STRONG; YEL-YELLOW

Table 2. Candidate Catalysts

aluminum chloride
strontium chloride
potassium ferrocyanide
zirconyl chloride
nickelous chloride
mercuric chloride
cadmium acetate
silicotungstic acid
titanium sulfate
hafnium tetrachloride
calcium iodide
cobalt chloride
calcium hydroxide
phosphomolybdic acid
cerric ammoniun nitrate
manganese (II) chloride
manganese (II) fluoride
manganese (III) chloride
chromium chloride
ferric chloride
cupric chloride
chromic acid
palladium acetate
potassium chloride
sodium molybdate
silver acetate
lead acetate
ceric hydroxide
magnesium acetate
cuprous chloride
zirconium nitrate
lead oxide
calcium acetate
platinum chloride
zirconium acetate
manganese pentacarbonyl bromide
manganese (III) meso-tetraphenylporhine acetate
dichlorotris(triphenylphosphine)ruthenium (II)

Table 3. Organic Vapors

benzyoyl chloride
benzaldehyde
anisaldehyde
N,N-dimethylforamide
piperidine
diethylamine
ethanolamine
diethylenetriamine
methylethylketone
diethyl carbonate
ethyl acetate
insect repellant (U.S. Army)
benzyl acetate
butyl ether
propylene oxide
anisole
benzyl chloride
4-picoline
hexene-1
aniline
acetylacetone
γ-butyrolactone
acetonitrile
diesel fuel

Table 4. Effect of Candidate Catalysts on Discoloration Reactions of Adsorbed Organic Vapors on Vycor Porous Glass

CANDIDATE CATALYST	ORGANIC VAPOR	STRENGTH OF CATALYTIC EFFECT
Manganese (II) Chloride	Piperidine	Strong
	Diethylamine	Strong
	Ethanolamine	Strong
Manganese (II) Fluoride	Piperidine	Moderate
Cupric Chloride	Aniline	Weak
Ferric Chloride	Methyl Ethyl Ketone	Weak
Silver Acetate	Piperidine	Weak
	Diesel Fuel	Weak
Cerric Ammonium Nitrate	Aniline	Weak
Chromic Acid	Aniline	Weak
	Propylene Oxide	Weak
	Acetylacetone	Weak

Table 5. Strength of Discoloration of Various Amine Vapors Adsorbed on Vycor Porous Glass/Manganese Chloride Detector

STRONG	MODERATE	WEAK
Piperidine	*n*-Butylamine	Phenethylamine
Diethylamine	*tert*-Butylamine	Cyclohexylamine
Isobutylamine	2-Methylpiperidine	Diallylamine
sec-Butylamine	Allylamine	Dibutylamine
	Triethylamine	

Table 6. Comparison of Vycor Porous Glass Detector with Liquid Crystal Detector in Carbon Bed Penetration Studies

DETECTOR TYPE	HEIGHT OF CARBON BED, cm	TEST VAPOR [a]	TIME TO POSITIVE SIGNAL (seconds)	
			Fresh Bed [b]	Loaded Bed [c]
VYCOR POROUS GLASS WITH Mn CATALYST [d]	3.5	diethylamine	117	55
LIQUID CRYSTAL [e]	3.5	acetone	214	54
	3.5	diethylamine [f]	120	80
	3.5	dichloromethane	140	32

[a] Air drawn through organic liquid at 1 liter/min.

[b] ASC Whetlerite Carbon Bed.

[c] ASC Whetlerite Carbon Bed loaded to 80% of capacity with DMMP

[d] Catalyst is manganese (II) chloride.

[e] Liquid Crystal K-15 on glass slide.

[f] Average of two determinations.

Table 7. Attractive Characteristics of Liquid Crystal Detector or use in Filter-Life Indicator

- Non-specific detector for organic vapors
- Not affected by water or water vapor
- Simple to use
- Good long-term stability
- Automatically and rapidly reversible
- Rapid response time
- Striking color change as the detection signal
- Detects high levels of organic vapors
- Does not respond to low levels of vapors

DESCRIPTION OF THE REVISED CONCEPT

Figure 6 is a sketch of the C-2 canister for the M-40 type protective masks modified with the proposed liquid crystal filter life indicator. Light from a light emitting diode (LED) is directed through a polarizer and then conveyed to a liquid crystal detector by a fiber-optic fiber. Using another optical fiber, the light emitted would be directed through another polarizer (crossed with respect to the first polarizer) and then to the eyepiece of the mask where the detection signal is seen as a color change in a small screen at the end of the fiber.

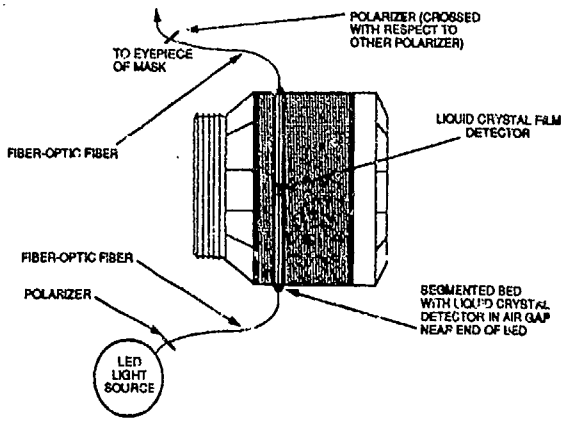

Figure 6. Liquid Crystal Filter-Life Indicator Modified G2 Canisterfor M-40 Protective Mask

The filter life indicator using a liquid crystal detector in the M-40 protective mask is shown in Figure 7.

The individual wearing the mask sniffs vapors of the nonpolar organic vapor and observes the time required to trigger a detection signal (a color change in the liquid crystal detector); the procedure is then repeated with the polar vapor. The times required for penetration of the polar and nonpolar organic vapors are then used to access the remaining filter life for strongly and weakly held CW agents respectively. Penetration times should be faster as the adsorptive capacity of the filter becomes depleted. Furthermore, the penetration rate of the nonpolar organic vapor probably could also be correlated with the amount of adsorbed water vapor contained in the carbon bed and, hence, might also indicate vulnerability to an unknown chemical agent whose rate of penetration of carbon beds is directly related to the quantity of adsorbed water in the bed.

An alternate and even simpler approach is shown in the artist's illustration (Figure 8).

Here a single pressure-activated cartridge containing a mixture of polar and non-polar organic vapors is used. The desirability of using a single cartridge with a mixture of vapors instead of separate cartridges for non-polar and polar vapors would depend on the outcome of future studies. When applied in the field, a "go/no-go" decision to keep or discard a filter canister would depend on whether or not a color change occurred within a preset time after the filter had been exposed to the mixture of test vapors. A timer activated at the start of the vapor challenge would signal when the required exposure time had been reached. In the artist's illustration (Figure 8), the "go/no-go" decision would be based (as shown on the instruction card) on a 1-min exposure. This exposure period was arbitrarily selected for the illustration and is not based on experimental data.

CONCLUSIONS

The best VPG detector developed detects only high levels of amines and hence is not promising. Based on preliminary data, the revised concept shows promise.

ACKNOWLEDGEMENTS

Appreciation is expressed to Mr. Joseph Pistritto, Robert Morrison, John Conlisk, Dr. David Friday, Dr. Chen Hsu, and Richard Newton for helpful discussions, and to Dr. Russell Drago (U. of FL) for suggesting some candidate catalysts for the study. The author also wishes to thank Vikki Henderson and Girish Munavalli for performing most of the experiments, Terry Callahan for preparing the loaded Whetlerite sample, John Parsons for constructing a cell holder, and Larry Rouiller for drawing artist's illustrations of the revised concept (Figures 7 and 8).

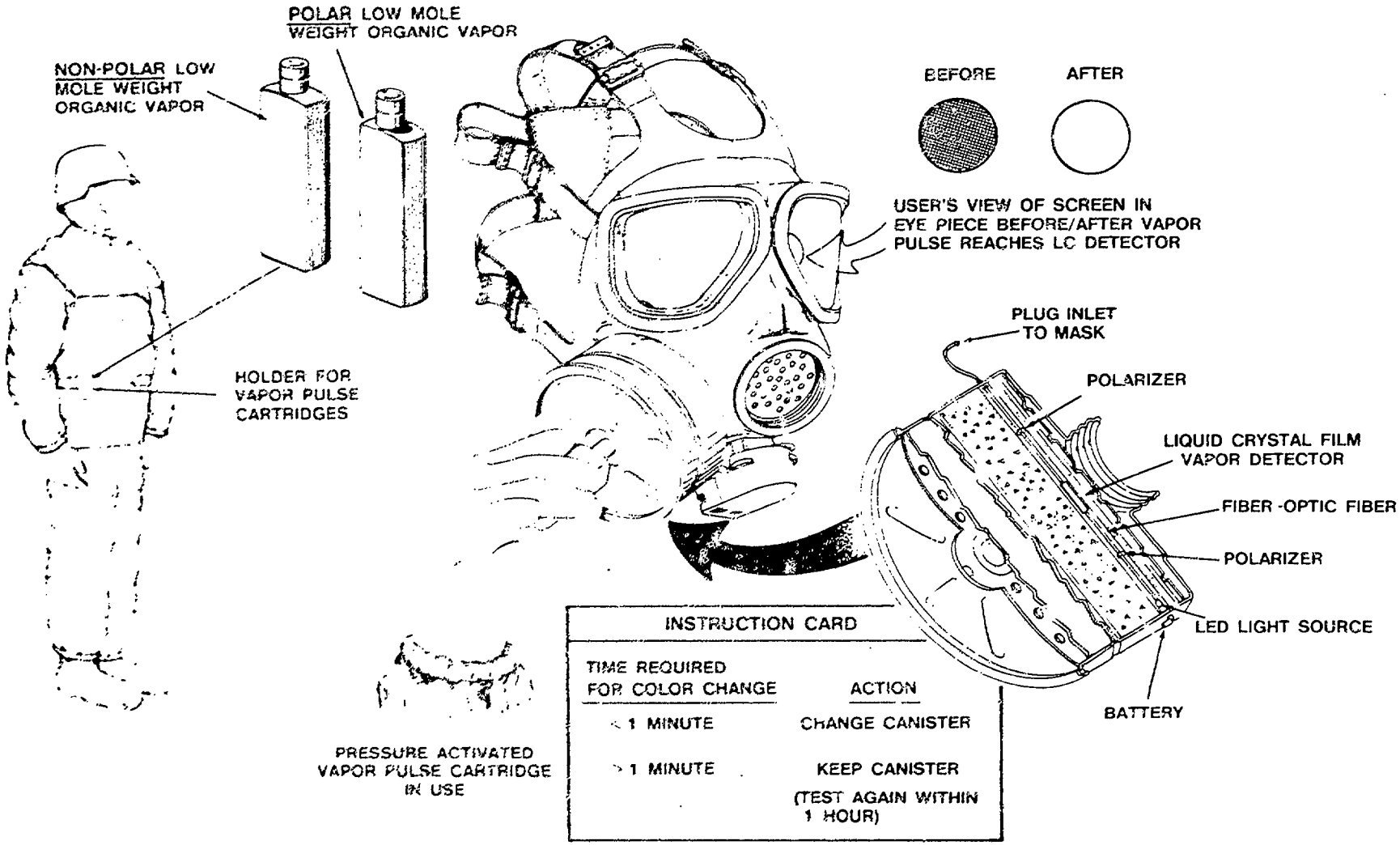

Figure 7. Liquid Crystal/Dual Vapor Pulse Filter Life Indicator for M-40 Type Protective Mask

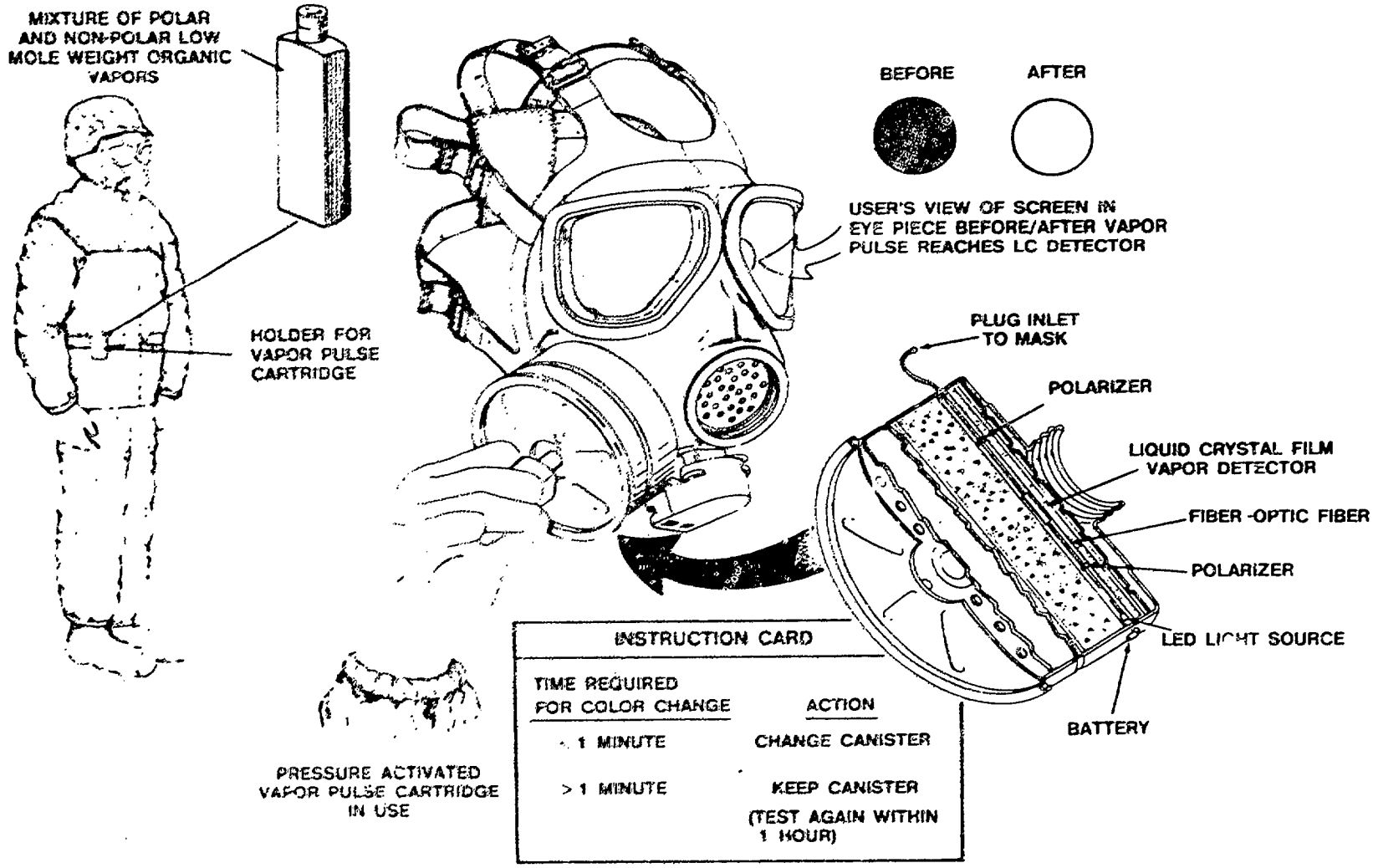

Figure 8. Liquid Crystal/Single Vapor Pulse Filter Life Indicator for M-40 Type Protective Mask

LITERATURE CITED

1. DTIC Search Control No. FF039E 88/07/21 covering the keywords "Residual Life" and "Filter Life." This reference is available in the CRDEC Technical Library.

2. T.J. Novak, E.J. Poziomek, and R.A. Mackay, "Use of Anisotropic Materials as Chemical Detectors", *Anal. Lett.*,Vol. 5, p 187 (1972).

Mr. Novak received a B.S. degree in chemistry from Drexel University in 1963 and an M.S. degree in chemistry from the University of Delaware in 1974. He is a research chemist in the Applied Chemistry Branch, Chemical Division, Research Directorate at CRDEC.

BLANK PAGE

H. D. Durst, CRDEC, and F. R. Longo, Drexel University

ENVIRONMENTAL EFFECTS ON THE LUMINESCENCE OF IODOSOBENZOIC ACID DERIVATIVES IN ORGANIZED MEDIA

Luminescence studies on *ortho*-iodosobenzoic acid using monochromatic excitation (310 nm) resulted in a broad, featureless luminescence band centered at 410 nm with a half-width of ~ 70 nm. This band significantly increases in intensity as excitation is repeated, both in aqueous and in microemulsion media. Concurrently a considerable amount of acid is generated. The catalytic power of the *ortho*-iodosobenzoic acid is appreciably reduced and, upon prolonged irradiation, is completely eliminated. During photolysis *ortho*-iodosobenzoic acid is transformed, resulting in a product that has an absorption maximum near that of IBA. Aqueous solutions of of IBA stored out-of-doors in sealed quartz vessels showed a 95% decease in catalytic power in 10 days. Product analysis of the photolyzed solution by means of GC/MS and FT/NMR indicate that the primary product of the photolysis is 2-iodobenzoic acid. Authentic samples of 2-iodobenzoic acid give absorption and luminescence spectra identical with the photolysis product.

Our studies of phosphate esters have demonstrated that their hydrolysis is accelerated in cationic micellar and microemusion media. In addition, hydrolysis is significantly catalyzed by the sodium salts of iodosobenzoic acid (IBA), iodoxybenzoic acid (IBX), and their derivatives. We had proposed empirical studies that would determine the environment of these catalysts in micellar and microemulsion organizates.

Introduction

During the last quarter century there have been an increasing number of investigations of the effects of surfactants on the rates and mechanisms of chemical reactions .[1,2] Surfactant systems have also been employed as media for organic synthesis and as models for enzymatic action.[3-8] These studies have been primarily concerned with the influence of normal micelles in aqueous solution, although processes in reversed micelles, lyotropic liquid crystalline phases, vesicles, and monolayers have also been examined. Common to all these systems is the presence of the microscopic oil/water interface.

In spite of the advantages of microemulsions, relatively few studies of chemical reactions in these media have been reported. Microemulsions are capable of dissolving large amounts of a great variety of solutes due to the presence of different phases, including the oil, aqueous, and unique interphase, over which there is a gradient in the dielectric constant ranging from ~2 to ~78. (Figure 1). Very nonpolar solutes will be located in the oily core of the microemulsion droplet; whereas, more polar substances will be distributed throughout the interphase and aqueous regions. Thus, the microemulsion medium makes it possible to bring nonpolar oil-soluble (lipids) and polar water-soluble reagents into contact.

The Nature of Microemulsions.

There is no universal agreement concerning the nature of the fluids that have variously been referred to as microemulsions,[9-12] solubilized micellar solutions, [13] and micellar emulsions.[14] These systems are translucent or transparent dispersions of oil-in-water (o/w) or water-in-oil (w/o) that contain one or more amphiphilic compounds

and are mechanically stable. There are some systems that are demonstrably only kinetically stable,[15-18] while many others[19-25] appear to be thermodynamically stable. It is often difficult to prove thermodynamic stability in these systems of complex composition; the important criteria for this determination include spontaneous formation and physical properties independent of order of addition of components. Furthermore, after being subjected to a "pulse" perturbation (ΔT, ΔpH, etc.), which causes phase separation, a microemulsion identical with the original must reform. Accounts of earlier work on thermodynamic stability and microstructure are presented in reviews by Shinoda and Friberg [26] and Prince.[27]

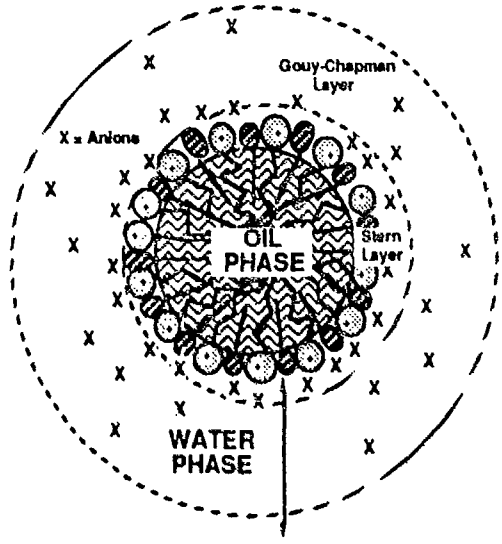

Figure 1. A Model of the Oil in Water Microemulsion Droplet

To obviate the problem of thermodynamic stability, Reed and Healy [25] suggested an operational definition: a microemulsion is a persistent, translucent combination of oil and water that may contain electrolytes and one or more amphiphiles. In this definition, the term 'persistent' is relative and is dependent upon the specific application. Amphiphiles are normally surfactants (soaps, alkylarylpolyethylene oxides, alkylated pyridine N-oxides, alkyl benzene sulfonates, tetraalkyl ammoniums, etc.) and frequently include cosurfactants such as C_4 to C_{10} alcohols (which are are not very water soluble), hydrotropes, and other polar compounds. Co-surfactants were originally employed to produce optical transparency or clarification.

Microemulsions are believed to consist of a dispersion of oil microdroplets in a water continuum or, vice versa, water microdroplets in an oil continuum. The volume occupied by the dispersed phase (phase volume) can be high (20 to 80%). The droplet diameter is on the order of 100 to 600 Å. In this size range, the droplets appear to be monodisperse,[10,12,29,30] although more recent work has provided evidence for a more complex structure in some systems.[31,32] Conceptually, the droplet may be divided into two major regions: the oil or water core and the surface or interphase region. The interphase region may be further subdivided into the Stern layer and the Guoy-Chapman layer. The Stern layer is the spherical volume element surrounding the oil core. It contains the surfactant head groups, the co-surfactant; and some counterions. Beyond this is the Guoy-Chapman layer, which contains the remaining counterions. Essentially all of the surfactant and part of the co-surfactant are located in the interphase region. A model of an o/w microemulsion is shown in Figure 1. Under appropriate conditions, a third phase that appears to be oil and water continuous may be detected. This phase has been called the middle or surfactant phase.[25,26] It has been variously suggested that this surfactant phase consists of bicontinuous structures,[33] lamellae of oil and water,[31] or molecularly dispersed solutions.[35]

A thorough survey of the literature from 1975-79, containing supplemental references, has been published by Holt.[36] All aspects of surfactant systems are more recently reviewed in the six volumes representing the proceedings from the 4th and 5th Symposia on Surfactants in Solution;[37] in particular, Volume 6, Part VII, is

entirely devoted to microemulsions (structure, stability, and composition) and chemical reactions in microemulsions.

Experimental Approach

The luminescence intensity and the wavelength maxima for excitation and emission are environment sensitive. Hence, by studying the ultraviolet (UV)-excited luminescence of IBA, IBX, and their derivatives over a wide range of solvent polarities, we had hoped to calibrate their emission in micellar and microemulsion systems. In such media, because of microscopic heterogeneity, the dielectric constant (D) ranges from ~ 2 in the oily core of the microaggregate to ~ 78 in the aqueous continuous phase (Figure 1).

Experimental Methods

Ultraviolet Exposure of IBA.

A 1 x 10^{-3} M solution of IBA(20 mL) in 0.03 M of borate buffer, pH 9.3, were placed in a shallow glass beaker and irradiated with UV light with a low intensity, hand-held, UV lamp. The UV light was incident to the surface of the solution. The solutions turned brown during the photolysis.

Kinetics.

Samples of 1 mL were removed from the irradiated solutions (described above) at t=0 and at intervals of time ranging from 4 to 130 min. These samples were diluted 1:2 with a concentrated microemulsion solution consisting of 36% CTAB, 36% 1-butanol, 8% hexadecane, and 20% borate buffer to give a microemulsion solution containing 18% CTAB, 18% 1-butanol, 4% hexadecane, and 60% borate buffer and 5 x 10^{-4} M irradiated IBA. The rate of hydrolysis of PNDP was then measured in each diluted sample. Values of k_{obsd} were corrected to account for the volume of water that had evaporated during the experiment. A graph of the first order rate constant, k_{obsd}, as a function of photolysis time is presented in Figure 2.

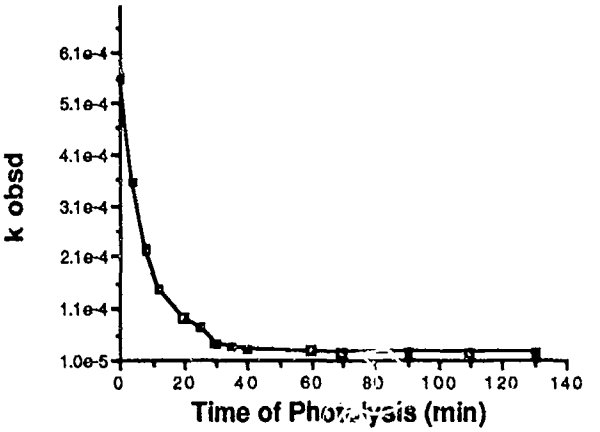

Figure 2. Low Intensity UV Irridiation
Graph of the first order rate constant, k_{obsd}, for the hydrolysis of *p*-nitrophenyl diphenyl phosphate (PNDP) in catalyzed microemulsion at pH 9.3 as a function of photolysis time of the catalyst, *o*-iodosobenzoate (IBA). The catalyst has been exposed to low intensity ultraviolet radiation for periods of time ranging from 0 to 130 minutes.

This experiment was repeated using a high intensity UV lamp. In this case, irradiation time per sample ranged from 30 sec to 25 min. Samples of 1 mL were diluted in a similar manner, and the rate of hydrolysis of PNDP was again measured. A graph of k_{obsd} as a function of time of radiation is presented in Figure 3.

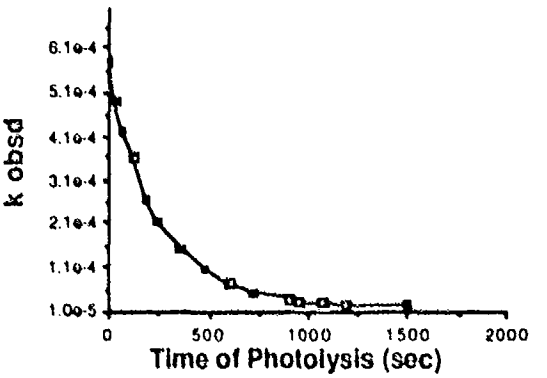

Figure 3. High Intensity UV Irridiation
Graph of the first order rate constant, k_{obsd}, for the hydrolysis of p-nitrophenyl diphenyl phosphate (PNDP) in catalyzed microemulsion at pH 9.3 as a function of photolysis time of the catalyst, *o*-iodosobenzoate (IBA). The catalyst has been exposed to high intensity ultraviolet radiation for periods of time ranging from 0 to 1500

Due to the low concentration of IBA in the irradiated solutions, the pH of the solutions did not change during the experiments.

The rate of hydrolysis of PNDP in uncatalyzed microemulsion containing 18% CTAB, 18% 1-butanol, 4% hexadecane, and 60% borate buffer was determined as a control baseline value. This value of k_{obsd}, based on an average of four determinations, was 2.63×10^{-5} sec^{-1}.

Natural Irradiation of IBA Solutions.

A 1×10^{-3} M solution of IBA (12 mL) in 0.03 M of borate buffer was placed in a sealed quartz tube and positioned in the sun for a total time of 8.5 days. The solution turned brown within 24 hr. Aliquots (1 mL) of the irradiated sample were diluted 1:2 with the microemulsion concentrate, and the rate of hydrolysis of PNDP was measured. Less than 4% of the catalytic activity of the IBA remained after 8.5 days.

Conformation Test for Presence of Iodine.

Since the solutions became brown during radiation, a starch test was performed to determine if I_2 was present. Starch (0.5 g) was added to 20 mL of formamide and heated. A solution of I_2/ I^- was prepared as a control, and two drops of the cooled starch solution were added. The solution turned blue. One drop of the unknown mixture was added to a solution of I^- in water. Upon dissolution, two drops of the starch solution were added. The solution did not turn blue.

NMR and Mass Spectroscopy Studies.

Aliquots (20 mL) of a solution containing 1×10^{-3} M of IBA in water were irradiated for 150 min with the low intensity, UV lamp. The value obtained for k_{obsd} in the irradiated sample/ microemulsion concentrate mixture was 2.12×10^{-5} sec^{-1}. This process was repeated six times. The irradiated samples were combined, evaporated to dryness, and submitted for NMR analysis. A more concentrated solution of IBA in water or in borate buffer was not photolyzed completely by the low-intensity lamp. Also, when the photolyzate contained borate buffer, the concentration of salt was too high to dissolve the sample sufficiently for an NMR analysis.

^{13}C spectra in dimethyl sulfoxide-d_6 indicated that the irradiated sample contained 27 separate peaks. Tentatively, the sample is a mixture of four compounds: 45% *o*-hydroxybenzoic acid, 27% *o*-iodobenzoic acid, 9% 2-iodo-4-hydroxybenzoic acid, and 19% of an unknown compound.

Direct probe mass spectroscopy confirmed the existence of *o*-hydroxybenzoic acid and *o*-iodobenzoic acid in the mixture. The typical patterns for the breakdown *o*-hydroxybenzoic acid and of *o*-iodobenzoic acid were indicated on the spectrum.

Results and Conclusions

Luminescence studies on the parent compound, IBA, led to very peculiar results. Using monochromatic excitation (310 nm), we observed a broad, featureless luminescence band centered at 410 nm with a half-width of ~ 70 nm. Surprisingly, this band significantly increased in intensity as excitation was repeated, both in aqueous and in microemulsion media. At the same time, a considerable amount of acid was generated. More significantly, the catalytic power of IBA was appreciably reduced and, upon prolonged irradiation, was completely eliminated. Consideration of these observations led to the conclusion that IBA undergoes photolysis, resulting in a product that has an absorption maximum near that of IBA. Aqueous solutions of of IBA stored out-of-doors in sealed quartz vessels showed a 95% decrease in catalytic power in 10 days.

Studies of the photolyzed solution by means of GC/MS and FT/NMR indicated that the primary product of the photolysis is 2-iodobenzoic acid:

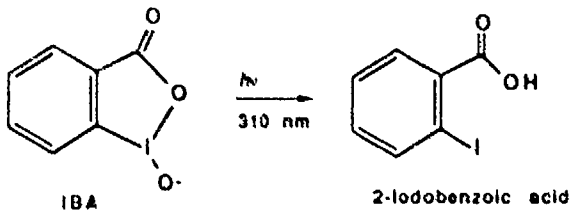

IBA 2-Iodobenzoic acid

In addition, authentic samples of 2-iodobenzoic acid gave absorption and luminescence spectra identical with the photolysis product.

The initial goals of the project will not be easily achieved because of facile photolysis of IBA in aqueous and microemulsion media. From a practical point of view, it appears that photolysis of IBA is not significant in terms of its incorporation into DECON formulations since solar radiation at 310 nm is of low intensity; more importantly, IBA and systems formulated with IBA will be stored in UV-opaque containers.

Acknowledgments

The authors wish to thank Dr. Patrick Nolan, Dr. Kieth Haddaway and Ms. Stephanie Garlick for their help and support of this project. Without their thoughtful comments and observations, this project would not have progresssed as it did. We wish also to thank Linda Szafraniec and Bill Beaudry for performing the NMR analysis for this project.

LITERATURE CITED

1. E. H. Cordes and R. B. Dunlop, "Kinetics of Organic Reactions in Micellar Systems," *Acct. Chem. Res.* Vol. 2, p 329 **(1969).**

2. E. J. Fendler and S. N. Fendler, "Reactions in Micellar Media," *Phys. Org. Chem.* Vol. 8, p 271 **(1970).**

3. J. H. Fendler and E. J. Fendler, "Catalysis in Micellar and Macromolecular Systems," Academic Press, New York, NY, **(1975).**

4. J. B. Rijnbout, "Stokes Principle of Reversion and the Optical Measurement of Soap Film Thickness," *J. Phys. Chem.* Vol. 75, p 2001 **(1971).**

5. A. Kitahara, "Solubilization and Catalysis in Reversed Micelles ," *Adv. Colloid Int. Sci.* Vol. 12, p 109 **(1980).**

6. S. I. Ahmad and S. Friberg, "Catalysis in Micellar and Liquid Crystalline Phases. I. The System Water-Hexadecyltrimethyl Ammonium Bromide-Hexanol," *J. Am. Chem. Soc.* Vol. 94, p 5196 **(1972).**

7. J. H. Fendler, "Surfactant Vesicles as Membrane Mimetic Agents: Characterization and Utilization," *Acct. Chem. Res.* Vol. 13, p 7 **(1980).**

8. J. T. Davis, "Structure of Organized Media," *Adv Catalysis*, Vol. 6, p 1 **(1954).**

9. T. P. Hoar and H. H. Schulman, "Transparent Water-in-Oil Dispersions: the Oleopathic Hydro-Micelle," *Nature* (London), Vol. 152, p 102 **(1943).**

10. J. H. Schulman, R. Matalon and M. Cohen, "The Role of the Cosurfactant," *Discuss Faraday Soc.* Vol. 11, p 117 **(1951).**

11. J. H. Schulman, W. Stockenius, and L. M. Prince, "Mechanism of Formation and Structure of Microemulsions by Electron Microscopy," *J. Phys. Chem.* Vol. 63, p 1677 **(1959).**

12. W. Stockenius, J. H. Schulman and L. M. Prince, "The Structure of Myelin Figures and Microemulsions as Observed with the Electron Microscope," *Kolloid. Z.* Vol. 169 , p 170 **(1960).**

13. K. Shinoda and H. Kunieda, "Conditions to Produce So-called Microemulsions: Factors to Increase Mutual Solubility of Oil and Water by Solubilzer," *J. Colloid. Interface Sci.* Vol. 42, p 381 **(1973).**

14. A. W. Adamson, "A Model for Micellar Emulsions," *J. Colloid. Interface Sci.* Vol. 29, p 261 **(1969).**

15. M. Clausse and P. Sherman, C. R. Hebd. "Theory of Luminescence Quenching," *Seanc. Acad. Sci., Ser C* Vol. 279, p 919 **(1974).**

16. M. Clausse, P. Sherman and R. J. Sheppard, "Dielectric Properties of Benzene-in-water Microemulsions in the Frequency Range 100 kHz - 5 MHz," *J. Colloid. and Interface Sci.* Vol. 56 , p 123 **(1976).**

17. C. Hermansky and R. A. Mackay, "Solution Chemistry of Surfactants," pp 723-730, K. L. Mittal, Ed., Plenum Press, New York, NY, **(1979).**

18. H. L. Rosano, T. Lan, A. Weiss, W. E. F. Gerbacia, and J. H. Whittan, "Transparent Dispersions: An Investigation of some of the Variables Affecting Their Formation," *J. Colloid. Interface Sci.* Vol. 72 , p 233 **(1979).**

19. K. Letts and R. A. Mackay, "Reactions in Microemulsions. I. Metal Ion Incorporation by Tetraphenylporphin," *Inorg. Chem.* Vol. 14, p 2990 **(1975).**

20. K.Letts and R.A.Mackay, Reactions in Microemulsions. II. Solubilization of Intermediates," *Inorg. Chem.* Vol. 14 , p 2993 **(1975).**

21. G. D. Smith, B. B. Garrett, S. L. Holt and R. E. Barden, "The Interaction of Copper(II) and N^{α}-Acyl-L-histidinol at the Interface of an Oil Continuous Microemulsion," *J. Phys. Chem.* Vol. 80, p 1708 **(1976).**

22. G. D. Smith, B. B. Garrett, S. L. Holt and R. E. Barden, "Properties of Metal Complexes in the Interphase of an Oil Continuous Microemulsion.2. Interaction of Copper(II) with the Side Chains of Lysine, Glutamine, and Methionine," *Inorg. Chem.* Vol. 16, p 558 **(1977).**

23. R. A. Mackay, N. S. Dixit, C. Hermansky, and A. S. Kertes, "Conductivity and Diffusion Measurements in Micellar and O/W Microemulsion Systems. A Comparative Study," *Colloids and Surfaces* Vol. 21, pp 27-39 **(1986).**

24. R. A. Mackay and R. Agarwal, "Electrochemical Studies in Nonionic Microemulsions," *J. Colloid Interface Science* Vol. 65, p 225 **(1978).**

25. R. L. Reed and R. N. Healy, "Improved Oil Recovery by Surfactant and Polymer Flooding," Academic Press, New York, NY, 1977.

26. K. Shinoda and S. Friberg, "Microemulsions: Colloidal Aspects," *Adv. Colloid Interface Sci.* Vol. 4, p 281 **(1975).**

27. L. M. Prince, "Emulsions and Emulsion Technology, Part I," p 125, K. J. Lissant, Ed., Marcel Decker, Inc., New York, NY, 1974.

28. L. M. Prince, "Microemulsions," Ed, Academic Press, New York, NY, 1977.

29. W. C. Tosch, S. C. Jones, and A. W. Adamson, "Distribution Equilibria in a Micellar Solution System," *J. Colloid Sci.* Vol. 31 , p 297 **(1969).**

30. C. E. Cook and J. H. Schulman, "Surface Chemistry," p 231, Munksgaard, Copenhagen, 1965.

31. Y. Tricot, J. Kiwi, W. Niederberger and M. Gratzel, "Application ^{13}C NMR, Fluorescence, and Light Scattering Techniques for Structural Studies of Oil-in-Water Microemulsions," *J. Phys. Chem.* Vol. 85, p 862 **(1981).**

32. E. Gulari, B. Bedwell and S. Alkafaji, "Quasi-Elastic Light-Scattering Investigation of Microemulsions," *J. Colloid Interface Sci.* Vol. 77, p 202 **(1980).**

33. L. Scriven, Micellization, "Solubilization and Microemulsions," Vol 2, p 877, K. L. Mittal, Ed., Plenum Press, New York, NY, 1977.

34. S. Friberg, I. Lapizynska, and G. Gillberg, "Microemulsions Containing Nonionic Surfactants - The Importance of the PIT Value," *J. Colliod Interface Sci.* Vol. 56, p 19 **(1976).**

35. D. O. Shah, R. D. Walker Jr., W. C. Hsieh, N. J. Shad, S. Dwivedi, J. Nelander, R. Pexinsky and D. W. Deamer, SPE 5815, Proceedings of the Improved Oil Recovery Symposium of Soc. Pet. Eng. of AIME, Tulsa, OK March 1976.

36. S. L. Holt, *J. Dispersion Sci. and Tech.* Vol. 1, p 423 **(1980).**

37. K. L. Mittal, and B. Lindman, Ed., "Surfactants in Solution. II In Volumes 1 to 3," 4th International Symposium, Lund, Sweden, 1982; Volumes 4 to 6, K.L.Mittal, and P.Bothorel, Ed., 5th International Symposium, Bordeaux, France, 1984.

38. J. H. Fendler, "Photochemical Solar Energy Conversion. An Assessment of Scientific Accomplishments," *J. Phys. Chem.* Vol. 89, p 2730 **(1985).**

Dr. H. Dupont Durst received his BA and MS degrees in Biochemistry from Louisiana State University, Baton Rouge Campus, and his Ph. D. in Organic Chemistry from the University of Minnesota, Minneapolis Campus. During the 1970's, while on the faculty at SUNY at Buffalo, he developed several new methods to conveniently use phase transfer catalysts for a large number of synthetic transformations. This work permitted an avalanche of methods by which simple procedures were developed for bimolecular transformations in organic solvents, transformations that previously had been considered very difficult to perform. In 1975, in collaboration with Professor George Gokel, he published one of the most frequently cited review articles in the area of phase transfer and crown ether catalysis. Other research areas to which he has contributed to include: development of new and novel reducing agents, biosynthetic studies of terpene and alkaloid metabolism, synthesis of "resonance twisted" arenes, reaction behavior in organized media, and the isolation and structure determination of marine natural products. Most recently, Dr. Durst has been investigating microemulsions as hosts for the degradative hydrolysis and/or oxidation of chemical warfare agents and other toxic materials. Dr. Durst, a past senior National Research Council Fellow at CRDEC, is currently Adjunct Professor of Chemistry at Drexel University and adjunct professor of marine chemistry in the Department of Marine Science, University of Puerto Rico, Mayagüez Campus.

Dr. Fred R. Longo received his BA degree from Villanova, his MS degree from Drexel, and his Ph. D. from the University of Pennsylvania. During the 1960's, in collaboration with Alan Adler, he discovered several convenient new syntheses for a large number of porphyrinic materials. This work permitted the avalanche of studies in which synthetic porphyrins have been used as models for heme, chlorophyll, and other natural pigments. Other areas he has contributed to include solvated electrons, transport properties in molten eletrolytes, and porphyrin chemistry. Most recently, Dr. Longo has been investigating microemulsions as hosts for the degradative hydrolysis and/or oxidation of chemical warfare agents and other toxic materials. Professor Longo is currently full professor of Chemistry at Drexel University and was appointed senior National Research Council Fellow here at CRDEC to pursue his interest in the chemistry of organized media.

BLANK PAGE

Maryalice Miller, CRDEC

MONOCLONAL ANTI-IDIOTYPIC ANTIBODIES AS TOXIN RECEPTORS

The goals of this research were to upgrade the present biotechnology capabilities of the Research Biotechnology Division through the establishment of a functional hybridoma production laboratory, and then to develop and produce monoclonal anti-idiotypic antibodies that, because of their unique structure and properties, could mimic the binding and function of actual toxin receptors. This project directly supports the U.S. Army Chemical Research, Development and Engineering Center (CRDEC) effort to develop receptor-based capacitance biosensors that possess specific pharmacologic profiles, thus enabling the development of a rapid mechanistic *in vitro* assay of cholinergic antagonists based upon receptor protein technology.

INTRODUCTION

The technique of cell hybridization or fusion can be applied to many problems in the biological and biomedical sciences. The theory of monoclonal antibody production is based on the hypothesis that each B lymphocyte within the mammalian spleen is capable of producing monospecific antibodies. Antibody-producing spleen cells have a finite life span and cannot be grown normally in culture. Tumors of these cells can be cultured easily and indefinitely. The hybridization of these two cells will produce a single cell with the antibody-producing capabilities of one parent and the eternal growth capacity of the other.

MATERIALS AND METHODS

Monoclonal antibodies that are specific for many areas on the surfaces of receptors and ion channel proteins are prepared by immunizing inbred mice with purified acetylcholine receptor, calcium and sodium channel proteins, or gamma-aminobutyric acid (GABA) receptors. These proteins were made available by Dr. Mohyee Eldefrawi of the University of Maryland Medical School, Baltimore, MD. After the initial immunizations, the mice are rested for 2 weeks, then given a booster dose of the receptor antigen. The presence of the desired antibody in the sera of immunized mice can be determined by enzyme-linked immunoassay (ELISA). The immunization period may vary from 3 to 12 weeks; this is dependent upon the immunogenicity of the receptor proteins used. Hybridization of the spleen cells from the immunized mice are made with one of three murine immortal partner cell lines (P3X-63Ag8.653, Sp2/0 Ag14, and NS-1). The cell lines were kindly donated by Dr. Matthew Pollack, of the Department of Medicine, Infectious Diseases Division, Uniformed Services University of the Health Sciences, Bethesda, MD. These cell lines are in cryogenic storage in Research Biotechnology Division's Hybridoma Repository.

Newly fused cells are grown in defined culture medium until the colonies are macroscopic in size. Culture fluid is sampled and tested in ELISA for the presence of the desired antibodies. Cells from the cultures that produce positive ELISA tests are cloned by limiting dilution technique to produce cultures that are derived from a single cell. Cloned cell lines that produce the desired antibodies can be held in cryogenic storage until needed.

Receptor-site specific monoclonal antibodies (idiotypic antibodies) produced by the first fusion can be purified and used as immunogens to induce the production of anti-idiotypic antibodies.

The functional sites of the antibodies produced in the second fusion can mirror the active sites found on the receptor proteins. Cell lines producing the anti-idiotype antibodies could be exploited as an inexhaustible supply of "receptor mimics" for use in biosensor development.

RESULTS

Progress continues to be made. The work completed to date has resulted in the establishment of a functional hybridoma production facility that can be used to the advantage and support of several current and future antibody and receptor-based detection programs in both the Research and Detection Directorates of CRDEC.

Ms. Miller received a B.S. degree in 1975 and an M.S. degree in 1979 in animal sciences at the University of Maryland, College Park, MD. She has eight years of experience in the field of human infectious and parasitic diseases and in hybridoma technology. She has been employed as a research biologist in the Biotechnology Division, Research Directorate, since July 1987.

A. Peter Snyder, CRDEC

Rapid Detection and Identification of Agents of Biological Origin by Mass Spectrometry

Pyrolysis-short column, gas chromatography-ion trap mass spectrometry (Py-GC/ITMS) was used as a tool to investigate the potential for the generation of trichothecene toxin and the generic and specific key microorganism components. In particular, short analysis times (under 6 min) and convenient, potentially portable instrumentation concepts were used. The results show that, for the first time, the major microorganism components, including the lipids and DNA/RNA nitrogen bases, could be produced and unambiguously identified, visually and analytically, during one Py-GC/MS experiment in under 6 min. This has important, transferable ramifications for portable Py-GC/ITMS instrumentation in terms of an information data base for an alarm algorithm and decision-making steps for the detection of agents of biological origin on the battlefield.

INTRODUCTION

Pyrolysis mass spectrometry (Py-MS) is currently being investigated as a candidate method for the development of a small, fieldable point detector for biological-warfare threat agents.[1]

The microbiological, medical, and biotechnological communities have taken highly complex living systems and tailored the *in vivo*/*in situ* experimental conditions to yield precise, yet trivial, response characteristics, e.g., a go/no-go, present/absent, or positive/negative analysis, expressed as a color or fluorescent change as indicators of viability and identification. Mass spectrometry, on the other hand, essentially uses a biological technique in sample interrogation and must necessarily contend with analyzing parts and pieces of these large molecular weight entities.

From an instrumental design perspective, Py-MS systems can be divided into two broad groups, namely, pyrolysis systems used in a vacuum and pyrolysis systems used at above ambient pressure. A major advantage of vacuum pyrolysis is the relative ease with which large polar or labile pyrolysis products can be detected. Unfortunately, the necessity for repetitive sample introduction through a mechanical vacuum lock is a designer's nightmare, since this greatly increases the potential for catastrophic equipment failure. An alternative approach is to introduce individual aerosol particles into the vacuum through a nozzle and skimmer arrangement. However, this imposes high pumping speed requirements, leading to greatly increased overall system weight and power consumption. Pyrolysis at ambient and superambient pressures requires subsequent transfer of pyrolysis products into the vacuum system by any of three possible routes: a semipermeable membrane, a molecular leak, or a capillary transfer line. Compared to the vacuum pyrolysis methods, all (super) ambient-pressure pyrolysis MS techniques suffer from an increased risk of losing large characteristic pyrolysis products during transfer from the pyrolysis zone to the

ionization region. This problem can be partly overcome by using atmospheric pressure ionization. However, this also tends to increase pumping requirements and further introduces widely different response factors for different classes of compounds.

The semipermeable membrane approach has been successfully used for chemical warfare agent detection, e.g., in the form of the German Mass Spectrometer (GEMS) or Mobile Mass Spectrometer (MM1) system. This method has the undisputed advantage of greatly reduced gas loads (and thus pumping requirements) while increasing operational reliability. However, the markedly high polarity and lability of many biothreat agents and/or their most characteristic pyrolysis products would seen to make it less attractive to use membranes in biodetection Py-MS systems. Finally, molecular leaks (pinholes) are easily clogged, especially under conditions where high concentrations of particulates are to be expected.

This leaves heated capillary transfer lines [gas chromatography (GC)] as an attractive way of introducing pyrolysis products into the vacuum of a mass spectrometer. Especially when using modern, fused silica capillary tubing coated with a chemically bonded, high-temperature stationary phase, high transfer efficiencies can be achieved for a wide range of chemical components while keeping pumping requirements in the low mL/min range. Furthermore, coated, capillary transfer lines offer the advantage of affording a definite degree of chromatographic separation, thereby adding a whole new dimension of chemical identification at minimal increase in cost, weight, power requirements, or overall complexity of the system.

The two main concerns in using a chromatographic separation step are: can sufficiently large and/or polar molecules be detected (the "specificity" issue), and how much time will this cost (the "response time" issue).

In addition to an instrumental method for rapid and reliable analysis of chemical agents, the Reconnaissance, Detection and Identification Master Plan mandates a similar capability for biological and toxin compounds. The key to a successful determination of presence as well as relative differentiation of a particular microbe from that of other types of microorganisms (i.e., on the genus, species, or strain level) is a knowledge of organism-characteristic biomarkers and/or patterns of organism-inherent components that are reproducibly accessible with a given instrumentation concept and not necessarily by a particular or individual piece of apparatus.

Pyrolysis-short column GC-Ion Trap Mass Spectrometry (ITMS) is explored as a rapid (<6 min) and convenient means of producing microorganism information for generic and specific discrimination. GC chromatograms of microgram amounts of different organisms provided highly similar responses for different strains with excellent reproducibility. These concepts are important for portable Py-GC/MS systems in terms of an alarm algorithm data base for the detection of agents of biological origin on the battlefield.

MATERIAL AND METHODS

Experiments were performed with the Finnigan MAT ion trap mass spectrometer (ITMS) system using a Hewlett-Packard model 5890 GC equipped with a silica capillary column coated (5-m long, 320-µm i.d.) fused with SE 30 (0.25 µm) and coupled directly to the ion trap. Pyrolysis was carried out with our split/splitless Curie-point pyrolysis reactor[2] and a Fisher Labortechnik, 1.1-MHz, 1.5-kW hf power supply. Experimental conditions were as follows: Curie-point temperature 610 °C, temperature rise time approximately 150 msec, total heating time 1 sec, split ratio 1:1, column flow 8 mL/min (He), reactor temp 300 °C, typical GC column temp program 100 to 320 °C at 40 °C/min and held isothermal for 5 min, MS interface temp 280 °C, ITMS temp 180 °C, typical MS scanning rate 1 spectrum/sec from m/z 100-620.

Fourteen, 3-day old bacteria were investigated, including the following bacilli: low virulent (LV) and virulent (V) anthracis (BA), one strain of cereus (BC), and two strains of subtilis (BS), thuringiensis (BT) and licheniformis (BL). One strain of *E. coli* (EC), *S. aureus* (SA), *Legionella pneumophila* (LP), and two strains of *Francisella tularensis* (FT) were also studied. All but one of the organisms

(*Legionella pneumophila*) were kindly supplied by Drs. Tony P. Phillips, (CDE, Porton Down, UK) and Leslie A. Shute (University of Bristol, Bristol, UK). These organisms were grown in Lab M nutrient broth for 3 days at 37 °C. The cells were harvested by centrifugation, washed with sterile, deionized, distilled H_20, and resuspended in 10 mL of similar grade H_20. The cells were killed by adding 10 mL of 6% H_20_2 and letting the suspension sit overnight. The cells were then centrifuged, washed, and freeze-dried. A 1-mg/mL suspension of *Legionella pneumophila* group I bacteria by Luc Berwald, FOM Institute, Netherlands, was heated-killed at 120 °C and then lyophilized. The 1.7-mg/mL suspensions of the organisms were prepared by adding 0.15 mL of methanol to 0.5 mg of the lyophilized bacteria, sonicating to effect a uniform dispersion and then adding 0.15 mL of deionized, distilled water. Three microliters, or approximately 5 µg of bacteria, were applied to the tip of a Curie-point wire, and the suspension dried in a stream of warm (40 °C) air.

RESULTS AND DISCUSSIONS

The toxin analyses consisted of a mixture of 100 ng each of five trichothecene toxins (deoxynivalenol, diacetoxyscirpenol, 3-acetyldiacetoxyscirpenol, T-2 tetraoltetraacetate, and T-2) and was pyrolyzed on a Py-GC-ITMS system with a temperature-programmed GC column and full mass scan information from m/z 100- 500. Figure 1 shows that all five toxins were separated, with T-2 eluting last in 2 min. Their characteristic high molecular weight and fragment reconstructed ion chromatograms (RICs), Figure 1, allow for a better degree of identification. Under similar instrumental conditions, except for a ballistic heating of the GC column, the same relative information is obtained with T-2 as the final eluting component at only 1 min.

The analysis of microorgamisms with the Py-GC-ITMS system produced a wealth of information that was found to provide orthogonal degrees/levels of microbe differentiation in terms of the complexity (i.e., organism characteristic) information and time (i.e., specific compound or group of compounds). This is a highly desirable concept, because different levels of information allow an identification/alarm software algorithm for a fieldable instrument to possess different stages of decision points with relative degrees of confidence at each stage.

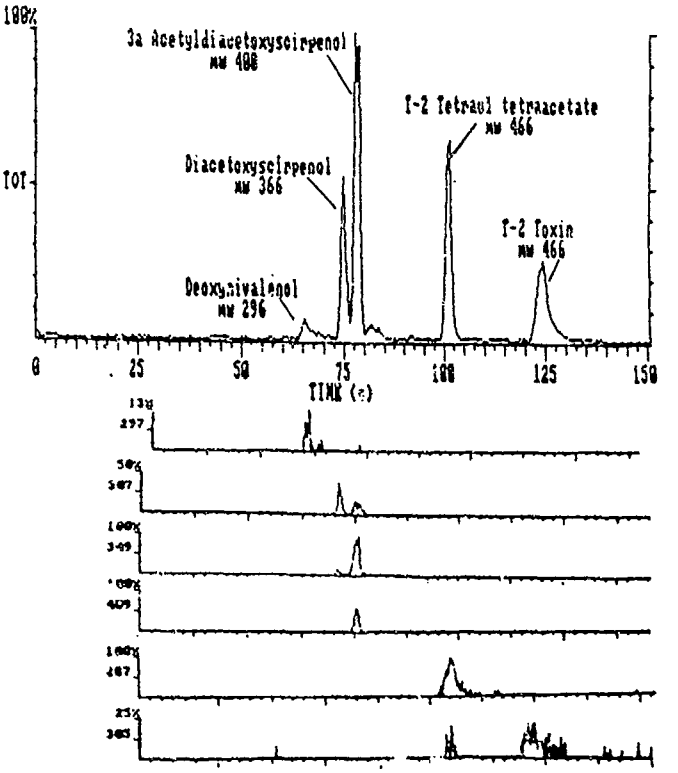

Figure 1. Toxin Elution from GC with corresponding RIC

Two to five microgram amounts of 14 different bacteria were investigated, including the following bacilli: low virulent (LV) and virulent (V) anthracis (BA), 1 strain of cereus (BC), and 2 strains of subtilis (BS), thuringiensis (BT) and licheniformis (BL). One strain of *E. coli* (EC), *S. aureus* (SA), *Legionella pneumophila* (LP) and two strains of *Francisella tularensis* (FT) were also investigated. Figure 2 presents the Py-GC-ITMS chromatograms of a virulent and a nonvirulent strain of *B. anthracis* as well as replicates. Two main regions can be discerned and lit within the 0-4.0-min and 4.5-6.0-min time domains. The last broad eluting feature is very reproducible. This is in part due to the fact that better signal sampling occurs in broader than in narrower, short-lived zones of elution. This feature is attributable to lipid/fatty acid components of high molecular weight (see below) of the microorganisms and is labeled as the lipid total ion chromatogram (TIC) region of the complete chromatograms in Figure 2.

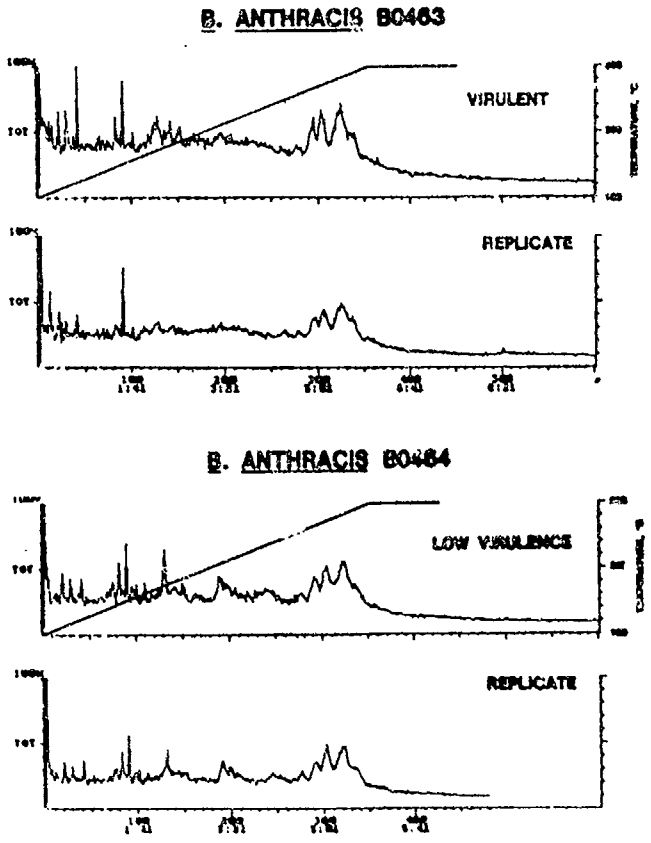

Figure 2. Lipid/fatty Acid Components of Virulent and Low Virulence *B. anthracis*

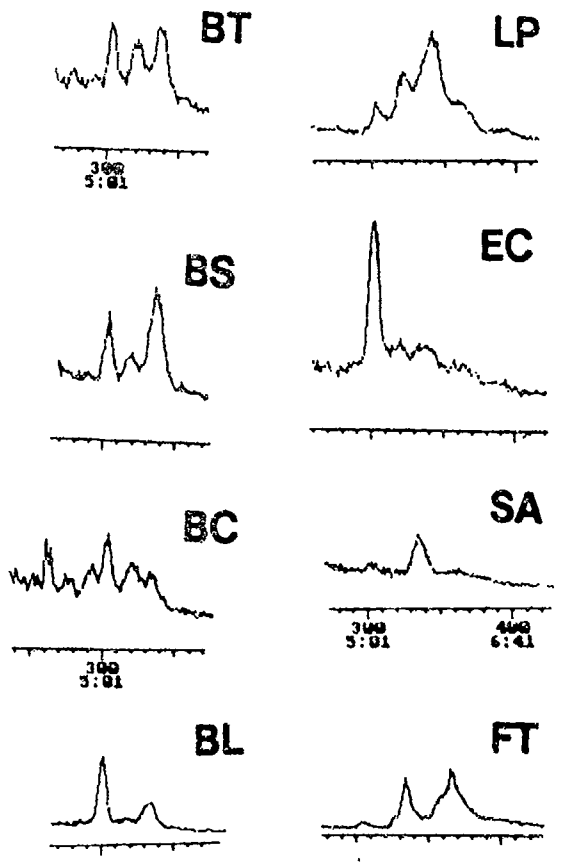

Figure 3. Lipid TIC Region of Several Bacterial Strains

Figure 3 displays the lipid TIC region from a strain of each different bacterial species and a satisfactory degree of differentiation can be achieved with just a visual analysis. The lipid TICs in Figure 3 were highly reproducible, and RIC plots of selected lipid components of high molecular weight were used to display their behavior over time (Figure 4). The m/z 494 and 508 ions varied in number of features, retention time, and relative intensity, while the m/z 522, 536, and 550 features varied only relative intensity for the 14 different organisms. Clusters of masses occurred from m/z 299 to greater than m/z 592 at regular 14 amu (methylene group) intervals and were only present in the lipid TIC envelope. This observation, along with their high boiling nature and mass spectra similar to that of lipid standards, provided good evidence that these compounds were indeed lipid.

Two separate analyses were performed on the data in Figure 4 for each organism strain. The maximum intensity of each RIC, regardless of retention time, was plotted (Figures 5 and 6), and the extracted ion mass spectra from the selected RICs were obtained (Figure 7). A satisfactory degree of organism differentiation can be achieved from a visual analysis of Figure 5. An excellent degree of reproducibility is shown in Figure 6 in that the (0) labeled data were taken in October 1987 with a Py-GC-ITMS system (40 °C/min ramp and DB-5 GC column) and the (triangle) labeled data were determined in March 1988 with an identical GC unit along with a 30 °C/min temperature ramp, an SE-30 GC column, and an ion trap detector (single MS) unit instead of the ITMS (MS/MS device). The information in Figure 7 is even more revealing in that, for each RIC series, a degree of differentiation is achieved

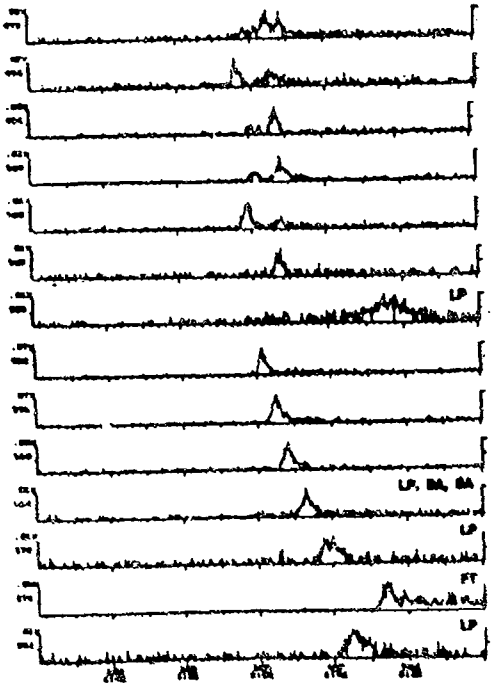

Figure 4. Representative RIC's from Lipid TIC's

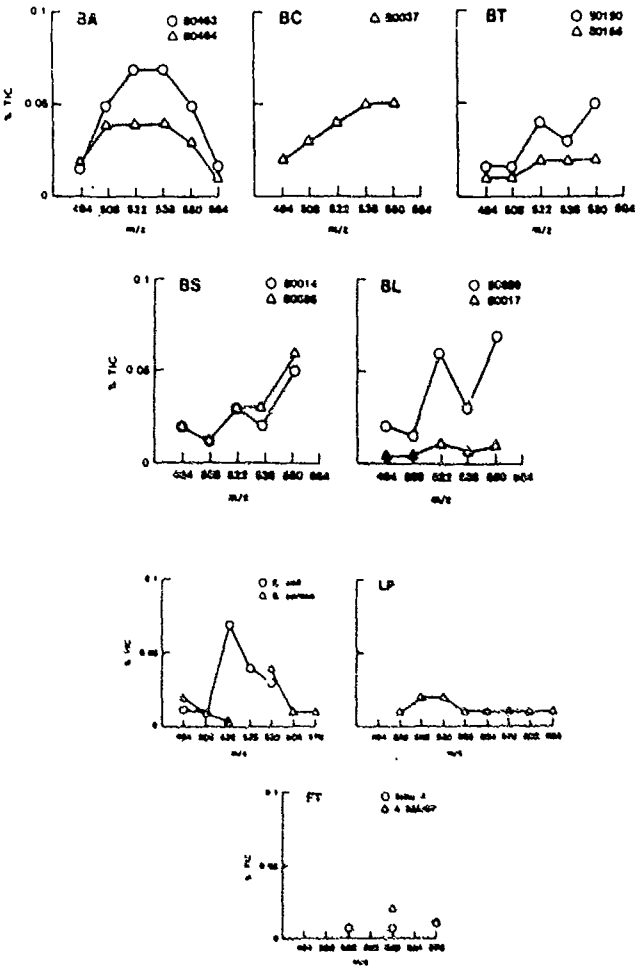

Figure 5. RIC Intensity Distribution

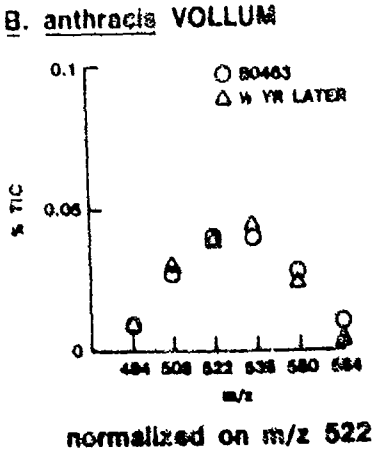

Figure 6. RIC Intensity Distribution Reproducibility

EXTRACTED MASS SPECTRA
FROM THE m/z 494 RIC

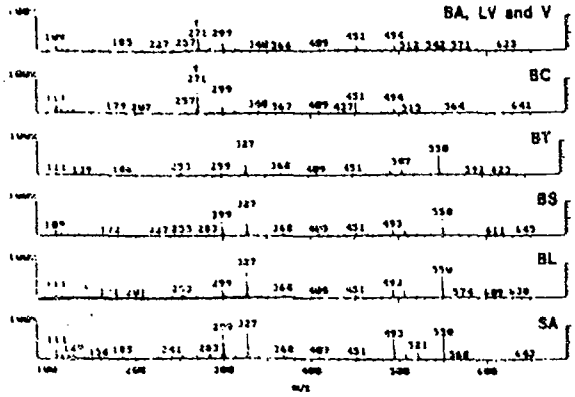

NOTE: RIC NOT PRESENT FOR LP, EC, AND FT

EXTRACTED MASS SPECTRA
FROM THE m/z 508 RIC

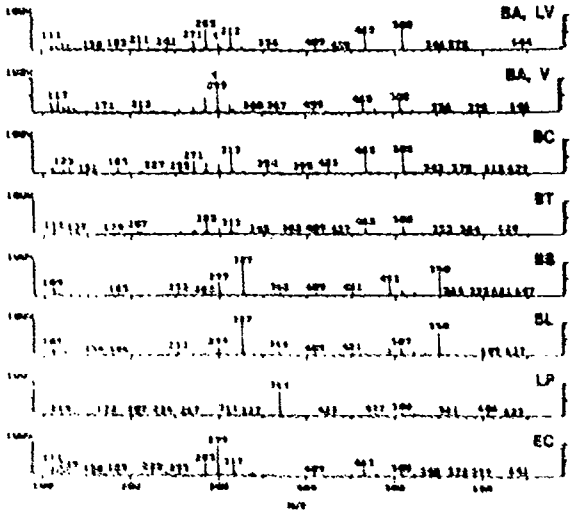

NOTE: RIC NOT PRESENT FOR BA AND FT

EXTRACTED MASS SPECTRA
FROM THE m/z 522 RIC

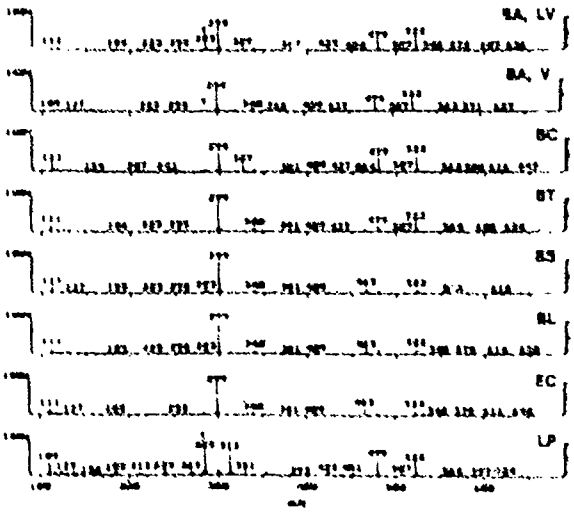

NOTE: RIC NOT PRESENT FOR BA AND FT

EXTRACTED MASS SPECTRA
FROM THE m/z 536 RIC

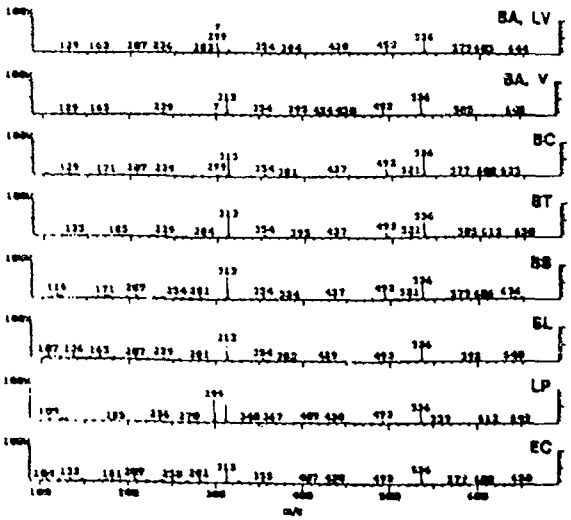

NOTE: RIC NOT PRESENT FOR BA AND FT

EXTRACTED MASS SPECTRA
FROM THE m/z 550 RIC

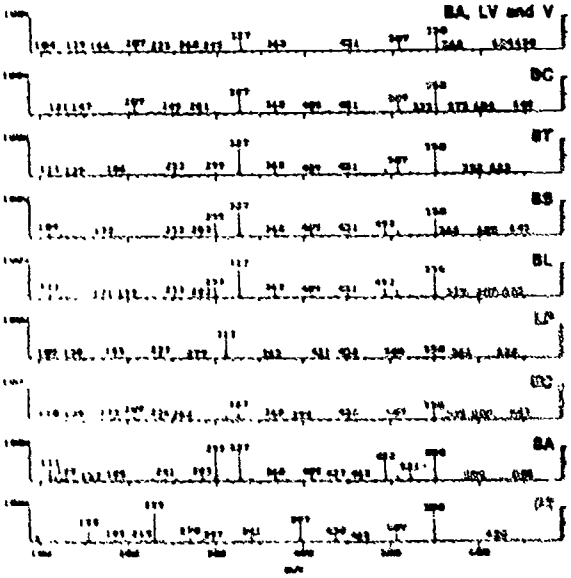

EXTRACTED MASS SPECTRA
FROM THE m/z 564 RIC

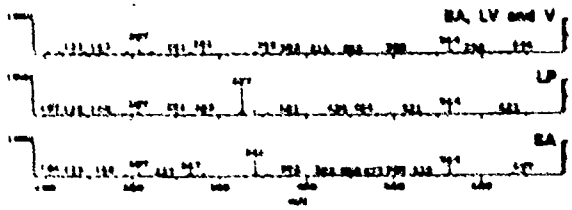

EXTRACTED MASS SPECTRA
FROM THE m/z 578 RIC

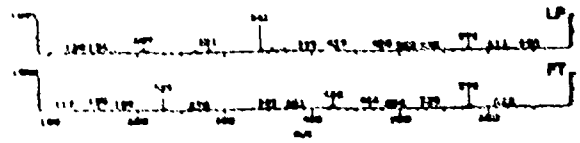

Figure 7. Extracted Ion Mass Spectra from Selected RIC's

with groups of bacteria, and direct, unambiguous and reproducible evidence is shown for the delineation of low virulent and virulent BA in the m/z 508, 522, and 536 RIC mass spectra with an under 6-min analysis per organism by Py-GC-ITMS. Bacilli can be grouped separately, depending on the RIC series, and the LP and FT organisms display quite different mass spectra in comparison to the bacilli.

Figure 8 shows an unambiguous detection of the adenine DNA/RNA base, which was identical in retention time and mass spectral content for all organisms studied. The data in Figure 9 was also obtained for every organism and provides indirect evidence of the thymine DNA base. Since all mass spectra were obtained in the m/z 100-650 range, the key m/z 59 thymine fragment was not part of the mass interrogation range. However, the m/z 126 and 135 RICs from the bacteria have the same retention times as that of the pure bases.

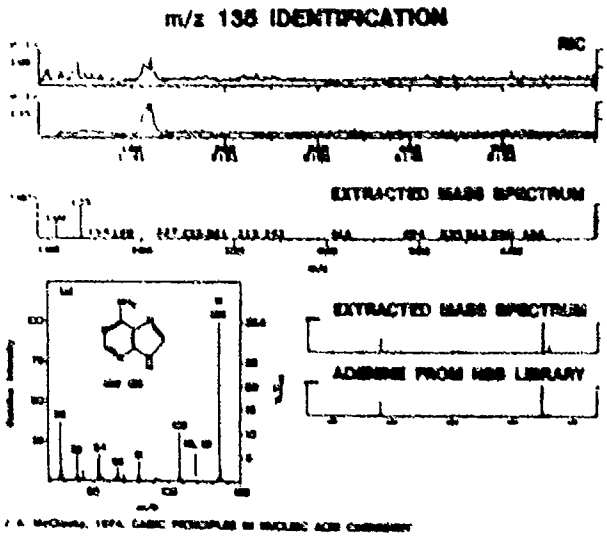

Figure 8. Unambiguous Detection of Adenine DNA/RNA Base

Figure 9. Indirect Evidence of Thymine DNA Base

CONCLUSIONS

The generation of information, such as the generic nucleic acid bases in under 2 min and the relatively more specific lipid material in 4.5-6 min, introduces attractive possibilities for computer software for decision algorithms for devices such as ion trap mass spectrometer systems. Time-dependent determination of suspect aerosol sample can occur. For example, if nucleic acid bases are not observed within minutes of a sample introduction, then another sample collection and interrogation would be in order, rather than continuing the analysis, because the decision algorithm should predict that no informative bacterial data would be obtained. With a positive DNA/RNA nucleic acid base response, the algorithm can continue interrogation on the same sample for possible high-molecular weight features in a subsequent time frame (i.e., for additional, more specific proof for the presence of bacteria). Furthermore, the MS/MS dimension could provide additional discriminative insight, especially for the species of high-molecular weight.

LITERATURE CITED

1. A.P. Snyder, W.H. McClennen, and H.L.C. Meuzelaar, "Rapid Microorganism Characterization with Pyrolysis, Short-Column GC- Ion Trap Mass Spectrometry," accepted for publication as a chapter in Proceedings of the First International Symposium on the Interface Between Analytical Chemistry and Microbiology, S.H. Morgan and A. Fox, Eds., Plenum Press, London, U.K., 1989.

2. Master Plan, Executive Summary, Reconnaissance, Detection and Identification of Chemical, Biological, and Toxin Agents, U.S. Army Chemical Research, Development and Engineering Center, Aberdeen Proving Ground, MD, and U.S. Army Chemical School, Fort McClellan, AL, August 1987 UNCLASSIFIED Report.

Dr. Snyder received a B.A. degree in chemistry from Mansfield University of Pennsylvania and then attended the State University of New York at Buffalo. In 1981, he earned a Ph.D. in inorganic chemistry from the Pennsylvania State University. He is a research chemist in the Spectroscopy Group, Analytical Division, Research Directorate, CRDEC.

Lynn Hoffland, Ronald Piffath, CRDEC, and Sterling Tomellini, University of New Hampshire

DEVELOPMENT OF ANALYTICAL PROTOCOLS AND AN EXPERT SYSTEM FOR EVALUATING AGENT DECONTAMINATION IN COMPLEX MATRICES

By combining infrared spectroscopy with an expert system, screening of unknown materials for the existence of specific chemicals will be facilitated. The expert system will identify trace levels of these specific chemicals in complex matrices (i.e., soils, leaves, sludge, etc.).

INTRODUCTION

The purpose of this project was to produce a working expert algorithm for screening unknowns in the infrared spectral region for trace amounts of chemicals of Army interest.

This work has been a joint project with Dr. Stirling Tomellini of the University of New Hampshire, (UNH). The algorithm was developed by Dr. Tomellini and tested at U. S. Army Chemical Research, Development and Engineering Center (CRDEC) on several different matrices.

METHODS

The algorithm developed would be an extension of a Program for Analysis of Infra Red Spectroscopy (PAIRS) that is used for identifying chemical functional groups in an infrared spectrum. The algorithm would be trained to identify several different chemicals in a complex matrix (soil, leaves, sludge, etc.) in trace quantities. The program will run on a PC (IBM compatible) and on the computer data system that controls the infrared spectrometer. The program will then be tested on several real world samples.

RESULTS

To date, 70 spectra have been sent to Dr. Tomellini, and he has plotted and checked them out. He has developed an improved user interface for the microcomputer (PC) version of PAIRS to allow the chemist to use the results of a spectral interpretation more efficiently. This advanced version was supplied to CRDEC in March, 1988 for testing.

The advanced microcomputer version of PAIRS was ported to the Nicolet 620 via a VAX 8600 at the University of New Hampshire (UNH). Appropriate modifications were made to PAIRS to allow it to run on the Nicolet 620. This system runs the Fourier Transform infrared spectrometer "FTIR" at CRDEC and UNH.

Programs have been developed to allow spectral data to be transferred directly from Nicolet DX and Nicolet SX FTIR software, (different instruments at CRDEC) to PAIRS compatible data files. This will significantly affect the generation of interpretation rules for compounds of interest to CRDEC.

An interface has been delivered to CRDEC to dump spectral files from three different infrared spectrometers to a microcomputer. This will allow this expert software to operate on any spectra generated in the spectroscopy laboratory at CRDEC.

In 1972, Dr. Hoffland received a B.A. degree in chemistry from Wartburg College, IA, and an M.S. in 1975 and a Ph.D. in 1980, in chemistry, from Northwestern University, IL. He has been at CRDEC since 1981 as a research physical scientist in the Analytical Research Division of the Research Directorate.

Wayne G. Landis and Mark V. Haley, CRDEC

REDUCTION OF THE IMPACT OF CHEMICAL POLLUTANTS BY DEGRADATIVE ORGANISMS

Dibenz-1,4-oxazepine (CR), a strong sensory irritant, has previously been reported as recalcitrant to degradation. Recently isolated bacteria show potential as a tool for the degradation of CR waste. Microcosms were prepared with soil samples taken from three locations around Aberdeen Proving Ground, MD. The microcosms were spiked with CR and placed in a darkened chemical exhaust hood for 3 mo. Water samples (2 mL) were taken from the microcosms and plated on nutrient agar spiked with CR, replica plating onto successively higher concentrations selected for organisms tolerant to CR. Bacteria isolates were found that have an extremely high tolerance to CR (200 mg/L). The isolated bacteria, identified as *Alcaligenes denitrificans denitrificans* strain CR-1, grows well on the microcosm media spiked with 200 mg/L of CR, but shows minimal growth on the microcosm media without CR. After 24 days the organisms are able to reduce the CR concentration from 150 mg/L to below 5 mg/L. Reduction ... toxicity of a CR solution treated with *A. denitrificans* CR-1 in standard *Daphnia magna* and algal toxicity tests has been demonstrated.

INTRODUCTION

Hazardous waste is a growing problem for our society. Biodegradation and its enhancement through biotechnology has been recognized as a potential tool for the remediation of hazardous waste. The Department of Defense, including the Army, has a tremendous hazardous waste disposal and remediation problem that ranges from the disposal of hundreds of thousands of pounds of contained waste to 400 to 800 sites needing remediation. Buildings must be decontaminated and disassembled. Soils and sediments are contaminated with a variety of toxic materials. The same types of materials are found at a variety of installations such as Rocky Mountain and Pine Bluff Arsenals. Cost of the clean up has been estimated to be 5 to 10 billion dollars over the next 10 years. Biodegradation and bioremediation hold the promise, yet unfulfilled, of detoxifying or degrading toxic materials at a lower cost than conventional methods.[1] Our program is an attempt to provide U. S. Army Chemical Research, Development and Engineering Center (CRDEC) with the technology to supply leadership in this arena.

The riot control material CR, is a persistent material that is highly toxic to a variety of aquatic organisms (Dennis W. Johnson, CRDEC unpublished data). CR was taken as a model compound for our studies on degradation of materials of military interest. In addition, theoretical studies were conducted to examine strategies of biodegradation based on the continuum of environments (Figure 1) and resource competition theory.

MATERIALS AND METHODS

CR was obtained from stock containers located at Pine Bluff Arsenal, Pine Bluff, AR. This material is the feedstock used in mixing for application as a riot control material.

Selection of a media was a two-step process. First, it was desired that a CR-degrading organism would be able to survive in a freshwater aquatic environment. Therefore, the media used in the Standardized Aquatic Microcosm assay (SAM media) consisting of mineral salts was chosen.

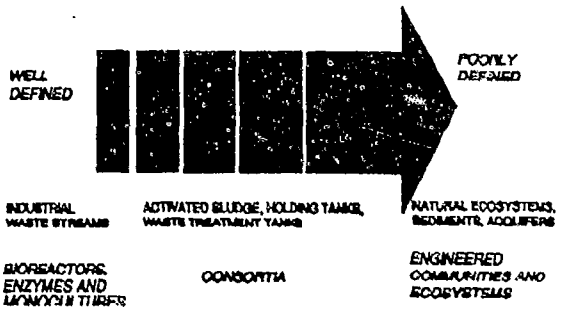

FIGURE 1. THE CONTINUUM OF ENVIRONMENTS IN XENOBIOTIC DEGRADATION
A wide variety of environments means that in order to eliminate toxic materials a variety of strategies must be employed. In waste streams from process plants an immobilized enzyme or bacteria in a bioreactor may prove sufficient. As complexity grows a single organism may not be bale to survive or compete in the contaminated environment. In order to clean up ecosystems an ecosystem level approach may have to be undertaken, incorporating a variety of organisms and trophic levels.

Soil and sediment samples from the Edgewood Area of the Aberdeen Proving Ground were inoculated into jars filled with SAM media containing 20 mg/L of CR and placed in the dark for 90 days. Two-mL water samples were then placed on agar plates spiked with CR. Replica plating onto successively higher concentrations of CR was then performed up to a concentration of 200 mg/L. The surviving organism was then examined for the ability to grow, using CR as a carbon source with the concentration of CR followed by liquid chromatography (LC). In further experiments, the degradation of possible intermediates of CR degradation, *o*-nitrophenol, cresol, catechol, and 3-methyl catechol, was examined.

Identification of the isolate CR-1, GC analysis of the phospholipids and more conventional metabolic and cytological methods were employed.

In examining the aquatic toxicity of the CR solution after partial degradation by the candidate bacterium, a stock solution of CR was inoculated 8 days before testing. A *D. magna* 48-hr toxicity test and a 96-hr algal toxicity test using *Selenastrum capricornutum* were conducted with the resultant solution according to current American Society for Testing and Materials (ASTM) methods.

The theoretical work was based on the resource competition models of Tilman[2] as applied to environmental toxicology by Landis.[3]

RESULTS

Following a 90 day incubation and isolation using successively higher concentrations of CR, an isolate was obtained that appeared resistant to CR toxicity. A gram negative motile bacterium (Figure 2) identified by several methods as *A. denitrificans denitrificans* (Figure 3), was able to degrade CR. After 21 days the organism reduced the CR concentration to below detectable limits using LC (Figures 4 and 5). The organism was also found to degrade the proposed intermediates *o*-nitrophenol, 3-methylcatechol, and catechol (Figure 6). Cresol, however, was not degraded, although efforts were made using both *in vivo* and *in vitro* methods.

FIGURE 2. SCANNING ELECTRON MICROGRAPH OF *ALCALIGENES DENITRIFICANS*
The bacterium is a gram negative rod of approximately 2 by 0.5 microns.

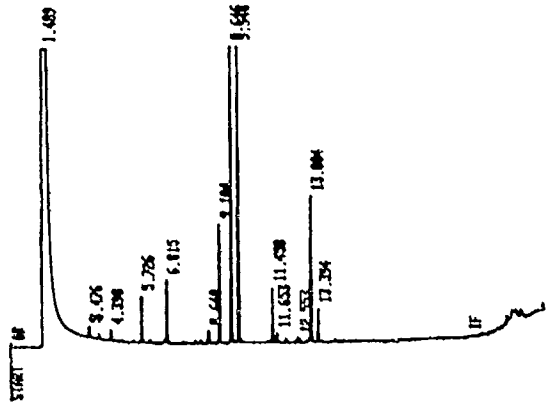

FIGURE 3. GC FATTY ACID ANALYSIS BY MICROBIAL I.D. INC. This analysis was used along with conventional metabolic and cytological methods to identify CR-1 as *A. denitrificans denitrificans*. Alcaligenes is a widely distributed soil and aquatic bacterium known for its ability to degrade a variety of xenobiotics.

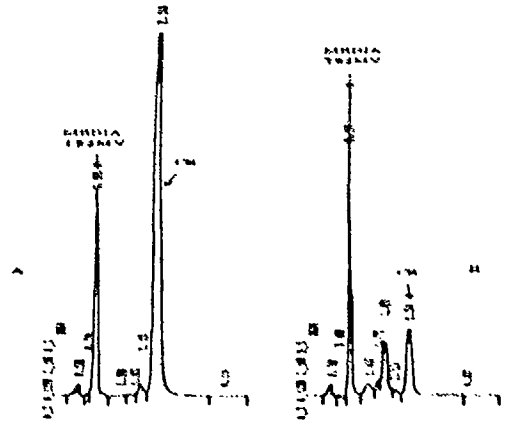

FIGURE 4. EXAMPLE OF A CHROMATOGRAM DEMONSTRATING THE DEGRADATION OF CR COMPARED TO CONTROLS Sam media containing CR and the *A. denitrificans* showed a significant decrease compared to controls not inoculated with *A. denitrificans*.

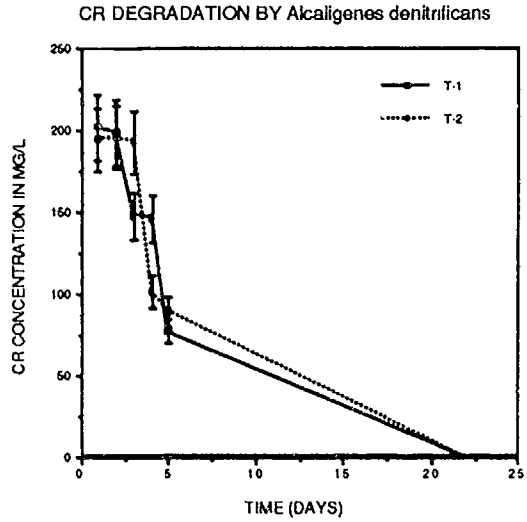

FIGURE 5. REDUCTION OF CR IN SAM MEDIA OVER A 23 DAY PERIOD CR was reduced to below detectable levels in the replicates containing the *A. denitrificans* isolate.

A. denitrificans was not harmful to controls in the 48-hr *D. magna* assay to examine toxicity reduction of a CR solution. After 8 days, the *A. denitrificans* was able to reduce the toxicity of CR by over 50%. In the 96-hr algal assay, the solutions inoculated with CR actually exhibited an enhancement of algal growth (Figure 7).

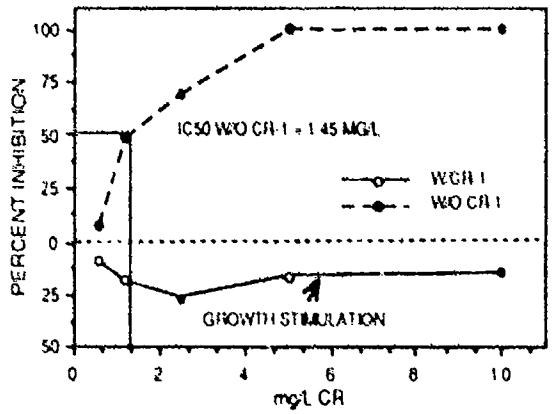

FIGURE 7. REDUCTION OF THE TOXICITY OF A CR SOLUTION BY A. DENITRIFICANS AS MEASURED BY THE 96 HR ALGAL TOXICITY TEST After a 5 day incubation period the CR solution inoculated with *A. denitrificans* reduced the toxicity of the material until it enhanced algal growth.

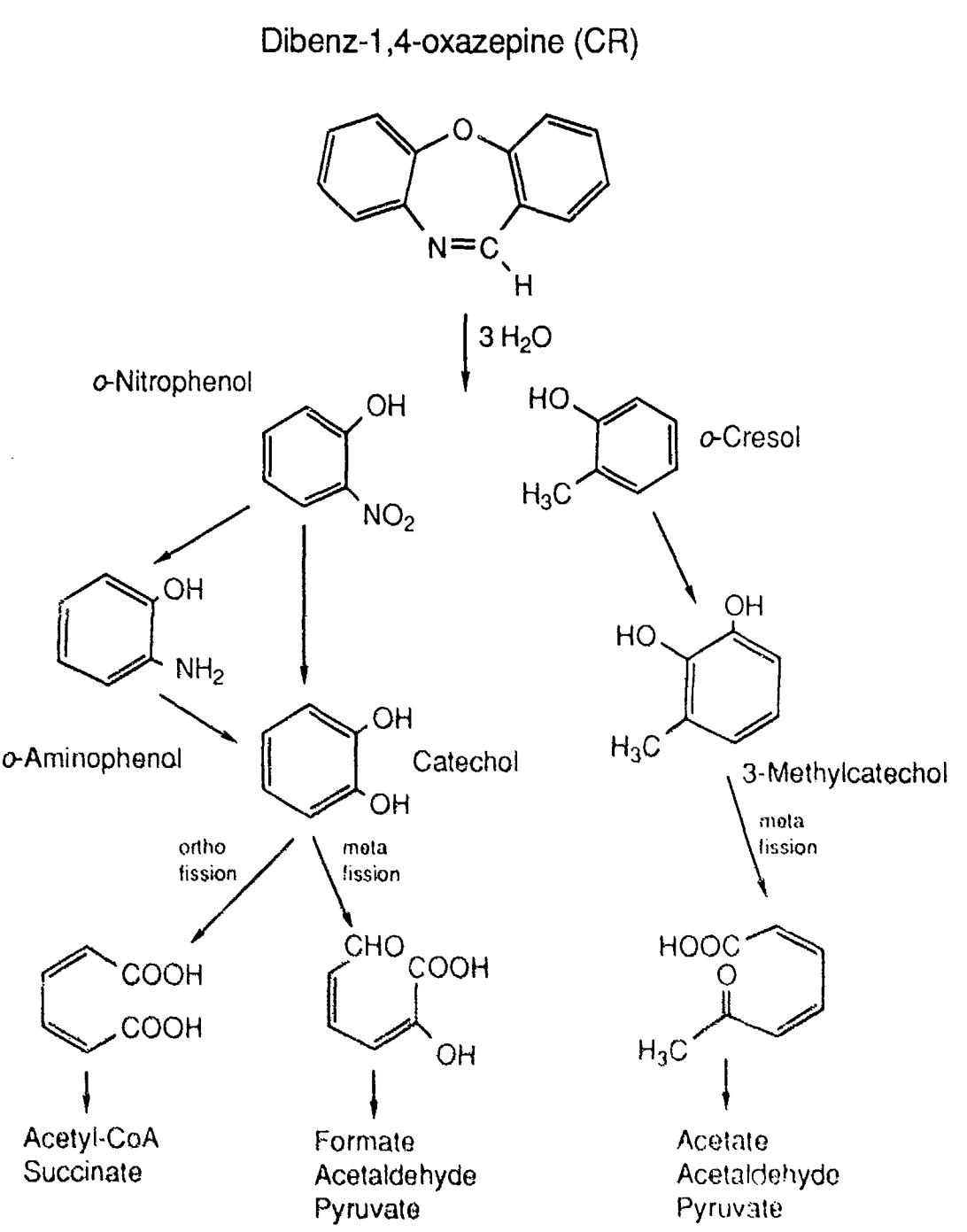

FIGURE 6. PROPOSED DEGRADATION PATHWAY FOR DIBENZO-1,4-OXAZEPINE
Originally proposed by J. DeFrank, the metabolism of the intermediates *o*-nitrophenol and catechol have been confirmed by M. V. Haley. However, cresol degradation has not been seen using both *in vivo* and *in vitro* methods. 3-Methyl catechol is degraded.

The resource competition models demonstrated that in situations of low xenobiotic concentration introduced degradative organisms may not be able to compete with naturally occurring microorganisms using alternate substrates. With the ratio of natural substrate to xenobiotic as in region 1(Figure 8), very little of the xenobiotic will be degraded before the introduced organism becomes extinct. In region 4 the degradative organism will quickly become extinct. However, in areas where the xenobiotic concentration is high but the natural substrate lower, regions 3 and 5, degradation of the xenobiotic may be almost complete and efficient.

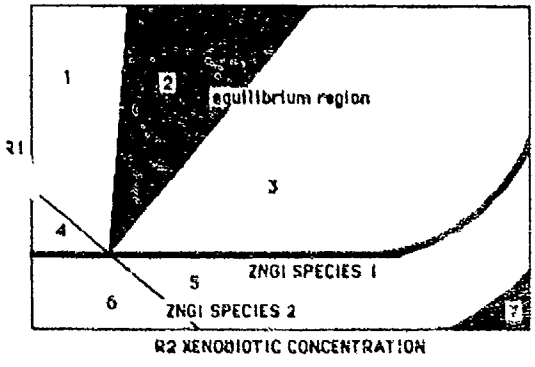

FIGURE 8. RESOURCE COMPETITION DIAGRAM FOR XENOBIOTIC DEGRADATION
The diagram is based on the resource competition models of Tilman with modifications to represent competition with one of the resources as a recalcitrant xenobiotic. With the ratio of natural substrate to xenobiotic as in region 1, very little of the xenobiotic will be degraded before the introduced organism becomes extinct. In region 4 the degradative organism quickly becomes extinct. In areas where the xenobiotic concentration is high but the natural substrate low, regions 3 and 5, degradation of the xenobiotic will occur.

DISCUSSION

The degradation of the riot control material CR has been demonstrated. Although unusual in many respects, CR can be degraded by a bacterial genus known for degradation of chlorinated aromatics and other materials.[4,5] Not as well characterized as the psuedomonads, Alcaligenes is a hardy genus known from both terrestrial and aquatic environments.[6] An important finding is that *A. denitrificans* is capable of degradation under conditions simulating a typical aquatic aerobic environment. Although more research is necessary for definitive answers, it seems possible to select for degradative organisms capable of surviving in natural environments. If found to be competitive with the natural flora, degradation in situ should prove workable. Another important finding is that *A. denitrificans* is not harmful to *D. magna* and also reduces the toxicity of the CR solution. Toxicity has not been totally eliminated and a consortia may be needed to degrade the metabolites to reduce the toxicity to acceptable limits.

Also significant is the work demonstrating the ratio of toxic xenobiotic to other natural substrates in determining the rate and outcome of degradation in a mixed culture. At low concentrations of xenobiotic, there may simply not be enough to allow the organism to survive in competition with native organisms. It might be necessary to use a cometabolism strategy to ensure degradation.

This program is ripe for further research and application. In FY89 we are planning to conduct a SAM assay to explore community level effects of CR degradation by *A. denitrificans*. A model bioreactor will be constructed using a porous substrate to examine the potential for CR demilitarization (Figure 9). The genetics and physiology of the degradation of *A. denitrificans* is now being explored. Finally, the resource competition models will be further developed and applied to understand the theoretical ecological framework of microbial degradation.

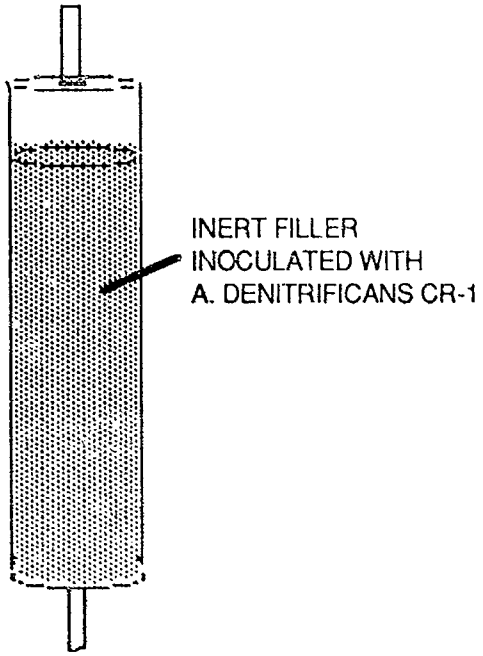

FIGURE 9. SCHEMATIC OF A CR BIOREACTOR It should prove fiesable to construct a bioreactor able to detoxify CR using *A. denitrificans* immobilized to a diatamaceous substrate. Such bioreactors may prove to be an inexpensive substitute to incineration for the destruction of hazardous materials.

CONCLUSIONS

- An organism has been isolated that is able to degrade the riot control material CR in a media modeled after a freshwater ecosystem.
- The responsible organism has been identified as *A. denitrificans* strain CR-1.
- In addition to CR, the organism also degrades nitrophenol and catechol.
- *A. denitrificans* can reduce the toxicity of a CR solution.
- *A. denitrificans* does not exhibit harmful effects to *D. magna*.
- Competitive interactions between degradative organisms and the natural flora may inhibit degradation *in situ* depending upon the xenobiotic to natural resource ratio

LITERATURE CITED

1 Reducing Risks from Environmental Chemicals Through Biotechnology Workbook, Office of Technology Assessment, OTA-BA-360, **1987**.

2. D. Tilman, Resource Competition and Community Structure, Princeton University Press, Princeton, NJ, **1982**.

3. W.G. Landis, "Resource Competition Modeling of the Impacts of Xenobiotics on Biological Communities," In Aquatic Toxicology and Environmental Fate: Ninth Volume , ASTM STP 921, pp 55-72, J. M. Poston and R. Purdy Eds., American Society for Testing and Materials, Philadelphia, PA, **1987**.

4. K. Furukawa, F. Matsumura, and K. Tonomura. "Alcaligenes and Acinetobacter Strains Capable of Degrading Polychlorineated Biphenyls," *Agric. Biol. Chem.* Vol. 42, pp 543-548 (**1978**).

5. F. Westmeier, and H. J. Rehm, "Degradation of 4-Chlorophenol in Municipal Wastewater by Adsorptive Immobilized Alcaligenes sp. A 7-2," *Appl. Microbiol. Biotechnol.* Vol. 26, pp 78-83 (**1987**).

6. K. Kersters, and J. De Ley, "Genus Alcaligenes Castellani and Chalmers 1919, 936," pp 361-373 In Bergey's Manual of Systematic Bacteriology, Vol 1, Eds N. F. Krieg and John G. Holt. Williams and Wilkins, Baltimore, MD, **1984**.

Dr. Landis has been at CRDEC since the spring of 1982 and is currently the Leader of the Ecological Toxicology Group in Environmental Toxicology Branch. After receiving his doctorate from Indiana University, Bloomington, IN, in 1979, he has made significant contributions in the field of aquatic toxicology, the ecology and genetics of protozoa, and the characterization of the organophosphate acid anhydrases (OPA). He has recently co-edited with W. Adams and G. Chapman the book Aquatic Toxicology and Environmental Fate: Tenth Volume published by the American Society for Testing and Materials.

Mr. Haley is a 1981 graduate of Millersville State University and has been a part of the Ecological Toxicology Group since April of 1982. He has played a major role in the implementation of the Standardized Aquatic Microcosm as a standard bioassay at CRDEC. Recently, Mr. Haley published several papers on the aquatic toxicity of heavy metals and the elucidation of the organophosphate acid anhydrases (OPA).

BLANK PAGE

Yu-Chu Yang, CRDEC

PHOTOCATALYTIC OXIDATION OF MUSTARD USING SEMICONDUCTOR OXIDES

The photooxidation of mustard (2, 2'-dichlorodiethyl sulfide) has been investigated in dilute solutions of 0.01 M in acetonitrile under ambient conditions. In the presence of 1mg/mL of titanium(IV) dioxide (TiO_2) after 24 hrs of irradiation at 350 nm, about 50% of the original mustard was converted to produce primarily mustard sulfoxide. A simultaneous photolysis also occurred, and additional products formed from free radical intermediates were identified. In the absence of the photocatalyst, mustard was photo-activated at 350 nm to react with oxygen dissolved in acetonitrile to form almost exclusively mustard sulfoxide.

INTRODUCTION

Since the awareness of fossil-fuel shortages in the seventies, a great deal of research has been directed towards the generation of electricity and fuels from sunlight. A number of semiconductor oxides have since been identified as catalysts that can be photo-activated to produce electron-hole pairs. These oxides also promote photooxidative reactions of organic molecules containing electron-donating functional groups in solution by an interfacial electron-transfer process.[1] Until recently, the above principle has not been applied to the decontamination of chemical agents. ARO-sponsored researchers. M.Gratzel and M. A. Fox showed that irradiated titanium(IV) oxide (TiO_2) could convert oxygen adsorbed on its surface to reactive superoxide anion. As a result, both the hydrolysis of a G-agent simulant[2] and the oxidation of unsaturated hydrocarbons[3] are catalyzed by photoactivated titania powders. In addition, Davidson and Pratt also demonstrated that a series of alkyl sulfides were oxidized to primarily sulfoxides and sulfones by the same method.[4]

It is the purpose of this project to investigate the oxidative degradation of mustard with air and sunlight on titanium oxide surfaces as a potential decontamination method. The method is of particular interest because air is being activated as the reactive oxidant; that transportation of unstable oxidants to the field is eliminated. The conversion of mustard and its simulants will be measured as a function of light irradiation and solvent property. The major reaction products will be identified and accurately quantified by GC, NMR, and GC/MS techniques. The following Scheme is proposed for the photooxidation of 2-chloroethyl sulfides ($RSCH_2CH_2Cl$ where R = $ClCH_2CH_2$ for mustard, CH_3 for CEMS) in general:

$$TiO_2 \xrightarrow{h\nu} e^- + h^+ \quad (1)$$

$$RSCH_2CH_2Cl + h^+ \longrightarrow RS^+\cdot CH_2CH_2Cl \quad (2)$$

$$RS^+\cdot CH_2CH_2Cl + O_2 \longrightarrow RS^+ CH_2CH_2Cl \quad (3)$$

$$O_2 + e^- \longrightarrow O_2^{-}\cdot \quad (4)$$

$$RSCH_2CH_2Cl + RS^+\cdot CH_2CH_2Cl + O_2^{-}\cdot \longrightarrow 2\,RSCH_2CH_2Cl \quad (5)$$

$$RS^+\cdot CH_2CH_2Cl + e^- \longrightarrow RSCH_2CH_2Cl \quad (6)$$

$$O_2^{-}\cdot + h^+ \longrightarrow O_2 \quad (7)$$

Scheme. Mechanism of Photooxidation of $RSCH_2CH_2Cl$ on TiO_2 Surface

EXPERIMENTAL METHODS

Material

Mustard was a distilled product. Gold-labelled titanium(IV) oxide (TiO_2) at 99.99% purity was obtained from Aldrich Chemical Company. The ^{13}C labelled CEMS was kindly prepared by Dr. Sankar Lal of Drexel University. HPLC grade acetonitrile(CH_3CN) and distilled water were used for the solvents. Mustard sulfoxide was prepared by adding mustard dropwise to an excess of concentrated nitric acid.[5] A white crystalline solid was obtained as the sulfoxide after all the liquid was evaporated at room temperature.

Photooxidation

A Rayonet Photochemical Chamber Reactor (Model RPR-100) was used for photooxidation. The reactor is equipped with 16 "black light" lamps of 24 watts. More than 90% of the intensity of the irradiated light is at 350 nm. At the center of the reactor chamber, where a pyrex reactor tube is placed, the black light irradiation is about 9200 microwatts/cm^2. An air-driven magnetic stirrer is installed in the reactor chamber base. An internal cooling fan keeps the chamber temperature within a 40-44 ^oC range when all the lamps are turned on.

To a 10-mL solution of 0.01 M sulfide in a pyrex reactor tube (8 in. long x 13 mm ID) was added 10 mg of TiO_2. The mixture was then sonicated for 15 min to form a uniform suspension. The tube was tightly closed with a ground-glass stopper and placed in the center of the reactor chamber. The lamps, stirrer, and fan were then turned on and reaction time was recorded. Some of the reaction mixture, 1 to 2 mL, was removed at specific sampling times. The titanium oxide particles were filtered out of the sample by using a 0.45 μm syringe filter. *n*-Octane was added to each of the liquid samples as an external standard (ES) for quantitative determination of the conversion of mustard with an HP 5880A GC. A Finnigan 5100 GC/MS instrument was used to further identify additional products in the samples. The ^{13}C NMR analyses of the simulant samples were made with Varian XL200 and Varian VXR-400s superconducting FTNMR instruments.

RESULTS AND DISCUSSION

PHOTO-INDUCED AIR OXIDATION OF MUSTARD

The simultaneous disappearance of mustard (HD) and appearance of mustard sulfoxide (HD=O) as a function of irradiation time at 350 nm are illustrated in Figure 1. During the first 12 hrs only a trace amount of sulfoxide was produced. But after 24 hrs of irradiation, half of the initial mustard was reacted to form primarily sulfoxide. The maximum rate of reaction was about 3.3×10^{-4} M/min between 12 and 36 hours. Beyond 36 hrs of irradiation, the yield of sulfoxide reduced and additional products were observed. The chromatogram of the reaction mixture at 36 hrs is shown in Figure 2.

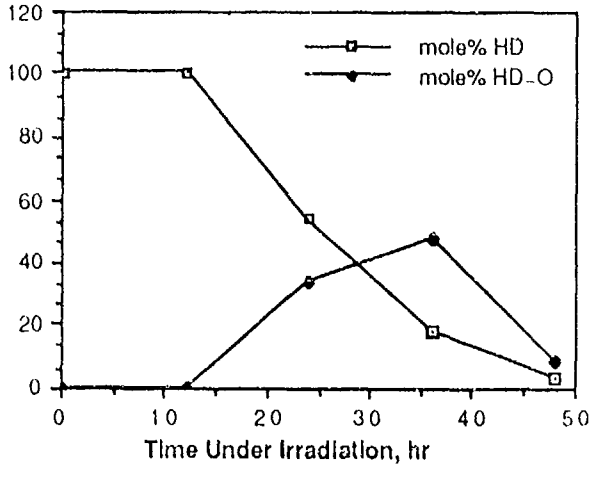

Figure 1. HD (0.01 M) in Acetonitrile with 1 mg/mL of TiO_2

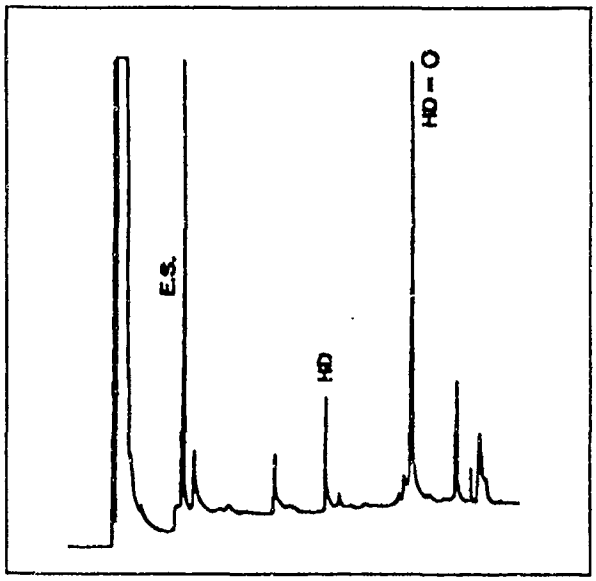

Figure 2. HD in CH_3CN/TiO_2 after 36 Hours of Irradiation at 350 nm

To measure the sulfoxide yield quantitatively, a concentrated sample containing 0.6 M pure mustard sulfoxide in acetonitrile was analyzed to detect any decomposition at elevated temperatures in the GC instrument.[6] Mustard was partially regenerated from the sulfoxide. Our result is consistent with that obtained by previous investigators who detected mustard in the distillate of sulfoxide under vacuum.[5] Identifications of additional products were accomplished by GC/MS in (Table 1). Different from reports in the literature, mustard sulfone, $(ClCH_2CH_2)_2SO_2$, was not formed in any significant amount due perhaps to the lack of excess oxygen in the atmosphere. Instead, mustard disulfide, $(ClCH_2CH_2)_2S_2$, was positively identified by comparison with the GC/MS characteristics of a pure sample. The disulfide was produced apparently from photolysis of the S-C bonds. These results suggest that both photocatalysis and photolysis reaction paths are present.

To verify the above result, a comparative study was made with a ^{13}C-enriched mustard simulant, $^{13}CH_3SCH_2CH_2Cl$ (CEMS), so that sample analysis can be independently accomplished by ^{13}C NMR methods. Tables 2

Table 1. Photooxidation of HD on TiO_2 Surface in CH_3CN After 12 Hours of Irradiation

Compounds	GC/MS-CI area%
MW=59	11.3
HD	41.2
$NCCH_2SCH_2CH_2Cl$	1.6
$Cl_2C_2H_3SCH_2CH_2Cl$	4.6
$ClCH_2CH_2S\text{-}SCH_2CH_2Cl$	9.0
$NCCH_2S\text{-}SCH_2CH_2Cl$	2.5
$ClCH_2CH_2S(=O)CH_2CH_2Cl$	7.4

and 3 list seperately the ^{13}C NMR and GC/MS analyses of the products identified as a function of irradiation time. As shown Figure 3, the simulant reacted faster, but product patterns similar to that of HD were observed. It was reported previously that the oxidation rate of a sulfide molecule increased with the nucleophilicity of the sulfur atom.[7] There are two electron-withdrawing chloroethyl groups in mustard, resulting in a lower nucleophilicity of the sulfur atom than that in CEMS. Therefore, CEMS oxidizes faster than HD. In the case of photooxidation, the same trend has been observed. However, the rate behaviors shown in Figure 2 seem to indicate that the maximum rates of both compounds were about the same. This may mean that a common rate-determining step, perhaps a diffusion process at the liquid-solid interface, is present for both reactants.

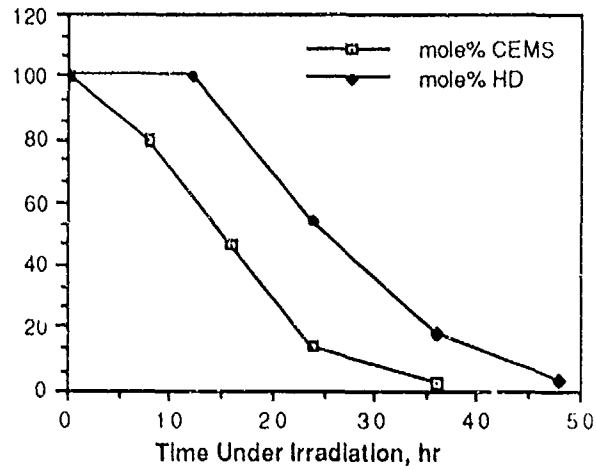

Figure 3. Sulfide (0.01 M) in Acetonitrile with 1 mg/mL of TiO_2

Table 2. Photooxidation of CEMS on TiO_2 Surface in Acetonitrile

(^{13}C NMR Analysis of Products, mole% product per mole CEMS reacted [a])

Z (Product = $^{13}CH_3$-Z)

	-S	-S[+b]	-S=O	-S(=O)$_2$	-O-	=O	others
NMR shifts (ppm)	*15.0*	*21.8 23.2*	*38.6*	*39.3*	*50.4*	*50.6*	*160's*
Time exposed to light, hr.							
0	100						0
8	80	2	7	3	-	-	7
16	46	4 10	19	3	5 2	-	11
24	14	5 12	34	10	6 3	6 4	6
36	2	2 1	4	43	2 1	6 10	25
24 [c]	3	-	42	28	3	8	17

[a] Integrated area of the carbon atom adjacent to nitrogen in acetonitrile (CH_3CN, *117 ppm*) was used as the internal standard.

[b] may be the disulfides $^{13}CH_3SSCH_2CN$ and $^{13}CH_3SSCH_2CH_2Cl$ shown in Table 3.

[c] no TiO_2

Table 3. Photooxidation of CEMS on TiO_2 in CH_3CN

GC/MS analysis

Irradiation Time, hr	*24*		*36*
Compound	CI area%	EI area%	EI area%*
$^{13}CH_3S\ S^{13}CH_3$	2.5	1.5	
MW=59	9.8	1.4	
$^{13}CH_3SCH_2CH_2Cl$	4.3	17.2	3.9
$^{13}CH_3SCH_2CN$	3.6	1.3	2.5
$^{13}CH_3SC_2H_3Cl_2$	5.2	5.5	4.5
$^{13}CH_3S\ SCH_2CN$	2.0	1.2	3.1
$^{13}CH_3S$-SCH_2CH_2Cl	15.5	21.2	7.1
$^{13}CH_3S(=O)CH_2CH_2Cl$	28.0	21.7	4.0
$^{13}CH_3S(=O)_2CH_2CH_2Cl$	0.9	0.6	
$^{13}CH_3S(=O)\ S(=O)CH_2CH_2Cl$	2.4	3.3	2.1
$ClCH_2CH_2S$-SCH_2CH_2Cl	9.1	20.0	5.3
$NCCH_2S$-SCH_2CH_2Cl	1.7	2.0	3.2
Trichloroethane	-	-	10.3
MW=144(1 Cl)			3.4

* plus many more unidentified compounds in small quantities MW=94(1 Cl), 130, 138, 122, 102, 80, 161(2 Cl), 169(2 Cl), 111, 148, etc.

Table 4. Photooxidation of 0.01 M CEMS in CH_3CN After 24 Hours Irradiation at 350 nm

Compound	GC/MS-EI, area%
MW=59	36.3
MW=115 (1 Cl)	8.2
$^{13}CH_3SCH_2CH_2Cl$	10.6
$^{13}CH_3SC_2H_3Cl_2$	1.0
$^{13}CH_3S$-SCH_2CH_2Cl	7.1
$^{13}CH_3S(=O)CH_2CH_2Cl$	23.8
$^{13}CH_3S(=O)_2CH_2CH_2Cl$	4.0
$^{13}CH_3S(=O)$-$S(=O)CH_2CH_2Cl$	1.5
$ClCH_2CH_2S$-SCH_2CH_2Cl	0.4

HOMOGENEOUS PHOTOLYSIS

Homogeneous solutions of HD and CEMS in acetonitrile were irradiated to investigate photolysis in the absence of titanium oxide. After 24-hrs irradiation, the conversions of both substrates were greater than the samples containing TiO_2. The ^{13}C NMR analysis of the CEMS sample is listed in Table 2 for comparison with the CEMS samples containing TiO_2. A chromatogram of the HD mixture after 24-hrs irradiation is shown in Figure 4. Again, GC/MS was used to further identify the reaction products (Table 4).

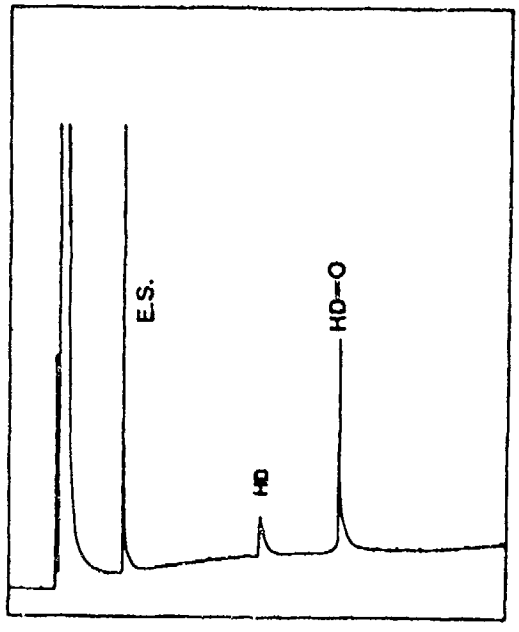

Figure 4. Photooxidation of 0.01 M HD in CH_3CN After 24 Hours of Irradiation at 350 nm

It seems that the light energy was absorbed more efficiently by the sulfide substrate in the absence of suspending TiO_2 particles. The photo-activated sulfide subsquently reacted with oxygen dissolved in the solvent to form sulfoxide as the major product. On the basis of the additional products identified by both NMR and GC/MS, the C-S bonds were broken by the light energy, and radical intermediates were produced. Variables that control the competing parallel reaction paths described above will be isolated and investigated in the future as a continuation of this study.

EFFECT OF WATER IN THE SOLVENT SYSTEM

Since it is desirable to use water as a decontaminant, a comparative study of the above photooxidation was made using an aqueous solvent system of 50 vol% of CH_3CN. The simulant had to be used because GC methods are not appropriate for aqueous samples. The products are listed in Table 5.

Photooxidation was significantly retarded by water, which absorbs photons. However, it is interesting to find that hydrolysis was almost completely prevented by light-induced reactions. This is perhaps due to the fact that photo-generated radicals form faster than the cyclic ethylenesulfonium ionproduced in the first and rate-determining step in hydrolysis.[8] However, in the absence of light, hydrolysis did occur and the dimer product, $(^{13}CH_3SCH_2CH_2)S^+(^{13}CH_3)(CH_2CH_2X)$ where X = Cl or OH with a second $^{13}CH_3S$ peak at *14.5 ppm*), was positively identified after 36 hrs of reaction (Table 5).[8] The TiO_2 suspensions were less stable in aqueous solutions. At each sampling interval, all of the titanium oxide powders had precipitated, leaving a clear solution in the test tube. The conversions of CEMS were about the same both in the presence and in the absence of the solid catalyst. This demonstrates that the titanium oxide powders had precipitated out of the solution and were not exposed to light for any significant period of time.

Table 5. Photooxidation of CEMS on TiO_2 Surface in an Equal Volume of Water-Acetonitrile Mixture

(^{13}C NMR analysis of products, mole% product per mole CEMS reacted [a])

		Z (Product = $^{13}CH_3$ -Z)			
		-S	$-S^+$	-S=O	others
NMR shifts,ppm		*14.9*	*23.3*	*37.7*	
Analysis Time, hr [b]	Time exposed to light, hr				
36	0	55	45	-	0
0	0	100	-	-	-
36	8	86	-	4	10
36	16	71	-	9	20
36	24	69	-	24	8
36	24[c]	63	5	20	3

[a] Integrated area of the carbon atom adjacent to nitrogen in acetonitrile ($CH_3\underline{C}N$, *117 ppm*) was used as the internal standard.

[b] Analysis time is time when sample was analyzed from time zero when CEMS was first mixed with the solvent.

[c] no TiO_2

SUMMARY

Both TiO_2-catalyzed photooxidation and homogeneous photolysis were identified in acetonitrile solutions of mustard and its simulant. Air has been the reactive oxidant to oxidize the sulfides to their corresonding sulfoxides thatdecompose at elevated temperatures. The conversions measured after 24 hrof irradiation at 350 nm suggest low quantum yields in the 3 to 5% range. The stability of TiO_2 suspension, as well as the conversions of photo-induced reactions of mustard, are significantly reduced by the presence of water.

Acknowledgments

The author appreciates the helpful discussions with Professor Mary Anne Fox of the University of Texas and Dr. J. Richard Ward of CRDEC; and thanks Dr. Patrick M. Nolan, CRDEC, for performing the initial experiments.

LITERATURE CITED

1. M.A. Fox, "Organic Heterogeneous Photocatalysis: Chemical Conversions Sensitized by Irradiated Semiconductors", *Accts. Chem. Res.* Vol. 16, pp 314-321 (1983).

2. C.K. Gratzel, M. Jirousek, and M. Gratzel, "Accelerated Decomposition of Active Phosphates on TiO_2 Surfaces", *J. Mol .Catalysis* Vol. 39, pp 347-353 (1987).

3. D.D. Sackett, and M.A. Fox, "Effect of Cosolvent Additives on Relative Rates of Photooxidation on Semiconductor Surfaces", *J. Phys. Org. Chem.* Vol. 1, pp 103-114 (1988).

4. R.S. Davidson, and J.E. Pratt, "The Titanium Dioxide Sensitised Photo-Oxidation of Sulphides", *Tetrahedron Lett.* Vol. 24, pp 5903-5906 (1983).

5. E.E. Reid, Ed. Organic Chemistry of Bivalent Sulfur, Vol. II, Chapter 5, Chemical Publishing Co. New York, N.Y. **(1960).**

6. F.A. Davis, L.A. Jenkins, and R.L. Billmers, "Chemistry of Sulfenic Acids. 7. Reason for the High Reactivity of Sulfenic Acids. Stablization by Intramolecular Hydrogen Bonding and Electronegativity Effects", *J. Org. Chem.* Vol. 51, pp 1033-1040 **(1986).**

7. Y.-C. Yang, L.L. Szafraniec, W,T. Beaudry, and F.A. Davis, "On Simulating the Oxidation Reactivities of Mustard and VX", accepted for presentation at the Scientific Conference on Chemical Defence, CRDEC, 15-18 November, 1988.

8. Y.-C. Yang, L.L. Szafraniec, W.T. Beaudry, and J.R. Ward, "Kinetics and Mechanism of the Hydrolysis of 2-Chloroethyl Sulfides", *J. Org. Chem.* Vol. 53, pp 3293-3297 **(1988).**

Dr. Yang graduated from Tulane University with a Ph.D. degree in physical chemistry. In 1983 she became an Associate in the Research Directorate of CRDEC, sponsored by the Associateships Office of the National Research Council. She later was employed by CRDEC as a research chemist in the Chemical Division and is currently assigned to the Decontamination Technology Branch in the Physical Protection Directorate.

BLANK PAGE

Brent R. Busey and Peter J. Stopa, CRDEC

AUTOMATED REAL-TIME SURFACE FLUORESCENCE BIOSENSOR

Two optical detection methods for monitoring immunoassays were subjected to qualitative engineering analysis. The primary goal was to develop an integral sensor/flow cell that would have low volume requirements, high sensitivity, and ease of production. One flow cell was built to monitor fluorescence. It incorporated a light-emitting diode, graded-index rod lenses, a fluorescence filter, and a photodiode. A second flow cell was constructed to monitor diffuse reflectance and optical transmission in a membrane-based colloidal-gold precipitation immunoassay. Each of the designs investigated exhibited insufficient sensitivity. Alternative designs were investigated and are proposed for future work.

INTRODUCTION

Direct detection of minimum infectious levels of biological organisms and minimum harmful levels of toxins requires analysis by extremely sensitive means. Current sampling methods produce only a small volume of very dilute sample. A sensor must be able to analyze such small samples with a high degree of sensitivity and selectivity. Detection Directorate of CRDEC is developing an automated detector for repetitive analyses of environmental samples. The goal of this project was to investigate an integral sensor/flow cell for use in this automated detector that would have high sensitivity, low sample volume requirements, and ease of producibility.

METHODS

Two optical methods were investigated for monitoring immunoassays in a miniature sensor/flow cell. The first was the measurement of fluorescence emitted from a small spot on the surface of a flat polymeric membrane. The light source and detector were arranged at 90° with respect to each other and at 45° with respect to the membrane surface. Several different flow cells were fabricated along the lines of the design shown in Figure 1. Excitation light was supplied either by an incandescent source with an excitation filter, or by a more narrow-band light-emitting diode (LED) without an excitation filter. For detection, a fluorescence filter was placed in front of a silicon photodiode. Fluorescent dyes (fluorescein and sulforhodamine 101 sulfonyl chloride) and antibodies conjugated to these dyes were used to determine gross sensitivity.

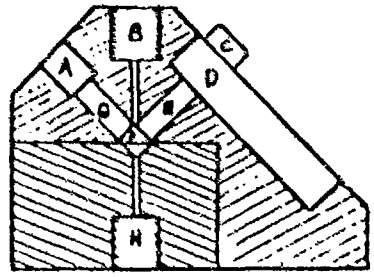

A - light emitting diode
B - fluid inlet fitting
C - photodiode
D - fluorescence filter
E - rod lens
F - sample chamber with filter diaphragm
G - rod lens
H - fluid outlet fitting

Figure 1. Cross sectional cut, full size, of the two-piece flow cell body

The second optical sensing method used was diffuse reflectance[1] or absorbance. While absorbance and reflectance measurements are

generally not as sensitive as fluorescence measurements (due to the large background intensity of the former two measurements), it was felt that the detector sensitivity in this case might be as good as or better than that of the fluorescence detector, due to a smaller number of optical components (and hence larger optical power throughput).

A low-volume flow cell was constructed that used diffuse background light from a battery-operated fluorescent flashlight to illuminate a 3- by 40-mm piece of polymeric membrane on which capture antibodies had been immobilized (Figure 2). Light reflected off the membrane (or transmitted through the membrane when the light source was placed on the opposite side of the membrane) was guided to silicon photodiodes by quartz rods, 1 mm in diameter, clad with a fluoropolymer. The quartz rods were placed above discrete spots on the membrane, allowing the monitoring of several independent locations. In principle, this would allow for the simultaneous analysis of several different substances in the sample, as well as providing negative control values.

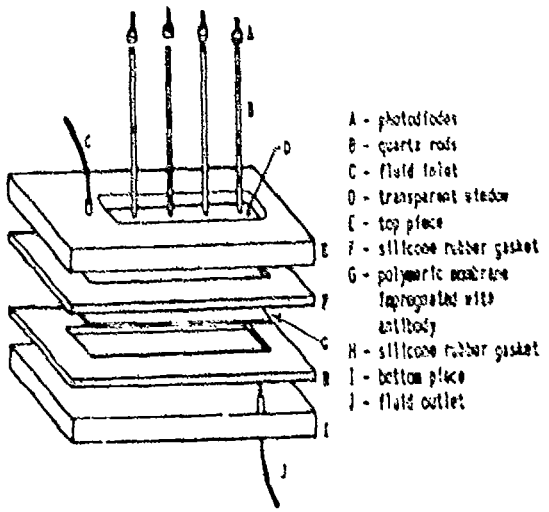

Figure 2. Exploded View of Low-volume Flow Cell for Measurement of Surface Reflectance at Multiple Sites

For this sensing approach, it is necessary that the formation of an optically dense product be linked to the immunological reaction. Several types of immunoassays involve the development of a colored product. One approach is enzyme-linked immunoassays, where a substrate is acted upon by an antibody-linked enzyme to produce a colored product. Some other types of immunoassays are based on the degree of formation of an immunoprecipitate, the presence of which is determined by changes in optical density at the bottom of a vial or on a piece of filter paper or membrane. The method chosen here was a colloidal gold immunoprecipitation reaction,[2] modeled after a commercially available assay. Figure 3 indicates how the presence of analyte in a sample causes the development of a dark spot on a membrane filter. The colloidal gold assay procedure was first applied to the detection of Rift Valley Fever virus using a nitrocellulose membrane in a 96-well microtiter plate assembly. This format allowed for rapid determination of the correct concentration ranges to use in the immunoassay. Unfortunately, due to problems with the immunological reagents as well as problems with the sensor hardware, the Rift Valley Fever assays got no farther than this initial screening.

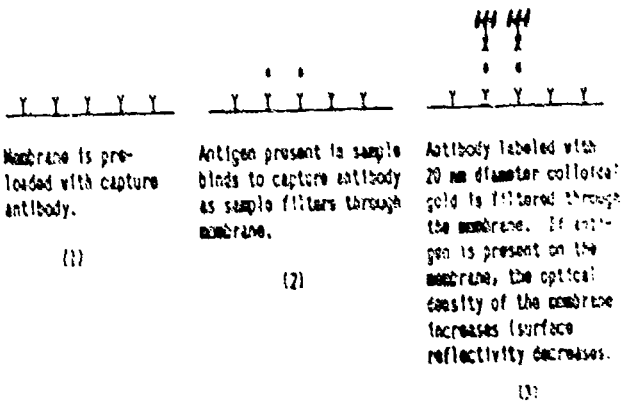

Figure 3. Sandwich Immunoassay Using a Colloidal Gold Conjugate

RESULTS

The detector built to monitor fluorescence had very poor sensitivity, using an incandescent source with an excitation filter or using an LED source with no excitation filter. The small physical dimensions of the internal sample chamber required the use of rod lenses (either graded index or step index) to channel light from the source to the sample chamber and thence to the detector. The multitude of optical interfaces then present, coupled with the small excitation spot in the sample chamber, resulted in very poor sensitivity, inadequate for monitoring the status of a fluorescent immunoassay. Custom-designed components, including antireflective coatings and index-matched materials, could possibly meet the sensitivity requirements.

Spectral reflectance and transmission absorbance measurements of colloidal gold immunoprecipitate spots, using the small flow-cell detector shown in Figure 2, were also of poor resolution. The sensitivity of the assembled detector was not as good as expected from results obtained with the subcomponents. The main difficulty lay not in the inherent sensitivity of the photodiode, but rather in a fiber optic-lensed detector's sensitivity to orientation with respect to and distance away from the monitored field.[3,4] Variations in background light intensity also reduced the detector's ability to quantitatively compare spatially separated spots. Based on the experimentation already performed, the strict control of these sensitive variables would allow an integral flow cell/detector to discriminate between optical density levels to a degree slightly better than that possible with the naked eye.

DISCUSSION

This study was of utility in that it demonstrates that the sensitivities of the primary sensors under development by Detection Directorate are hard to match with alternative designs. In recognition of this, current efforts have been refocused on adapting these primary sensors to the field detector application.[5] Research on the primary sensors is continuing with normal project funds. In addition, a FY 89 ILIR proposal has been submitted to investigate a promising variation in the monitoring of optical density in an immunoassay. In this application, a video camera is used to monitor the optical density of different spots on a membrane, using the colloidal gold immunoprecipitation reaction or some type of enzyme-linked immunoassay. The video camera method has the advantage of being able to simultaneously monitor hundreds of different sites and of being able to provide for background subtraction, contrast enhancement, and automated spacial adaptation due to inconsistencies between successive membranes. On the other hand, it is a more complex detector (with regard to size, power requirements, and data processing requirements) and may not be easily adaptable to a small volume flow cell.

LITERATURE CITED

1. G.F. Kirkbright, R. Narayanaswamy, and N.A Welti, "Studies with Immobilised Chemical Reagents Using a Flow-cell for the Development of Chemically Sensitive Fiber-optic Devices," *Analyst* Vol. 109, pp 15-17 (1984).

2. De Mey, J.R., "The Preparation of Immunoglobulin Gold Conjugates (IGS Reagents) and their use as Markers for Light and Electron Microscopic Immunocytochemistry," in Immunohistochemistry (A.C. Cuello, Editor), John Wiley & Sons, New York, pp 347-372 (1983).

3 Damuck, W. E. Jr., "Electro-Optic Detection Comparing Lensed and Fiber Optic Systems," *InTech*, pp 115-117 (1985).

4. Krohn, D.A., "Inside Fiber Optic Sensors," I & CS - *The Industrial and Process Control Magazine*, pp 57-58 (1983).

5 Busey, B R., Thames, K.E., *et al.*, "Fiber Optic Waveguide Detector For Use in Fluorescence Immunoassay," Technical Report 88051, U S. Army Chemical Research, Development and Engineering Center, Aberdeen Proving Ground, Maryland, 1988.

The University of Utah, Salt Lake City, UT, awarded Mr. Busey a B. S. degree in Chemistry in 1978 and an M. S. degree in Bioengineering in 1984. He works in the Detection Technology Division of Detection Directorate, specializing in the development and testing of sensors for the detection of chemical and biological agents.

Mr. Stopa has B. S. and M. A. degrees in Biochemistry from the University of Scranton, Scranton, PA. He recently joined the staff at CRDEC in the Detection Technology Division of Detection Directorate. He formerly worked for the Rapid Diagnosis Group at the U.S. Army Medical Research Institute of Infectious Diseases at Fort Detrick, MD and is responsible for the development of biological reagents for the Bio-Chemical Detector program.

Chen C. Hsu, CRDEC, and Yi H. Ma, Worcester Polytechnic Institute

Development of New Hydrophobic Regenerable Adsorbents, II

Four zeolite samples (ZSM5) with Si/Al ratios of 120, 240, 480, and 5202 were prepared and characterized. Results indicate that (a) the saturation adsorption capacity in four zeolite samples decreases in the following order: *n*-hexane > methanol > water, (b) the saturation adsorption capacity of water in zeolite samples decreases as the Si/Al ratio increases, (c) the effect of Si/Al ratio on the equilibrium adsorption capacity of organics is significant for methanol, but is small for *n*-hexane, (d) diffusion coefficients of organics and water in zeolite samples follow the same order, water > methanol > *n*-hexane, and (e) the diffusion coefficient decreases as the Si/Al ratio increases. A comparison was made among F-silicalite, silicalite, and ZSM5, and the results show that F-silicalite has superior performance in terms of hydrophobicity and adsorption capacity. The equilibrium coadsorption capacity of DMMP and water on silicalite, with Si/Al ratios of 1062 and 126, was also measured; there were 16% and 19% reductions respectively, in adsorption capacity under 67% RH.

INTRODUCTION

Zeolites are porous aluminosilicate crystals composed of SiO_4 and AlO_4 tetrahedra arranged in various geometric patterns. The tetrahedra are linked together at the corners by sharing oxygen ions to form ordered lattices. These lattices can be visualized as three-dimensional combinations of chain, layer, and polyhedra. Cations are present in the porous aluminosilicates. Some of these cations can be readily exchanged by placing crystals containing a given cation in a solution containing another cation. The adsorptive and catalytic properties of zeolites may be altered by the presence of different cations. More recently, zeolites have been engineered to handle specific molecules for a wide range of engineering applications, ranging from separation of xylene isomers to conversion of methanol to gasoline. Of particular interest are the hydrophobic and shape-selective properties and thermal stability of the pentasil zeolites (e.g., silicalite) and dealuminated zeolites. Zeolites have been extensively used in industrial separation and purification processes, such as air separation,[1,2] hydrogen purification,[3,4] and hydrocarbon separations.[5,6] One of the major drawbacks in using zeolites for air purification is its hydrophilic property. However, it has been shown that dealuminated zeolites, such as aluminum-deficient mordenite, possess hydrophobic property while the change in adsorption capacity for other adsorbates, such as cyclohexane, is relatively small.[7] Furthermore, high siliceous zeolites, such as silicalite and ZSM5, exhibit considerable hydrophobic properties while retaining shape-selective properties.[8]

The adsorbents used for the high-performance cyclic adsorption processes require the characteristics of high hydrophobicity and easy regenerability. Zeolites with high Si/Al ratios have been identified as possessing hydrophobic property. Previously, we have studied silicalite and F-silicalite in terms of their saturation adsorption capacity and diffusion coefficients with water and

organics. In this study, we have prepared and characterized four zeolite samples (ZSM5) with Si/Al ratios of 120, 240, 480, and 5202. The saturation adsorption capacity and hydrophobicity of activated carbon, silicalite, F-silicalite, and ZSM5 were compared. Additionally, the equilibrium coadsorption capacity ofdimethyl methyl phosphonate (DMMP) and water was also measured with silicalite samples of Si/Al ratios of 1062 and 126.

EXPERIMENTAL METHODS

The results from the previous study indicate that zeolites with higher Si/Al ratios have higher hydrophobicity. Additional zeolite samples (ZSM5) with Si/Al ratios of 120, 240, 480, and 5202 were prepared in the laboratory by hydrothermal processes; their physical properties are summarized in Table 1. The equilibrium adsorption isotherms and diffusion coefficients were measured with the same apparatus described previously. Briefly, the measurements were carried out with an assembly of Cahn RG electro-balance. The entire system was housed in an insulated cabinet to maintain a constant temperature. The sample was dried under 10^{-4} torr and 350 °C until no weight change was observed. At the start of a run, the adsorbate was admitted into the assembly. The change in adsorbent weight as a function of time was continuously recorded until equilibrium was achieved. To measure the equilibrium coadsorption capacity of DMMP and water, two modes of experiments were used. First, DMMP was admitted into the system after the sample was saturated with water. Second, DMMP was introduced into the system after water was evacuated from the water-saturated sample.

Table 1. Physical Properties of ZSM5 and ZSM8 Samples

Sample No.	Type	Si/Al Ratio	Particle Size (μm)
1	ZSM5	120	9.46
2	ZSM5	240	6.33
3	ZSM5	480	5.30
4	ZSM5	5202	4.26
5	ZSM8	240	7.34

RESULTS AND DISCUSSION

The equilibrium adsorption isotherms of *n*-hexane, methanol, and water in zeolite samples with four different Si/Al ratios at 25 °C are shown in Figures 1-3. The saturation adsorption capacities at 25 °C are listed in Table 2. It appears that the equilibrium saturation capacity for water decreases with increasing Si/Al ratio; however, the saturation adsorption capacity for n-hexane and methanol increases as the Si/Al ratio decreases. This is consistent with the earlier results. The saturation adsorption capacity for the three compounds in each ZSM5 sample decreases in the following order: *n*-hexane > methanol > water, further substantiating the hydrophobic and organophilic nature of ZSM5.

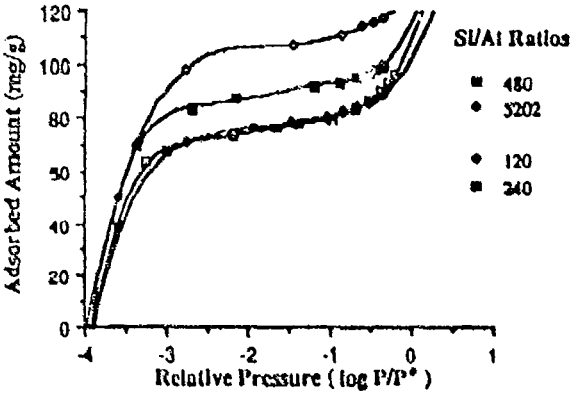

Figure 1. Adsorption Isotherms for *n*-Hexane in ZSM5 Samples

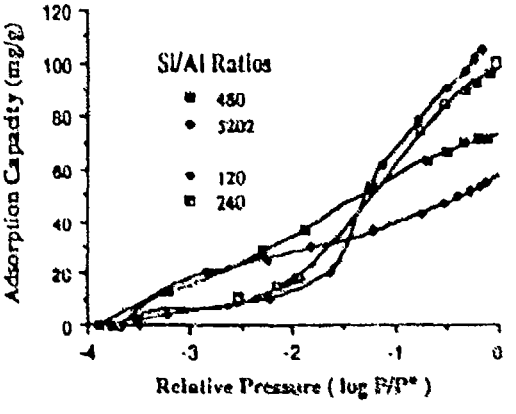

Figure 2. Adsorption Isotherms for Methanol in ZSM5

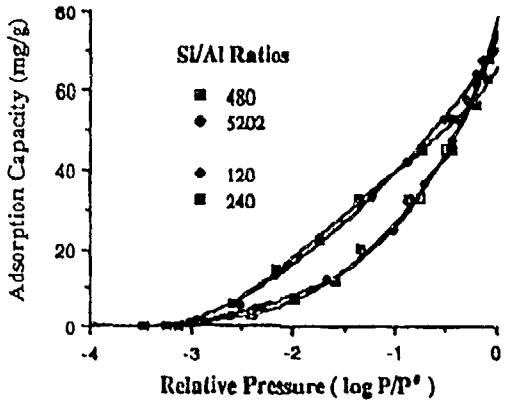

Figure 3. Adsorption Isotherms for Waterl in ZSM5

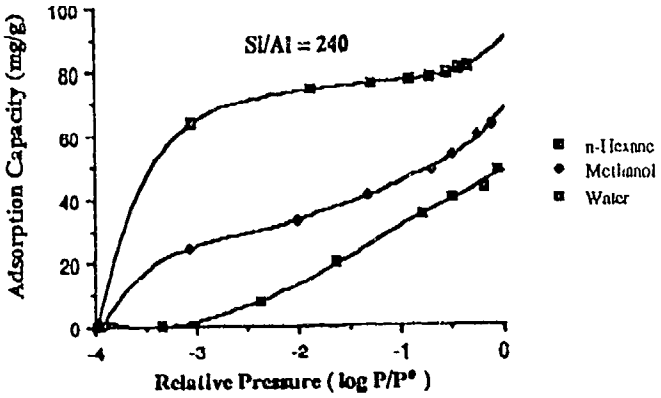

Figure 4. Equilibrium Adsorption Isotherms for ZSM8

Table 2. Saturation Adsorption Capacities of Organics and Water in ZSM5 at 25 °C

	Adsorption Capacity (mg/g)			
	Sample No.			
Adsorbate	1	2	3	4
n-Hexane	95.2	95.9	96.4	118.2
Methanol	57.2	72.1	95.0	105.2
Water	67.0	64.2	63.3	61.0

Additional measurements of ZSM8 samples were also made and equilibrium adsorption isotherms are shown in Figure 4. ZSM8 also exhibits hydrophobic property although the saturation adsorption capacity for n-hexane is somewhat lower than that of ZSM5 with the comparable Si/Al ratio due possibly to the difference in crystal structure.

The adsorption rate curves were also measured at 25 °C. A typical plot of the fractional uptake as a function of time for methanol, *n*-hexane, and water is shown in Figure 5. The diffusion coefficients determined at low sorbate concentration are tabulated in Table 3. The diffusion coefficient appears to decrease with increasing Si/Al ratio. Furthermore, the diffusion coefficient appears to be affected by the size of the diffusing molecules with water having the highest diffusion coefficient and *n*-hexane being the lowest.

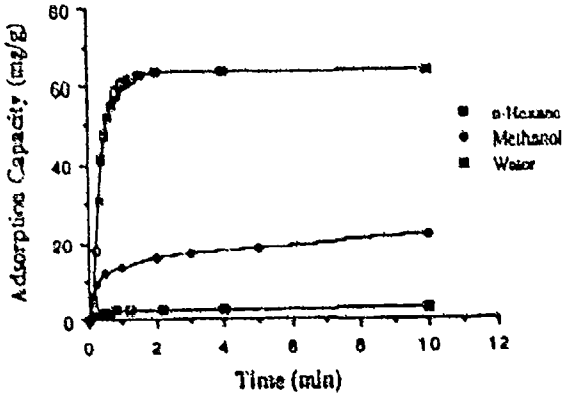

Figure 5. Adsorption Rate Curve of Organics and Water in ZSM5 at 25 °C

Table 3. Diffusion Coefficients of Organics and Water in ZSM5

$(D \times 10^{-9}\ cm^2/sec)$

Adsorbate	Sample No. 1	2	3	4
n-Hexane	6.87	5.67	4.97	1.63
Methanol	8.99	8.41	7.35	4.27
Water	15.87	14.06	11.89	7.30

Combined with the previous results, the saturation adsorption capacities of activated carbon,[9] F-silicalite, silicalite, and ZSM5 was compared inTable 4. It is obvious that activated carbon is the least hydrophobic; F- silicalite, silicalite, and ZSM5 are 46, 12, and 7 times more hydrophobic, respectively. The saturation adsorption capacities of methanol and n-hexane in F-silicalite, silicalite, and ZSM5 are between 1 and 2 times less than that of activated carbon; for benzene, activated carbon has about 4 to 5 times greater adsorption capacity than the other adsorbents studied. From the hydrophobicity data obtained so far, F-silicalite is considered to be the better adsorbent for cyclic adsorption processes (i.e., pressure swing and temperature swing adsorptions).

Table 4. Comparison of Saturation Adsorption Capacities of Activated Carbon, F-Silicalite*, Silicalite*, and ZSM5* at 25 °C

Adsorbate	Activated Carbon	F-Silicalite	Silicalite	ZSM5
Water	43.65%	0.95%	3.8%	6.1%
Methanol	17.60%	9.20%	12.0%	10.5%
n-Hexane	22.25%	9.92%	13.2%	11.8%
Benzene	40.94%	8.40%	10.1%	- - -

* Si/Al Ratios of F-silicalite, Silicalite, and ZSM5 are >200, 1062, and 5202, respectively.

The results of the equilibrium coadsorption capacity measurements at 22-24 °C are shown in Tables 5 and 6. In all cases, silicalite with an Si/Al ratio of 1062 showed better DMMP adsorption capacity than that with an Si/Al ratio of 126 in the RH range of 7% to 66%, indicating that a high degree of hydrophobicity improves DMMP adsorption. There is also a significant improvement in DMMP adsorption under relatively higher RH after the evacuation of the water-saturated sample. In the first mode of experiment (Run Nos. 2 and 3), where DMMP was introduced into the system after the sample was saturated with water, the reduction of adsorption capacity of DMMP is 2.3% and 32.4% for silicalite samples with an Si/Al ratio of 1062 under 7% and 24% RH, respectively. For the silicalite samples with an Si/Al ratio of 126, the reduction was 9% and 27% under the same conditions. In the second mode of experiment (Run Nos. 4 and 5), where the water-saturated samples were evacuated before DMMP was introduced, the reduction of DMMP adsorption capacity is 18% and 16% for silicalite samples with Si/Al ratios of 1062, and 22% and 19% for those samples with Si/Al ratio of 126 under 30% and 67% RH, respectively.

When water was removed from water-saturated samples, the DMMP adsorption capacity was increased. In all cases, however, in the presence of water, the adsorption capacity of DMMP on silicalite samples was decreased. Based on the earlier data, it is conceivable that F-silicalite samples would have less effect due to water.

CONCLUSIONS

- The saturation adsorption capacity in four zeolite samples (ZSM5) decreases in the following order: *n*-hexane > methanol > water.
- The saturation adsorption capacity of water in ZSM5 decreases as the Si/Al ratio increases
- The effect of Si/Al ratio on the equilibrium adsorption capacity of organics in ZSM5 is significant for methanol, but is small for *n*-hexane.

Table 5. Equilibrium Coadsorption Capacity of DMMP with Water on Silicalite Sample (Si/Al = 1062) at 22-24 °C

Run No.	1	2	3	4	5
Water Partial Pressure (mmHg)		1.464	5.110	6.337	14.000
Water Equilibrium Adsorption Capacity (mg/g)		9.800	32.800	13.000*	11.900
DMMP Partial Pressure or Total Pressure (mmHg)	0.678	<1.464#	<5.110#	0.788	0.520
DMMP Equilibrium Adsorption Capacity (mg/g)	129.000	126.000	87.100	106.000	108.000

*Adsorption Capacity Measured After Water Vapor Was Removed From the System.

#Introduction of DMMP Into the System Caused the System Pressure.

Table 6. Equilibrium Coadsorption Capacity of DMMP with Water on Silicalite Sample (Si/Al = 126) at 22-24 °C

Run No.	1	2	3	4	5
Water Partial Pressure (mmHg)		1.464	5.110	6.337	14.000
Water Equilibrium Adsorption Capacity (mg/g)		18.300	--	23.000*	21.300
DMMP Partial Pressure or Total Pressure (mmHg)	0.678	<1.464#	<5.110#	0.788	0.520
DMMP Equilibrium Adsorption Capacity (mg/g)	113.000	103.000	82.700	88.000	91.300

*Adsorption Capacity Measured After Water Vapor Was Removed From the System.

#Introduction of DMMP Into the System Caused the System Pressure.

- Diffusion coefficients of organics and water in ZSM5 with four different Si/Al ratios follow the order: water > methanol > *n*-hexane. Additionally, the diffusion coefficient decreases as the Si/Al ratio increases.

- The test results of the equilibrium coadsorption capacity of DMMP with water show significant reduction in capacity on silicalite samples. For silicalite samples with Si/Al ratios of 1062 and 126, the reduction is 16% and 19% under 67% RH.

- In terms of hydrophobicity, F-silicalite has superior performance compared to the other three adsorbents (activated carbon, silicalite, and ZSM5). In terms of organic adsorption capacity, activated carbon is the best adsorbent.

LITERATURE CITED

1. G. A. Sorial, W. H. Granville, and W. O. Daly, "Adsorption Equilibria for Oxygen and Nitrogen Gas Mixtures on 5A Molecular Sieves," *Chem. Eng. Sci.* Vol. 38, p 1517 (**1983**).

2. N. H. Berlin, U.S. Patent No. 3,280,536 (Oct 25, 1966) to EXXON Research and Engineering Company.

3. H. A. Stewart , and J. L. Heck, "Pressure Swing Adsorption," *Chem. Eng. Prog.* Vol. 65 (9), p 78 (**1968**).

4. R. T. Cassidy, ACS Symposium Series 135, "Adsorption and Ion Exchange with Synthetic Zeolite, " W. H. Flank (Ed.) p 247 (**1980**)

5. W. J. Asher, M. L. Campbell, W. R. Epperly, and J. L. Robertson, "Storage Hydrocarbon Processing" Vol. 48 (1), p 134 (**1969**).

6. W. J. Asher, *et al.*, U. S. Patent No. 3,070,542 (1962) to EXXON Research and Engineering Company.

7. N. Y. Chen, "Hydrophilic Properties of Zeolites," J. Phys. Chem. Vol. 80, p 60 (**1976**).

8. H. Nakamoto, and H. Takahachi, "Hydrophobic Natures of Zeolite ZSM-5," *Zeolites*, Vol. 2, p 67 (**1982**).

9. W. A. Noyes, Jr., Summary Technical Report of the National Defense Research Committee, Division 10, p 142 (**1946**).

Dr. Hsu was awarded a Ph.D. in physical chemistry in 1972 from the University of Utah, Salt Lake City, UT. He has been at CRDEC since 1982 as a research chemist in the Chemical Division of the Research Directorate. He also serves as a technical consultant to the U.S. Air Force on the catalytic air purification system for the airframe-Chemical and Biological Agents Protection System.

CHEMICAL RESEARCH, DEVELOPMENT AND ENGINEERING CENTER

PERSONNEL SUMMARY FY88

The U.S. Army Chemical Research, Development and Engineering Center (CRDEC) is the largest tenant on the 4,435 acres that form the Edgewood Area of Aberdeen Proving Ground, Maryland. The CRDEC's facilities use 1,314,129 square feet of space in 240 laboratory, administrative, industrial, and storage buildings.

The mission of the CRDEC is to manage and conduct the research, development, and engineering activities to provide a credible deterrent to chemical attack through a strong defensive posture and an adequate retaliation capability should deterrence fail. CRDEC is the AMCCOM Executive Agent for all research, exploratory, advanced, and engineering development and biological defense. CRDEC plans and conducts the Technology Base Program for Chemical Material for Joint Service Application. It participates in the international research, development, and standardization programs as the primary U.S. Army laboratory for chemical and biological defense materiel and chemical weapons materiel. The Center plans and conducts the Army research, exploratory development, advanced development, and engineering development for obscuring smoke/aerosol systems.

S & E DISTRIBUTION BY PROFESSION

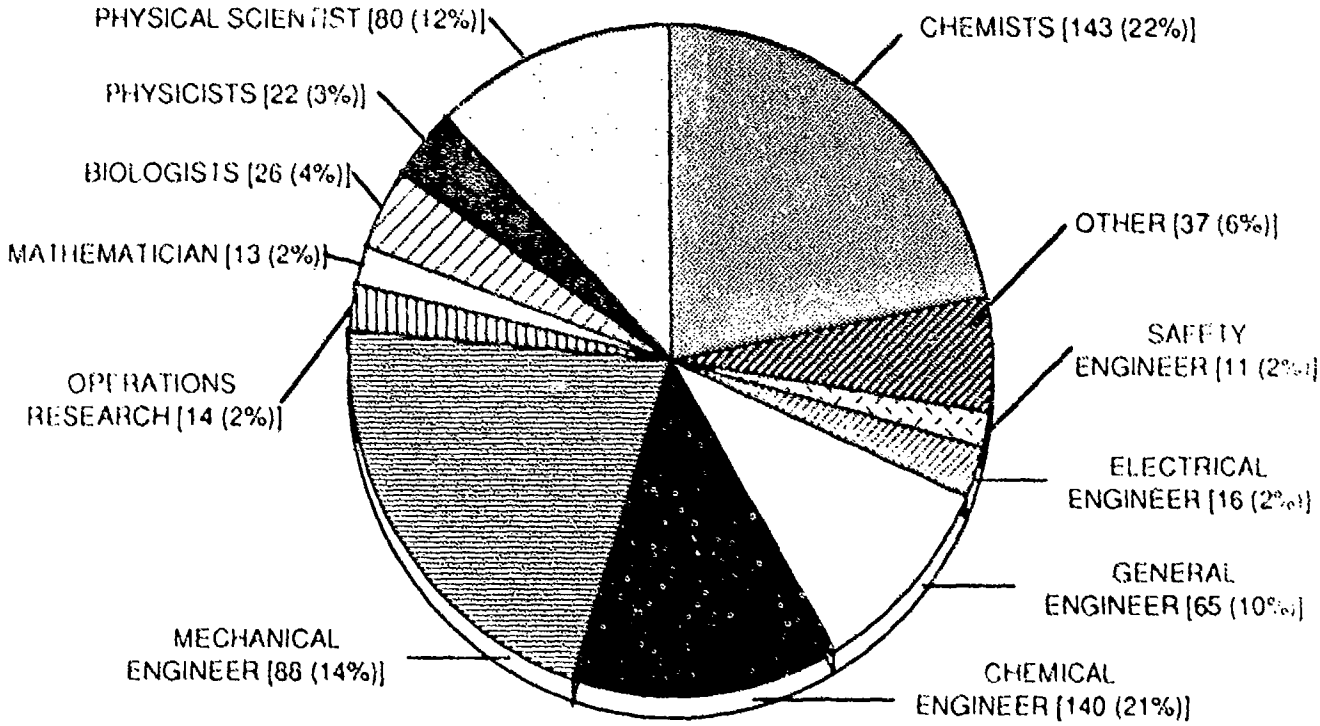

CIVILIAN PERSONNEL: FY88 = 1273

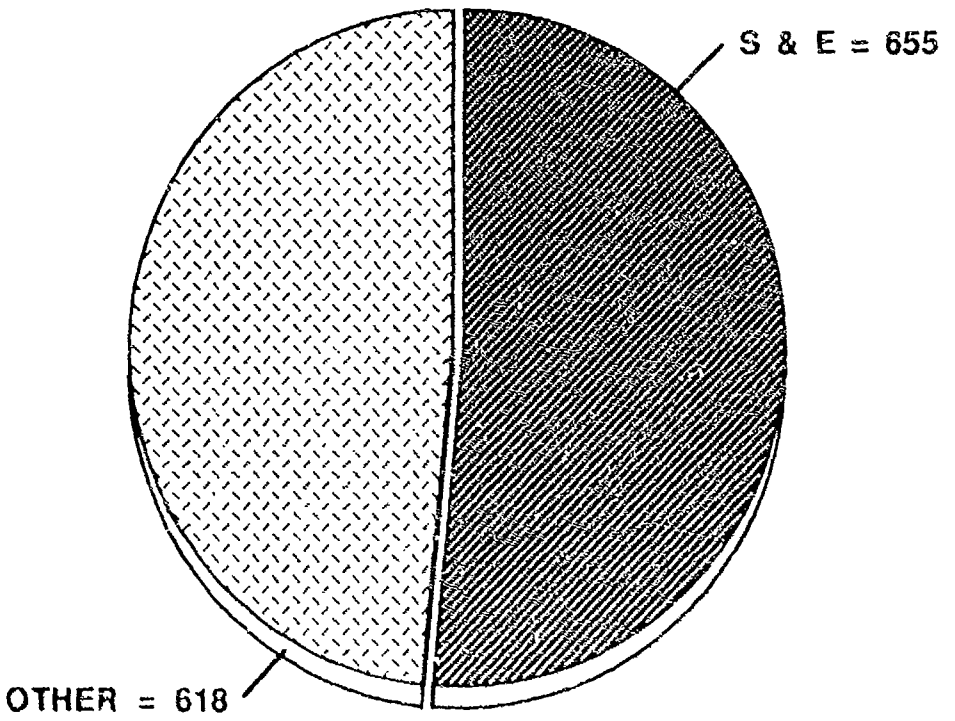

S & E DISTRIBUTION BY DEGREE

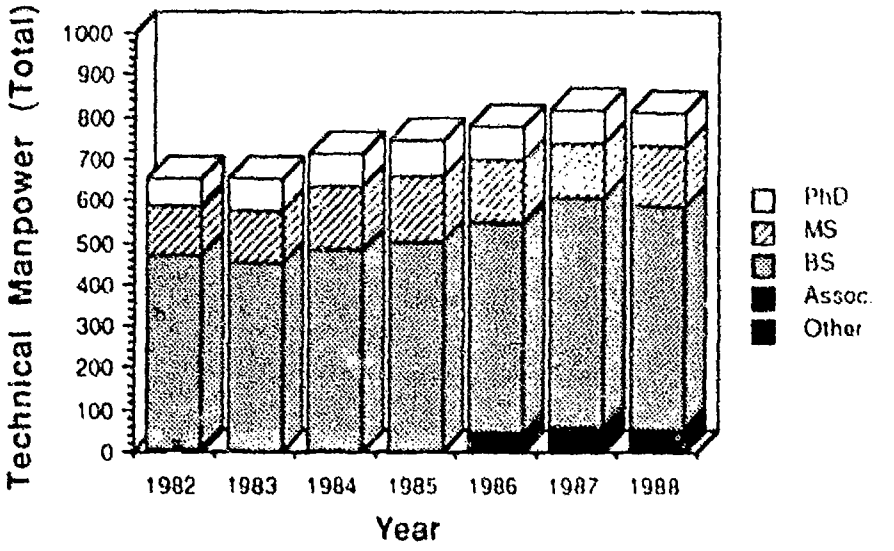

CRDEC NEW HIRES FY85-FY88